Aero – Propulsive Model Design from a Commercial Aircraft in Climb and Cruise Regime using Performance Data

by

Magdalena TUDOR

THESIS PRESENTED TO ÉCOLE DE TECHNOLOGIE SUPÉRIEURE
IN PARTIAL FULFILLMENT FOR A MASTER'S DEGREE
WITH THESIS IN AEROSPACE ENGINEERING
M.A.Sc.

MONTREAL, JANUARY 23, 2017

ÉCOLE DE TECHNOLOGIE SUPÉRIEURE
UNIVERSITÉ DU QUÉBEC

BOARD OF EXAMINERS

THIS THESIS HAS BEEN EVALUATED

BY THE FOLLOWING BOARD OF EXAMINERS

Ms. Ruxandra Mihaela Botez, Thesis Supervisor
Department of Automated Manufacturing Engineering at École de technologie supérieure

Mr. Thien-My Dao, Chair, Board of Examiners
Department of Mechanical Engineering at École de technologie supérieure

Mr. Guy Gauthier, Member of the jury
Department of Automated Manufacturing Engineering at École de technologie supérieure

THIS THESIS WAS PRENSENTED AND DEFENDED

IN THE PRESENCE OF A BOARD OF EXAMINERS AND THE PUBLIC

ON JANUARY 19, 2017

AT ÉCOLE DE TECHNOLOGIE SUPÉRIEURE

Dedication

This thesis is dedicated to the memory of my mother Ecaterina.

ACKNOWLEDGMENTS

First of all, I would to thank to Madame Ruxandra Mihaela Botez for the opportunity to study Aerospace Engineering at the ETS, and who suggested me this research topic. The work was performed at the Research Laboratory in Active Controls, Avionics and Aeroservoelasticity (LARCASE) under Dr. Botez' supervision. Furthermore, I would like to express my sincere appreciation for her passionate mentorship, understanding and financial support throughout my Master's program.

My great consideration and gratitude towards the LARCASE team, who encouraged me, and which has shared me, with so much patience and joy, their aerospace engineering knowledge, specifically to PhD students Ghazi Georges, Dancila Bogdan Dumitru, Dancila Radu Ioan, Murrieta-Mendoza Alejandro, Roberto S. Félix Patrón, Gabor Oliviu Sugar, and Andreea Koreanschi and to the Research Associate Mr. Oscar Carranza, for his valuable technical support.

Finally, I am grateful to my father Paul, and especially my husband Petre, for their support, the patience and great care, without which this goal would not have been achieved.

LA CONCEPTION D'UN MODÈLE AERO-PROPULSIF D'UN AVION COMMERCIAL EN REGIMES DE MONTÉE ET EN CROISIÈRE À PARTIR DES DONNÉES DE PERFORMANCE

Magdalena TUDOR

RÉSUMÉ

Les conséquences sur l'environnement de la demande croissante dans le transport aérien, qui ont été prises en compte dans le développement de l'industrie aéronautique, ont été estimées par IATA en 2012 à 2% des émissions mondiales de dioxyde de carbone. Les acquis historiques des progrès scientifiques et techniques dans le domaine de l'aviation commerciale ont contribué à cette estimation, et même la recherche d'aujourd'hui continue de faire des progrès pour aider à réduire les émissions de gaz à effet de serre.

Les progrès, dans la conception et la technologie des modèles d'avions commerciaux et des moteurs, ont été destinés à améliorer, effectivement et efficacement, les performances de vol, mais aussi la planification de vol de ces types d'avions. Derrière ces progrès, des bases des données numériques d'un avion, qui vient d'être générées, en tant que sources de référence, la plupart du temps sont évaluées comme "confidentielles" par les constructeurs d'avions, et très rarement, elles sont traitées comme sources partagées avec ceux qui font la modélisation de l'avion et de son moteur.

La littérature de spécialité présente plusieurs modèles aéro-propulsifs d'un avion, déjà mis en œuvre, mais aucun d'entre eux n'est conçu sans avoir accès à des données numériques du moteur, en plus, il faudrait être en mesure de générer, en montée et en croisière, une base de données numériques qui peut être appliquée directement dans un processus d'optimisation des profils de vol des aéronefs.

Cette thèse a pour but d'apprendre à concevoir des modèles aéro-propulsifs pour la montée et de croisière, en utilisant des méthodes d'identification et de validation des systèmes, à travers lesquelles les performances d'avion sont calculées et stockées sous la forme la plus compacte et la plus facile d'accès à ces types de données, afin d'être utilisées dans les techniques d'optimisation du profil de vol.

Les modèles aéro-propulsifs développés dans cette recherche ont été étudiés sur deux avions appartenant à la classe d'avions commerciale. Pour chaque avion, la méthodologie a fait preuve d'une très bonne précision. Les modèles étudiés, qui prouvent avoir une bonne précision, pourraient être adaptés à d'autres avions de la même classe, même s'il n'y a pas d'accès à des données de vol du moteur. Encore plus, les résultats de la recherche ont démontré, en quelque sorte, que ces modèles pourraient économiser de l'argent pour les compagnies aériennes, par le fait qu'un très grand nombre d'essais en vol pourrait être évité,

pour chacun des cas étudiés. En outre, l'équipe du laboratoire en commande active, avionique et aéroservoélasticité (LARCASE) de l'ÉTS gagne un accès direct à ces données des performances pour ces types d'avions, dans l'intérêt de créer de nouveaux algorithmes d'optimisation applicables à d'autres types d'avions.

Mots-clés: aviation commerciale, modèles aéropropulsifs, des données numériques des performances, méthodes d'identification et de validation du système, processus d'optimisation des profils de vol

AERO – PROPULSIVE MODEL DESIGN FROM A COMMERCIAL AIRCRAFT IN CLIMB AND CRUISE REGIME USING PERFORMANCE DATA

Magdalena TUDOR

ABSTRACT

IATA has estimated, in 2012, at about 2% of global carbon dioxide emissions, the environmental impact of the air transport, as a consequence caused by the rapidly growing of global movement demand of people and goods, and which was effectively taken into account in the development of the aviation industry. The historic achievements of scientific and technical progress in the field of commercial aviation were contributed to this estimate, and even today the research continues to make progress to help to reduce the emissions of greenhouse gases.

Advances in commercial aircraft, and its engine design technology had the aim to improve flight performance. These improvements have enhanced the global flight planning of these types of aircrafts. Almost all of these advances rely on generated performance data as reference sources, the most of which are classified as "confidential" by the aircraft manufacturers. There are very few aero-propulsive models conceived for the climb regime in the literature, but none of them was designed without access to an engine database, and/or to performance data in climb and in cruise regimes with direct applicability for flight optimization.

In this thesis, aero-propulsive models methodologies are proposed for climb and cruise regimes, using system identification and validation methods, through which airplane performance can be computed and stored in the most compact and easily accessible format for this kind of performance data. The acquiring of performance data in this format makes it possible to optimize flight profiles, used by on-board Flight Management Systems.

The aero-propulsive models developed here were investigated on two aircrafts belonging to commercial class, and both of them had offered very good accuracy. One of their advantages is that they can be adapted to any other aircraft of the same class, even if there is no access to their corresponding engine flight data. In addition, these models could save airlines a considerable amount of money, given the fact that the number of flight tests could be drastically reduced. Lastly, academia, thus the laboratory of applied research in active control, avionics and aeroservoelasticity (LARCASE) team is gaining direct access to these aircraft performance data to obtain experience in novel optimization algorithms of flight profiles.

Keywords: commercial aircraft, aero-propulsive model, aircraft performance data, climb and cruise regimes, system identification and validation methods, flight profile optimization, flight management system

TABLE OF CONTENTS

LIST OF TABLES

LIST OF FIGURES

Page

LIST OF ABREVIATIONS

A300, A310, A320	Airbus family
ADC	Air Data Computer
AE	American Engineering unit system
AFM	Aircraft Flight Manual
APM	Aircraft Performance Model
ASCII	American Standard Code for Information Interchange
AT	Air Transport
ATAG	Air Transport Action Group
ATC	Air Traffic Control
ATM	Air Traffic Management
ATS	Air Transportation Systems
BADA	Base of Aircraft Data
B757, B767	Boeing family
CAR	Canadian Aviation Regulations
CFR	Code of Federal Regulation
CO_2	Carbon dioxide
CS	Certification Specification
DS	Dynamic System
EASA	European Aviation Safety Agency
EEC	Eurocontrol Experimental Center
ÉTS	École de Technologie Supérieure

EoM	Equation of motion
FAA	Federal Aviation Administration
FM	Flight Manual
FMS	Flight Management System
GA	Genetic Algorithm
IATA	International Air Transport Association
ICAO	International Civil Aviation Organization
ISA	International Standard Atmosphere
LARCASE	Laboratory of Applied Research in Active Control, Avionics and Aeroservoelasticity
LS	Least Squares
MACH	Mach number
MATLAB/SIMULINK	MathWorks Software product
NACA	National Advisory Committee for Aeronautics
NDB	Navigation Data Base
NexGen	Next Generation Air Transportation System
NLR	National Aerospace Laboratory of the Netherlands
NM	Nelder-Mead algorithm
PE	Prediction Error
PDB	Performance Database
PSO	Particle Swarm Optimization
SA	Situation Awareness level
SAC	Standard Aircraft Characteristics

SAGE	System for assessing Aviation's Global Emissions
SESAR	Single European Sky ATM Research
SI	International System Units
TCCA	Transport Canada Civil Aviation
US	United States
VS	Vertical Speed
VSI	Vertical Speed Indicator

LIST OF SYMBOLS AND UNITS OF MEASUREMENTS

a	speed of sound
a	input parameter of a static model
a_{LR}	temperature variation coefficient (−0.0065°K/m or −0.0035°R/ft)
AF	acceleration factor (dimensionless)
AR	wing aspect ratio (dimensionless)
b	output parameter of a static model
b	wingspan (ft)
c	wing chord
csv	comma separated values
CAS	calibrated airspeed (KCAS)
C_D	drag coefficient (dimensionless)
C_L	lift coefficient (dimensionless)
C_{D0}	zero-lift drag coefficient (dimensionless)
C_{Di}	induced drag coefficient (dimensionless)
C_{Dmin}	minimum drag coefficient (dimensionless)
D	drag force (lb_f)
e	Oswald efficiency coefficient (dimensionless)
f	non-linear real-valued function
f_{err}	function error
FB	fuel burn (kg)
FL	flight level (ft)

g	acceleration of gravity (9.8 m/s^2 or 32.174 ft/s^2)
GW	gross weight (kg or lb_m)
h	altitude (ft)
$h_{traveled}$	total distance traveled (nm)
H_{Dist}	horizontal distance traveled (nm or nmi)
ISA	international Standard Atmosphere
IAS	indicated airspeed (KIAS or nm/h)
k	time index
k	drag due to lift factor
lb_f	pound force
lb_m	pound mass
L	lift force (lb_f)
LS	least-squares model
M	Mach number (dimensionless)
M_{LS}	matrix of independent variables
MSL	mean sea level
N	discrete value points
p	pressure
PA	pressure altitude (ft)
q_c	dynamic pressure (Pa or lb_m/ft^3)
R	real gas constant (287 J/kg °K) or (1716 ft lb_f/slug °R)
RoC	rate of climb (ft/min)
$\sin\gamma$	climb gradient (dimensionless)

S	reference wing's area (ft^2)
SLST	sea-level static thrust
t	wing thickness
t	instant time
t_c	time to climb (min)
T	temperature
T	thrust force (lb_f)
T_{sfc}	engine specific fuel consumption coefficient (dimensionless)
TAS	true air speed (KTAS or knot)
TAT	total air temperature
u	input
V	speed (knot)
$\bar{V}$	average true airspeed (knots or kts)
$\dot{w}_f$	fuel flow (kg)
W	weight force (N or lb_f)
x_{cg}	center of gravity position
y	actual system' response
y_m	model response
z	function of the process output
ΔISA	standard temperature deviation (℃)
Λ_{LE}	leading edge sweep angle (°)
α	angle of attack

δ	pressure ratio (dimensionless)
ε	error
$\boldsymbol{\gamma}$	adiabatic constant of an ideal gas (1.4)
γ	flight path angle
θ	vector of parameters
θ	temperature ratio (dimensionless)
$\boldsymbol{\theta}$	set of minimized arguments
ρ	density (lb/ft^2)
θ_i	set of parameters
$\boldsymbol{\theta}^*$	unique solution of the equation error method
σ	density ratio (dimensionless)

Subscript and Superscript Notations

$0strat$	Initial stratosphere altitude
c	Compressible air mass
cg	Center of gravity
$data$	Flight data
$Dist$	Distance traveled
err	Error
h	Altitude
LE	Leading edge
LR	Lapse rate
m	Model
MSL	Mean sea level

sfc	Specific fuel consumption
S	Static
T	Total
^{T}	Transposed
$\underset{Dist}{^{estim}}$	Estimated distances traveled, related to a position i
$\underset{i}{^{estim}}$	Fuel burnt, related to a position i

INTRODUCTION

The transport of people and the goods across the globe has become a necessity and is no longer a luxury. Commercial aviation, as part of the air transportation industry, has significantly gained in popularity to meet global expectations.

In April 2014, the Air Transport Action Group (ATAG) reported that close to three billion passengers boarded an aircraft somewhere on Earth (ATAG, 2014). This global mobility has had a positive impact on the global economy, opening new international markets and facilitating the globalization of production (Budd and Goetz, 2014). However, this global mobility of goods and people has a direct negative impact on the environment. Its contribution to climate change therefore requires global action to reduce global carbon emissions.

In 2012, almost 2% of carbon dioxide (CO_2) of the world's total carbon emissions was due to airline operations (ATAG, 2014; IATA, 2013). Even if the aviation industry's impact on the environment is relatively low compared to that of other sectors, the aerospace industry has undertaken to reduce net aviation CO_2 emissions by 50%, with respect to those of 2005 by 2050, despite of increasing its activity. In 2013, IATA investigations have predicted that to reduce the air transport's carbon footprint from commercial airline fuel burn by a number of 3.2% until 2020 and of 2.9% by 2030, the air transport (AT) system have to safely improve their fuel efficiency based on the airline operational procedures (IATA, 2013). Even if the airlines are not the only contributors of this reduction process, according to the IATA' estimations, a 3.2% carbon emissions reduction could be safely accomplished with the help of an optimized air traffic management (ATM) system. Thanks to several cooperative efforts, the aircraft industry has already found some solutions to make this goal attainable.

A decade ago, studies based on flight tests for airplanes flying in formation demonstrated that a 20% reduction in airplane drag leads to an 18% savings in fuel economy, as well as a 10% reduction in carbon dioxide emissions (Okamoto, Rhee and Mourtos, 2005). Commercial

aircraft manufactures have focused on fuel efficiency since as early as 1930 (Peeters, Middel and Hoolhorts, 2005).

To improve fuel efficiency, and thereby to implicitly lower their carbon footprints, Airbus and Boeing have developed and applied advanced wing technologies on existing commercial airplanes. Airbus is a pioneer in the design of wingtip devices. These devices have been applied on the A300 and A310, reducing the spiral-shaped vortices formed during the flights at their wingtips. Airbus has continued to improve this type of research, applying large sharklets (i.e. blended winglets) wingtip devices on the A-320. These have allowed to the A-320 savings up to 4% in fuel burn, as well as annual savings in CO_2 emissions for each of their aircrafts (Airbus, 2015). It has been demonstrated that an aircraft equipped with winglets can climb more efficiently than an aircraft having no winglets. Also, these wingtip devices helps the aircraft to achieve cruise altitudes faster at lower thrust settings (Peeters, Middel and Hoolhorts, 2005).

The statistics are also impressive for the other giant manufacturer, Boeing. The Federal Aviation Administration (FAA) published a report in January 2015 which noted that the Boeing-737N (the Max) was going to burn 14% less fuel than the Boeing-737-800NG (FAA, 2015). According to Boeing, the Winglet Advanced Technology on the 737 MAX has optimized its wing performance, achieving a fuel efficiency of 1.8% (DTTL, 2014). On the B-747-400, the winglet design shown a 3.5% benefit in terms of cruise drag reduction (Blake, 2009).

Aerodynamic studies and their applications have been made at a reduced scale, such as an airplane's wing and with conventional materials. The use of advanced materials on the B-787 and B-777X, such as carbon composites, have allowed improvements compared to using only conventional materials (DTTL, 2014). "Smart materials" have been used to morph the wings of an aircraft. Wing "morphing techniques" improve the aerodynamic characteristics and performance of a wing airfoil by changing its shape without using standard control surfaces. Several studies have shown that the design of a morphing aircraft wing may reduce an aircraft's fuel consumption. An optimal (or sub-optimal) wing shape can be found for a

specific flight phase including take-off, climb, cruise, and descent (Gabor, Koreanschi and Botez, 2012; 2013; Gabor et al., 2014).

To achieve the fuel reduction goal by 2050, also, the engine manufacturers must improve engine efficiency. In September 2014, Airbus evaluated the latest generation of power plants: PurePower PW1100G-JM from Pratt & Whitney and CFM International's LEAP-1A, on the A320NEO "New Engine Option" of the Airbus A320 family. According to Airbus, the A320's improvements have resulted in significant predictions such as 15% in fuel savings per aircraft, and by 2020, 20% fuel burn improvement per seat (Airbus, 2014).

Another way to reduce CO_2 emissions in aviation is the development of sustainable alternative fuels. One alternative to safely replace conventional kerosene jet fuel is to use "biofuel". After an impressive number of tests, three different types of biofuel were approved in June 2014. Even though the high cost of biofuel was a barrier, 21 airlines used alternative fuels for commercial flights in 2014 (IATA, 2014).

As mentioned in the ICAO 2010 Environmental Report, the design and manufacturing of an aircraft can take more than 10 years (ICAO, 2010). Implementing technological improvements into a fleet in service is a long and costly process. The airspace industry is therefore working in collaboration with academia to find alternative solutions, such as new aircraft trajectory optimizations methodologies for fuel cost reduction (Murrieta Mendoza, 2013; Mendoza and Botez, 2014; Patron, Botez and Labour, 2013; Murrieta-Mendoza and Botez, 2014a; Murrieta-Mendoza and Botez, 2014b; Patrón and Botez, 2014; Patrón et al., 2013a; Patrón et al., 2013b ; Patrón, Berrou and Botez, 2014 ; Dancila, Botez and Labour, 2012). According to Jensen (Jensen et al., 2014; Jensen et al., 2013), most aircraft in the United States do not fly at their optimal trajectories in terms of altitudes and speeds. Therefore, to reduce fuel consumption, an optimization of the vertical profile would be a value-added, low-cost option (Patron, Botez and Labour, 2012; Patron, Botez and Labour, 2013; Patrón et al., 2013; Dancila, Botez and Labour, 2012). Vertical flight profile trajectory optimization is considered as the pivotal function of the Flight Management System (FMS) due to its capacity for flight cost reduction (Sibin, Guixian and Junwei, 2010).

The FMS, as an airborne electronic device employed in most commercial aircraft manages each flight, computes the optimal flight profiles (i.e. the vertical and lateral profiles) to minimize the flight costs in terms of flight time, and also the total fuel burnt (Botez, 2006). To predict the optimal flight trajectory, the FMS needs an Aircraft Performance Model (APM) that estimates the horizontal distance traveled and the amount of fuel burnt (Murrieta-Mendoza and Botez, 2014; Murrieta-Mendoza, Botez and Ford, 2014; Dancila, Botez and Labour, 2013; Dancila, Botez and Ford, 2013). Predicting the optimal flight trajectory also requires the input data of an associated aircraft performance model, along with the operational instructions corresponding to its trajectory as well as the weather data. This proves how important is to have a well investigated and advanced FMS, which rely otherwise on the most reliable aircraft performance model (Sibin, Guixian and Junwei, 2010).

The behaviour of an aircraft in the classical way is described by a set of non-linear equations, called Equation of Motion (EoM), as proposed by Ghazi, G. (Ghazi, 2014) or by Vincent et al. (Vincent et al., 2012). As any electronic device, the FMS has a limited processing capacity. A simplified physical model must firstly be defined by a set of equations of motion, whose solutions are usually numerical. These solutions are then stored in so called the numerical database or look-up tables, easily adapted to the FMS architecture.

The objective of this thesis is to provide a complete methodology to conceive an Aircraft Performance Model (APM) from flight tests in climb and cruise regimes by creating look-up tables from aero-propulsive models. These aero-propulsive models were designed to meet the need of the Laboratory of Applied Research in Active Control, Avionics and Aero-Servo-Elasticity (LARCASE) team, of FMS manufacturers (CMC Electronics Esterline) and of the aircraft manufactures.

The obtained performance data by applying these proposed aero-propulsive models can be used by researchers to create algorithms and or simulations for the flight trajectory optimization in the vertical plane, in the climb and cruise phases (Murrieta-Mendoza, Botez and Ford, 2014; Dancila, Botez and Labour, 2013; Dancila, Botez and Ford, 2013). These

models in climb and cruise regimes were created using the numerical database of a commercial aircraft. In the climb as well as cruise flight phase, the aircraft performance for the flight tests involves a combination of aircraft aerodynamics and engine attributes (i.e. parameters).

It should be emphasized that the aircraft manufacturers are looking for the methodology that creates a numerical database using the measured flight parameters, and with a high reliability for a minimum number of flight tests (US, 1993). With these measurements collected from flight tests and stored in aircraft performance charts and tables, manufacturers can fulfill the aircraft specification compliances and utilities for a particular aircraft. Practice has revealed that the aircraft engines are not adequately equipped to collect the in-flight measurements (US, 1993). These measurements of the engine thrust are very important, as they are used to build an engine model, as part of the aero-propulsive model of any aircraft. Therefore, to create a complete aero-propulsive model, an aerodynamic model has to be developed. The aerodynamic model is also based on the measurements of the flight tests. Even with a minimum amount of information, i.e. the unknown engine performance data, this thesis proposes a complete methodology for identifying an Aero-Propulsive Model (APM) in climb and cruise regimes using numerical database of an Aircraft A. In a vertical plane (i.e. a plane perpendicular to the ground) the climb and the cruise regimes represent two essential segments of the commercial and military airplane flight profiles (Hull, 2007). The aircraft manufacturers goal is to build a reliable aero-propulsive model with a minimum access to aircraft information, and to a minimum number of flight tests. The proposed methodology to build these aero-propulsive models in the climb and cruise phases has showed a good prediction also for another numerical database of an Aircraft B belonging to the same aircraft commercial class.

This thesis shows how to create flight numerical database, without any prior engine information, in climb and cruise regimes, with a minimum flight tests number while retaining a good level of accuracy. Comparing to the existing methodologies, the new proposed methodology is therefore less costly (more economical) in terms of time and money (i.e. based on the number of the flight tests saved) for a commercial aircraft manufacturer.

This thesis research is structured on three large chapters. A literature review and a summary of the theoretical concepts are presented in Chapter 1, followed by the proposed methodology and the research problem statement under its assumptions in Chapter 2. Once the objectives, limitations and the methodology have been described, the results and discussions are analyzed in details in Chapter 3. Finally, the conclusions followed by recommendations summarize the contribution of this research topic in the aerospace field.

This research work was realized in collaboration with and was sponsored by CMC Electronics Esterline, partner of the LARCASE. The main objective was to create an aircraft performance model, in the climb and cruise regimes, using numerical database of a commercial aircraft as reference source.

CHAPTER 1

RESEARCH PROBLEM CONTEXT

This chapter defines the main terms of the research topic, including the definitions, concepts, theories and methods utilized for modeling an airplane in the climb and cruise regimes. This chapter includes a detailed description of the research problem, along with the assumptions made to orient the approach. A thorough review of the literature related to this topic is incorporated throughout.

1.1 General context

Governments and the airspace industry are looking for new strategies to achieve air transportation savings in the best interest of the planet. To constraint, and thus to reduce worldwide aviation emissions, Europe and the United States (US) have worked together in the creating and interoperating these systems: Single European Sky ATM Research (SESAR) and Next Generation Air Transportation System (NexGen) latest (Murrieta-Mendoza et al., 2015). The cooperation between Flight Management Systems (FMSs) and Air Traffic Management (ATMs) systems is possible made by use of navigation algorithms, utilized as simulation tools, and wherein future ATMs could generate modifications in flight plans to keep them (i.e. the flight plan) active (Flathers III, Allerton and Spence, 2010). Aviation applications have continually been designed to allow safe aircraft' separation and to improve the communication infrastructure among airliners, aircraft pilots, and Air Traffic Controllers (Murrieta-Mendoza et al., 2015; Theunissen, Rademaker and Lambregts, 2011).

The new aircraft/engine technologies and operational procedures also reflect the industries objective to reduce both fuel consumption and the emissions of carbon dioxide (CO_2), carbon monoxide (CO), hydrocarbons (HC), nitrogen oxides (NO_x), and sulphur oxides (SO_x), computed as (SO_2).

To measure the efficiency of reducing global fuel burn and its environmental impact, the US Federal Aviation Administration (FAA) has developed simulation aircraft and engine models

at local/regional (dependent on weather) and at global levels (Fleming et al., 2006). The engine model has the particularity that it is assigned by default as being among the most popular ones of the airline fleet. Called the System for assessing Aviation's Global Emissions (SAGE), this high fidelity computer model is helping the international aviation community to estimate aircraft fuel burn and emissions, as well as to make available databases and methodologies (Fleming et al., 2006). SAGE has also the ability to model variations in the parameters, as well as flight trajectories, aircraft performance (such as fuel flow) and aircraft motion data (as the operations database at the individual flight level), etc.

Optimization techniques have been studied for flight trajectories in the Aviation Industry, especially via the required criteria of minimum flight time and/or fuel consumption. These techniques, implemented on a number of FMS generations, have allowed flight crew to achieve the desired trade-off between time and fuel costs. National and international aeronautical organisation policy makers have imposed ambitious goals, such as safety improvements, increased FMS efficiency, and, last but not least, environmental sustainability.

In other words, to plan and to control the air traffic flow, in order to predict optimal flight trajectories, the ATC/ATM applications, as decision support tools, are using the most accurate Aero-Propulsive Models (APM(s)). Additionally, at that precise information on the main flight phases of a predictable flight, an APM can be employed to estimate the aircraft numerical databases, in order to obtain the exact trajectories estimates. However, the literature has few notable researches on the subject of APMs used for flight trajectory estimation.

1.2 Literature review

Sibin et al. in (Sibin, Guixian and Junwei, 2010) created a method to build an Aircraft Performance Model (APM) for FMS by using the performance data of a flight simulator prototype. As reported by Sibin' team, the data structure requirements of the performance

database from their FMS flight simulator were dependent on the Object-oriented Technique, and the aerodynamic model. Meanwhile, their engine performance data has been known, as it was provided by the flight simulator prototype system. Most aircraft manufacturers hesitate to provide the aero-propulsive data to researchers, making access to aircraft performance data quite difficult. However, this research thesis comes out with the novelty through that an Aero Propulsive Model (APM) can be created without any access to engine performance data.

Two years later, Sibin et al. in (Sibin, Li and Han, 2012), proved that their Particle Swarm Optimization (PSO) algorithm improved the trajectory optimization of the Boeing 737-800 aircraft in its vertical flight profile. Their work relied on the mass point and rigid body dynamics theory (Lu, 2007; Sibin, Li and Han, 2012). This approach is used in trajectory optimization process in order to reduce the complexity of aircraft behaviour and to enhance the real-time system performance in the online computation for FMS system. Accordingly to the same authors (Sibin, Li and Han, 2012), there are other Aircraft Performance Models (APMs) constructed by Peng, under non-real-time circumstances in (Junyi and Rongzhen, 1997), and by Wang in (Wang and Yang, 2008), both accordingly to the Aircraft Flight Manual (FM).

Another Aircraft Performance Model (APM), called also Base of Aircraft DAta (BADA) is developed and maintained by Eurocontrol in collaboration with the aircraft manufacturers and operating airlines. It contains the aircraft model specifications and the datasets, and is created for needs in aircraft trajectory simulations, and for their predictions using air traffic modelling and simulations tools.

Camilleri et al. (Camilleri et al., 2012) described the structure and the main features of an APM, developed to model the Airbus A320 performance in climb, cruise and descent regimes, over its entire operational flight envelope. They used the BADA information to validate their APM.

Gong and Chan in (Gong and Chan, 2002) presented a technique to obtain an Aero-Propulsive Model (APM) from the available time-to-climb data, which can be found in any flight manual (pilot's manual or operations manual). They performed two case studies, one study on a Boeing 737-400 for which the time-to-climb and the aero-propulsive data were known, and the other study on a Learjet 60. Boeing's INFLT, as part of a NASA aircraft performance software package from a cooperative research project with Boeing, computed the aircraft performance of most Boeing aircraft types. The engine thrust force estimated from an available engine model helped them to build the propulsive model. This engine model was scaled so that it could optimize the trajectory predictions for a Learjet 60. Good results were obtained when the predicted trajectories were compared to those obtained from radar tracking. However, their methodology did not take into account the engine fuel consumption or the fuel burnt, and therefore their APM could not be used to solve the current optimization trajectory problems.

Baklacioglu and Cavcar in (Baklacioglu and Cavcar, 2014) applied a genetic algorithm (GA) to obtain an aero-propulsive model (APM) from the flight manual data (Boeing 737-400 Operations Manual) of a transport aircraft in order to determine the climb and descent trajectories. But, contrary to Gong and Chan (Gong and Chan, 2002), their propulsive model was based on a semi-empirical equation. Their work involved an identification process to establish the model coefficients for a Pratt & Whitney JT9D-7A engine at different altitudes and Mach numbers. The predicted time to climb resulted from the obtained model was compared with the predicted from the flight manual data.

Eight years after Gong and Chan's research, Vallone and Mcdonald in (Vallone, 2010; Vallone and McDonald, 2010) analysed the supersonic light fighter, the Northrop F-5, and the McDonnell Douglas DC-10, a three-engine jet performances. The information was gathered from the Aircraft Flight Manuals (AFM), the Standard Aircraft Characteristics (SAC) charts, and the Jane's All the World's Aircraft or even the Wikipedia website.
According to the authors, the drag polar and engine deck models for these airplanes were created based on known aircraft data, using the inverse problem process. Based on the

engines' characteristics, Vallone (Vallone, 2010) built some functions for the fitting of the drag polar and the engine deck (engine model) for the Northrop F-5 and the McDonnell Douglas DC-10.

Ghazi et al. in (Ghazi, Botez and Tudor, 2015) developed a methodology to design an aero-propulsive model (APM) from flight tests, and built a performance database (PDB) to predict the Cessna Citation X performance in the climb regime. A total of 70 flight tests were performed at the Research Laboratory in Active Controls, Avionics and Aeroservoelasticity (LARCASE) on a Research Aircraft Flight Simulator (RAFS) for the Cessna Citation X business aircraft. This is a level D aircraft research flight simulator, manufactured and designed by CAE Inc., for which 9 of the 70 flight tests were used in the model identification process, and the rest (61) of flight tests were used for the model validation process. The estimations of the model based on this methodology had a 100% success rate for both flight tests categories used for model identification and validation. The aero-propulsive model and the interpolation methods used by Ghazi et al. to create the PDB were sufficiently accurate (maximum deviation of less than 5%) and could be further adapted for their use on other aircrafts.

The originality of this research thesis comes from the fact that an aero-propulsive model was set up, with no a priori propulsion model information. In previous studies, Gong (Gong and Chan, 2002), and Vallone (Vallone, 2010; Vallone and McDonald, 2010) had a priori propulsive model information available, which helped them to build their aero-propulsive models. Additionally, the new proposed methodology of this accurate aero-propulsive model studied in climb and cruise regimes, was created based only on the physical approach of the problem, and it was developed based on a minimum amount of flight test data required for the identification process.

1.3 Background

1.3.1 Aero-Propulsive Model and Aircraft Performance Definitions

An aircraft Aero-Propulsive Model is described with the help of two mathematical sub-models. The first sub-model, called “aerodynamic model” is based on aerodynamic analysis, using the computation of aerodynamic forces (lift and drag) that are specific for each of the two configurations (climb and cruise) analyzed. The second sub-model, called “propulsive model” is related to the propulsion (power plant, propeller or engine), and estimates the driving thrust force and the engine performance.

This “aero-propulsion model” is designed to improve the aircraft performance. Aircraft performance is characterized by the way in which an airplane performs under a specified set of conditions in order to achieve its intended purpose of flying from point *A* to point *B*. An airplane’s performance is measured by use of:

- The physics of flight;
- The lift, drag, and thrust coefficients;
- Estimation methods;
- Performance Data such as PDB, lookup tables, and flight test data for experimental data representation.

An aircraft is a market product; therefore, it has to meet performance standards fixed by laws. Gudmundsson (Gudmundsson, 2013)) and Maris (Maris and Vandevivere, 2014) presented information on commercial aviation laws, as controlled in the USA, in Europe and in Canada, according to the different rules summarized in Table 1.1.

Table 1.1 Certification source for
Commercial Aviation

	Rules
USA	14 CFR Part 25
Europe	CS-25 (EASA)
Canada	CARs, Part V (Part 525), TCCA (Part 521)

The progress in the design and technology of aircraft models and in ATM-FMS systems has strengthened the role of ATC services. The ATM en-route system submits the pre-planned aircraft trajectories estimated by Flight Management Systems (FMSs) to other airplanes, and to the ground ATM processors (Suchkov, Swierstra and Nuic, 2003). In (Suchkov, Swierstra and Nuic, 2003), Suchkov mentioned that one of the problems that the ATC service faces today is that not all airplanes are equipped with onboard FMSs, even if all FMSs have the ability to plan efficiently flight profiles.

An Aero-Propulsive Model (APM) was built to meet the need to optimize aircraft vertical profiles, mainly used by FMSs, in order to find the most economic flight paths in terms of time or fuel consumption.

1.3.2 Numerical Database and Flight Management System

The FMS is the key with which to responds to most of the airlines' economic worries in terms of fuel and time costs (Creedon, 1983). In 1982, Boeing began to install FMSs on B-757 and B-767 as standard equipment, and later Airbus installed FMSs on the A310. These FMSs became standard for most commercial airplanes: the Airbus A300-600, A320, A321, A330, A340, Boeing 737-300/400/500, B747-400, and B-777, the Fokker100, and the McDonnell Douglas MD-11 and MD-90) (Liden, 1995).

The industry was not prepared for this “revolutionary advance in the management of the flight” as mentioned by Liden in his paper (Liden, 1995). Therefore, in order to meet the aircraft manufacturers’ and the airlines’ requirements, different FMS versions were designed, and during the ensuing years, new features and improvements have been added in the FMS architecture. Customers’ requirements have been met thanks to the flexibility and functionality of the FMSs’ software architecture. Due to the anticipated air traffic growth, and to the FMSs inclusion in the ATM systems, an upgrading to hardware technology should give better ratings to FMS’s market (Liden, 1995).

The airlines and the airplane manufacturers have decided to use FMSs as a long-term solution for automatized flight planning, and recording flight procedures. The computerization of the FMS has revealed remarkable advances, including pilot workload reduction, increased flight safety, the insertion of large route databases, and trajectory optimization tools (Igor and Atkins, 2001). As a very complex avionics system, an FMS has the capability to predict and optimize the flight plan based on the following parameters: weight or gross weight, aircraft type, engine and performance characteristics, winds, air temperature, etc. Other parameters include the airspeeds, Mach numbers, and altitudes needed to produce four-dimensional (4D) flight profiles (lateral and vertical), as explained by Collinson and Walter (Collinson, 2011; Walter, 2001).

The FMS architecture includes functions for navigation, flight planning, trajectory prediction, performance computations, and guidance (Walter, 2001). These functions are supported by the Navigation Data Base (NDB), and the performance database (PDB) of the airplane. The NDB must be updated monthly, while the PDB should be updated whenever a change in an aircraft’s performance characteristics occurs (e.g. an engine retrofit). The PDB encloses aircraft/engine model performance data, which is composed of the drag, thrust, fuel burnt or fuel flow (depending on the flight regime), and the speed/altitude of aircraft flight envelope. The flight envelope is defined by Shin in (Shin et al., 2011) as the safe flying area of an aircraft, as described by certain variables.

A vertical flight profile, calculated along a lateral path, is composed by the 3 regimes of climb, cruise and descent.

Trajectory optimization problems usually have the following inputs: the center of gravity position (x_{cg}), the speed (V), the weight (W) or gross weight (GW), the ISA (International Standard Atmosphere) temperature deviation (ΔISA), the altitude (h). The output parameters of these problems are expressed in terms of the fuel burn (FB), the horizontal distance travelled (H_{Dist}) or (d) for the climb regime, and the fuel flow ($\dot{w}_f$) for the cruise regime.

1.3.3 System Identification Methods

The behaviour of an aircraft, defined as a Dynamic System (DS), is the main concern of aeronautical engineers. They have to choose, from many features, those that are necessary and sufficient to accurately describe the DS' objectives (Bosch and Klauw, 1994). The art of modeling firstly requires a thorough understanding of the basic problem in the real world by means of a "model". For this reason, the real dynamic system behaviour is described by functions that are mathematical representations of the system properties.

Aerospace literature reveals a range of approaches to achieve adequate models. Bosch and Klauw (Bosch and Klauw, 1994) emphasize that a model can be developed by considering prior knowledge of the process. For example, a mass is assumed to be a point mass, without a physical size. More, prior understanding of the process can enrich the structure of a model with supplementary information. The identification techniques are further introduced. These techniques help to find approximated values for the model parameters, dependent on to the inputs and the outputs of experimental observations and measurements.

The following classification system supports a means to choosing a mathematical model to describe an aircraft as a dynamic system. Bosch and Klauw classified the models to describe a dynamical system as follows (Bosch and Klauw, 1994):

- "Mathematical models" used to study the dynamics of a system with the aid of non-linear differential equations, and assumed to be very flexible;
- "Scale models" for situations where mathematical models are not accurate enough or cannot be computed fast enough; these models are created by examining a physical process or system, and then building it on a reduced scale in order to survey their loads during wind tunnel tests at lower cost;
- "Verbal models", with examples in sociology and psychology, in which a system is too difficult to be mathematically modeled. There must be some understanding of the qualitative relations between the system variables.

Once we understand that a mathematical model can be applied to determine an aircraft's motions through the air, then, according to the same authors (Bosch and Klauw, 1994), the mathematical models may be subdivided into:

- "Static or steady state model" that describes the relationship between the input u and the output y of a function, which can be linear or nonlinear. A static model with the output y, parameters a and b of the function, and the input u is depicted in Figure 1.1.

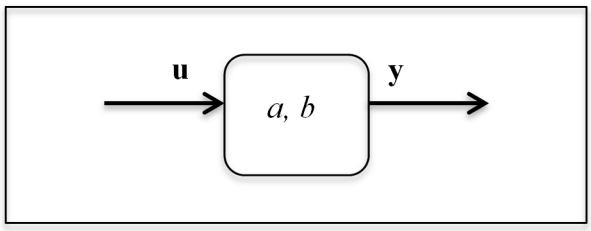

Figure 1.1 Static model representation

This type of model is described as a time independent computing system, and whose forces are balanced. It is also a means to view an airplane as a system, for example: an aircraft that is not intended to fly is called "static model", and is also known as an aircraft used for the testing and/or development of new designs.

- “Dynamic models”, which are mostly based on simulations, designed to understand the behaviours of a system by means of analysis. Typically, they are represented by differential equations, or presented as stochastic or matrix models such as black models or other such complex models.

Both the static and the dynamic models described above are “deterministic” models. These deterministic models are all those in which the output parameters are accurately determined. The aircraft may thus be designed using static and dynamic models.

The research problem analysis about the mathematical models of an airplane is continuing to be explored by means of the definitions regarding to the inputs and outputs of their parameters, and to investigate the most appropriate way to achieve their best approximation.

1.3.3.1 White, gray and black models

Starting from some basic physical laws and known parameters, we can create what is known as a ”white-box” model, that is a theoretical model. Therefore, this model could be described by some sets of equations. Under other circumstances, with no prior information, the model has to be developed from the measured data, and because lacking information about the system internal structure and its internal relations, the model is known as an empirical ”opaque” (black-box) model.

Our aero-propulsive model (i.e. an aircraft modeled after a DS concept) is a combination between these two models, and is known as a “grey” model or a “hybridization” of the above two models. Representative of a semi-empirical model class, the aero-propulsive model has unknown parameters which are computed from the experimental data, and they are also based on the theoretical (i.e. the numerical database) model built.

Mathematical modeling by means of parameter estimation is one of the techniques needed to determine a system' characteristics (i.e. the aircraft performance parameters determined from aerodynamics and propulsion data).

Aircraft parameter estimation is the most well-known example of system identification methodology, which helps to solve the engineering inverse problem of model determination and validation through a set of observations (i.e. the flight tests data) (Hamel and Jategaonkar, 1996). Hamel et al. (Hamel and Jategaonkar, 1996) also state that the system identification methods had become the most appropriate base for model validation in research and industry, by managing aircraft design and by improving risk and cost reduction in the ideal implementation of both existing and new-generation aircrafts.

Parameter estimation is a method of using observations from a dynamic system (DS) (i.e., any aircraft as a physical system) to develop a mathematical model that represents the system' features to an acceptable degree. This is a process of determining the unknown parameters of a mathematical model based on input–output data (flight data), and can be expressed graphically, as shown in Figure 1.2.

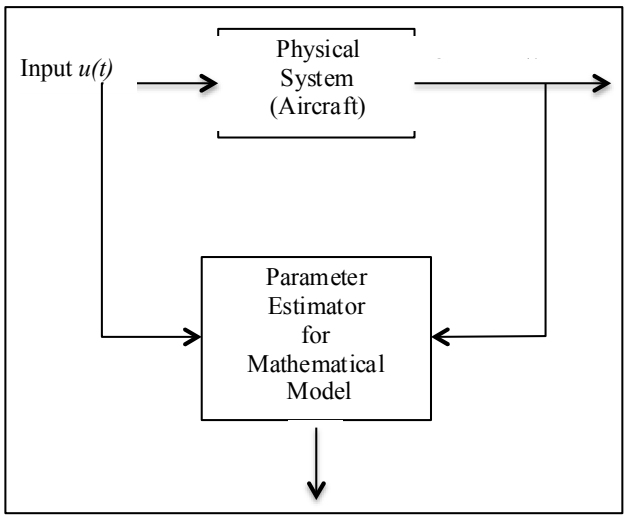

Figure 1.2 Estimation of the parameters of a mathematical model

The estimation process is the crucial step in the model's performance, which we are seeking to improve it, and which depends on the accuracy of its parameter estimates. The created model is described by a finite set of parameters, whose values are calculated by applying the estimation techniques. The problem of parameter estimation is based on an optimization of the error function that generates a set of equations that will estimate the dynamic system (DS) parameters. The objective is to obtain optimal estimates of the unknown parameters that best describe the behaviour of the DS. Basically, the path is found based on a least square error minimization between the model response (y_m) and the actual system' response (y).

With the arrival of the high-speed computers, experienced techniques like the innovative methods based on artificial neural networks have found increasing applications in parameter estimation problems (Raol, Girija and Singh, 2004). The black box model, used as a predictor, is a neural network that can approximate a function without seeing the structure of the approximated function. It is an efficient tool for computing models.

System identification is simply a form of mathematical approximation of a real-life system. The idea is to derive a model of acceptable accuracy from the available flight data. This model is the best approximation of the real description of an aircraft (Ljung, 2010). In real-life, practical systems or real-life objects (i.e. aircraft) are non-linear, and therefore the approximated model should be matched to the data of the system (i.e. the flight data or any AFM data). The parameters of the matched model need to be estimated.

According to Zadeh, a system identification developed from system theory and accepted by the aerospace industry says: "System identification (determination, on the basis of observation of input and output, of a system within a specified class of systems to which the system under test is equivalent; determination of the initial or terminal state of the system under test)" (Zadeh, 1962)

Based on Zadeh definition, the system identification process includes a model structure definition built on mathematical equations and the estimation of parameters defining the model. Schematically, Figure 1.3 describes the system identification concept.

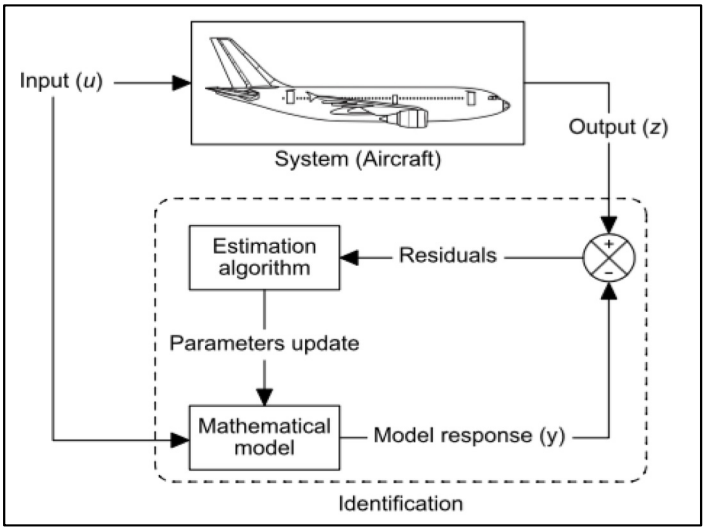

Figure 1.3 System identification concepts

The identification process described in Figure 1.3 could be achieved through the following three steps:

- Measurements and experiments have to be performed to create the aircraft performance data, as a required information;
- Mathematical model of the observed system (i.e., an aircraft) must be defined, using a set of equations, and
- Procedure or estimation method that automatically feeds the model with the model parameters should be done in order to reduce the modelling errors between the real system and the observed model.

As shown in Figure 1.3, the estimation algorithm from the identification concept is fed with the residuals or function errors (f_{err}) (i.e. the model error). The residual is a function that depends of the output (z) of the DS and the output of the mathematical model or model response ($y\ or\ y_m$) expressed as follows:

$$f_{err} = f_{err}(z, y_m) \tag{1.1}$$

Because of these residuals, the identification problem becomes an optimization problem. This means that the objective is to find a model (i.e. model error) for which the function error f_{err} reaches a minimum; this process is also known as a minimization problem. However, following the model error optimization, the parameters defining the model are updated accordingly to the estimation methods and algorithms.

1.3.4 Estimation Methods and algorithms

Generally, the mathematical model of a Dynamic System (DS) has the following form:

$$y(t) = f[\mathbf{u}(t), \boldsymbol{\theta}] \tag{1.2}$$

where y is a vector that contains the outputs of the model, $\mathbf{u} = [u_1(t), u_2(t), \dots, u_n(t)]^T$ is a vector of independent variables that has an impact on the model (e.g. gross weight, altitude, speed), $\boldsymbol{\theta} = [\theta_1, \theta_2, \dots, \theta_p]$ is a vector of parameters describing the model, and f is a nonlinear real-valued function (i.e. the functions of components of the parameter vector). The output is uniquely determined by the dependent variables (e.g. aerodynamic forces) at an instant time t, as a vector of their measured/observed values. The finite number of arguments from vector $\boldsymbol{\theta}$ is known as the state of the black box, at time t. These arguments or parameters of $\boldsymbol{\theta}$ are not directly measurable, and therefore they must be estimated from a set of measurements obtained from the real system. These measurements are expected from the outputs of the model plus an additional modeling error.

The linear time-invariant model corrupted by the modeling error vector $\varepsilon(k)$ is presented in the following form:

$$z(k) = y(k) + \varepsilon(k) \tag{1.3}$$

where $z(k)$ is a vector consisting of the measured/observed variables (i.e. the outputs of the dynamic system), k is the discrete time index and $y(k)$ is the vector composed of the outputs

of the mathematical model. These outputs are the parameters' estimates obtained by use of the mathematical model. If the outputs estimated by the physical model become close enough to the outputs measured by the real system, the values of the error vector thus become much smaller.

The objective of an estimation algorithm is to find the sets of parameters estimated (i.e. the vectors of the parameters) θ_i, $i = \{1, \dots, p\}$ that minimize the differences between the measured outputs $z(k)$ and the predicted outputs $y(k)$. An estimation algorithm that solves the minimization problem has a mathematical form (i.e. a numerical optimization) as follows:

$$\boldsymbol{\theta}^* = \arg[min\|z - y\|^2] = \arg\left[min\left(\frac{1}{N-1}\sum_{k=0}^{N}\varepsilon^2(k,\theta)\right)\right] \tag{1.4}$$

where N is the number of available input and output samples, and θ is the vector of the parameters to be estimated, at time instant k (Tomita, Damen and Van Den Hof, 1992). It is known also as Least Squares (LS) error method equation with the property to be "quadratic-in-the-parameters". According to Tomita et al. (Tomita, Damen and Van Den Hof, 1992) the method provides a good prediction model. To estimate the parameters of a linear model, more exactly the airplane's aerodynamic parameters, there are different approaches. The parameter estimation methodology used in this research relies on the linearity and non-linearity of the model under investigation.

1.3.4.1 Least Squares (LS) Method

The Least Squares (LS) method is used in the parameter estimation algorithm to find the best fit to a set of measured data (e.g. the flight data). Therefore, for a special case, when an output of the model $y(k)$ is a linear polynomial as function of $\boldsymbol{\theta}$ (a matrix), which are the parameters to be estimated (multiple inputs), the model's outputs are expressed as follows:

$$\begin{aligned} y(k) &= \theta_1 u_1(k) + \theta_2 u_2(k) + \cdots + \theta_n u_n(k) \\ &= \mathbf{u}^T(k)\boldsymbol{\theta} \end{aligned} \tag{1.5}$$

According to Hamel (Hamel and Jategaonkar, 1996) equation (1.5) is a "direct approach" to airplane parameter estimation for data analysis, and is known as the "equation error method". This linear estimation problem is solved using a deterministic method that is applied for N discrete value points, those for which the measurements $z(k)$ are accessible. Therefore, equation (1.3) can be written as follows:

$$\begin{aligned} z(1) &= \mathbf{u}^T(1)\boldsymbol{\theta} + \varepsilon(1) \\ z(2) &= \mathbf{u}^T(2)\boldsymbol{\theta} + \varepsilon(2) \\ &\vdots \\ z(N) &= \mathbf{u}^T(N)\boldsymbol{\theta} + \varepsilon(N) \end{aligned} \tag{1.6}$$

either in matrix form:

$$\mathbf{z} = \mathbf{M}_{LS}\boldsymbol{\theta} + \boldsymbol{\varepsilon} \tag{1.7}$$

where $\mathbf{z} = [z(1), \dots, z(N)]^T$ is the fixed measurement vector, $\boldsymbol{\varepsilon} = [\varepsilon(1), \dots, \varepsilon(N)]^T$ are the N x 1 vectors, and $\mathbf{M}_{LS}$ is the N x n matrix containing independent variables:

$$\mathbf{M}_{LS} = \begin{bmatrix} u_1(1) & u_2(1) & \cdots & u_n(1) \\ u_1(2) & u_2(2) & \cdots & u_n(2) \\ \vdots & \vdots & \cdots & \vdots \\ u_1(N) & u_2(N) & \cdots & u_n(N) \end{bmatrix} \tag{1.8}$$

By assuming that $\left(\mathbf{M}_{LS}{}^T\mathbf{M}_{LS}\right)$ is invertible, a unique solution of equation (1.4) is given by:

$$\boldsymbol{\theta}^* = (\mathbf{M}_{LS}^T\mathbf{M}_{LS})^{-1}\mathbf{M}_{LS}^T\mathbf{z} = \mathbf{M}_{\boldsymbol{LS}}^{\dagger}\boldsymbol{z} \tag{1.9}$$

where $\mathbf{M}_{\boldsymbol{LS}}^{\dagger}$ is the Moore-Penrose pseudo-inverse of $\mathbf{M}_{LS}$, and $\boldsymbol{\theta}^{*}$ represents the Least Squares solution of the minimization problem expressed by equation (1.4), and which is equivalent to the set of modeling errors (Ghazi et al., 2016). The detailed information about this methodology is presented in Chapter 2.

The Moore-Penrose inverse matrix was named after the two mathematicians who have participated to create this matrix. Moore E.H. developed the matrix for its mathematical research interest, in 1920. Then Penrose R. improved the Moore's matrix in 1955, which has the form used today. These days, the mathematicians have opportunity to construct a unique matrix, as a pseudo-inverse matrix, which solves an inconsistent LS system, and that gives the minimum norm and the closest solution (Ross, 2014). For this reason, this method is a very good alternative, being used for parameter estimation purposes.

The most impressive particularity of the Least Squares (LS) method is that it is a non-iterative method, as it does not require any preliminary information about the investigated system. In addition, the matrix $\mathbf{M}_{LS}$ given by equation (1.8) is non-singular, and it guarantees that a solution is always possible (Ghazi et al., 2016). The popularity of using the LS method to solve inverse problems comes from the fact that the Least-Squares estimates are retrieved easier and with minimal computation. The accuracy of the estimated parameters is a required part of the parameter estimation method.

1.3.4.2 Prediction-Error (PE) Method

The Prediction-Error (PE) method allows the parameters estimation for the non-linear function (i.e. the model) f that minimizes the sum of squared errors between the measured output and the predicted output. The choice of the optimization algorithm depends on the structure of the function f.

The Matlab® Optimization Toolbox™ has many algorithms available, but the Nelder-Mead (NM) algorithm was the selected in this research thesis. This NM technique is a heuristic

search method proposed by John Nelder and Roger Mead in 1965 (Daamen, Buisson and Hoogendoorn, 2014). It is a gradient-free optimization method, and is used since 2004 in the car-following model calibration to develop the model parameter estimates. The NM method, as one of the most widely applied direct search method has the particularity to be used for "nonlinear unconstrained optimization". This nonlinear unconstrained optimization algorithm the considered parameters do not have upper or lower bounds. By a nonlinear optimization we find the "optimal" model's parameters, which give the best fit to the sample data. Known as the "downhill simplex" algorithm (Daamen, Buisson and Hoogendoorn, 2014; Lagarias et al., 1998), this iterative method is based on a minimization routine. The aim of the method is to minimize a scalar-valued nonlinear function of *n* real variables (parameters) starting from an initial value, without any derivative information, but utilizing only the function values. Therefore, the methodology presented in Chapter 2 describes the way to find the initial parameters' of vector $\boldsymbol{\theta}$ that defines the model. The algorithm is designed to converge to a local minimizer, as solution of a non-linear system of equations, and it can be applicable nearly from any crude approximations or starting points (Dennis Jr and Schnabel, 1996). To run this algorithm, we used the *fminsearch* routine, as a Matlab® optimization tool (MathWorks, 2013). This method has the particularity to be iterative, for this reason this initial values of the parameters are very important.

1.3.5 Model Verification/Validation

To verify the estimated model, we used a criterion called the "model predictive capability". To verify the flight-estimated models, we fixed the model parameters to their estimated values, and then the model is run by inputs which are different from those used in the estimation process. The model's responses are then compared with the flight data measurements in order to determine the predictive capabilities of the estimated model.

1.3.6 Physics and Parameters of Flight

The physics of flight and its parameters are given by an atmospheric model, and used as a reference in the interest of creating an aircraft design or trajectory. The atmospheric parameters are used to control engine and aircraft performance, as well as for aircraft design.

1.3.6.1 The International Standard Atmosphere (ISA) model

In 1952, the International Civil Aviation Organization (ICAO) introduced the International Standard Atmospheric (ISA) model (ICAO Document 7488/2). This hypothetical model, viewed as an ideal atmosphere, consists of tables that indicate the parameters for the pressure (p), density (ρ), temperature (T) and the speed of sound (a). These parameters are changing over a range of altitudes during the flight, and these changes must be considered as stated in the literature by Talay (Talay, 1975), Cavcar (Cavcar, 2000), and Botez (Botez, 2006). In this ISA model, the atmosphere is assumed to be free from dust, moisture and water vapour, and in the absence of winds or turbulence, which is not the case in real-life (Talay, 1975). The altitude that needs to be considered is the Mean Sea Level (MSL). This is the reference altitude where the air is clean, dry, and acts as a perfect gas.

The standard pressure (p) at a given altitude is determined based on the following assumptions:

- Temperature is standard;
- Air is an ideal gas, whose pressure is obtained using the equation of state:

$$p = \rho RT \tag{1.10}$$

where R is the real gas constant estimated to 287 J/kg °K or 1716 ft. lb_f/slug °R (Asselin, 1997; Botez, 2006). The above-mentioned atmospheric parameters influence engine/aircraft performance and aircraft design. Their performances can be calculated and compared for various atmospheric conditions sets.

The altitude determined from the measured pressure, known as the pressure altitude (PA), is stated in m/ft or in.

The flight level (FL) represents the altitude expressed in 100's of ft, and is given in the next equation:

$$FL = PA/100 \tag{1.11}$$

The troposphere, the most important layer to aeronautics, is the atmospheric layer considered from the mean sea level (MSL) to 11km or 36,089ft. In the troposphere, the temperature decreases linearly with the altitude, while in the next layer, between 11km to 21km or 70,000ft, called the stratosphere, temperature is constant. Similarly, the speed of sound (a) varies with the temperature. The density and pressure decrease rapidly with altitude.

The variation of these parameters, for each of those atmospheric layers, is described by Asselin (Asselin, 1997) and Botez (Botez, 2006).

In the troposphere, the temperature function of altitude h has the expression given by Asselin in ((Asselin, 1997), page 312):

$$T_h = T_{MSL} + a_{LR}h \tag{1.12}$$

where a_{LR}, the temperature variation coefficient, is a constant whose value is -0.0065°K/m or -0.0035°R/ft, and for which the indices LR denote the "lapse rate".

The pressure as function of altitude h is described by Asselin in ((Asselin, 1997), page 312):

$$p_h = p_{MSL}\left(\frac{T_h}{T_{MSL}}\right)^{(-g/a_{LR}R)} \tag{1.13}$$

where g is the gravitational acceleration (9.8 m/s^2 or 32.174 ft/s^2).

The density as function of altitude h is expressed in the following form from Asselin's book ((Asselin, 1997), page 313).

$$\rho_h = \rho_{MSL}\left(\frac{T_h}{T_{MSL}}\right)^{(-1-g/a_{LR}R)} \tag{1.14}$$

As noted by Botez in (Botez, 2006), in the stratosphere, only the pressure and the density varying, as shown in the next equations:

$$p = p_{0strat}e^{\frac{-g\Delta h_{strat}}{RT_{strat}}} \tag{1.15}$$

$$\rho = \rho_{0strat}\, e^{\frac{-g\Delta h_{strat}}{RT_{strat}}} \tag{1.16}$$

where p_{0strat} and ρ_{0strat} are the pressure and density, respectively, at the initial stratosphere altitude, T_{strat} is the stratosphere temperature that is equal to 216.66°K, or -56.5°C or 390°R, and Δh_{strat} is the measured altitude (Dancila, 2011).

The last parameter of the standard atmosphere model is the Local Speed of Sound (a_h) or the LSS, as given in the following form (Asselin, 1997; Botez, 2006).

$$a_h = \sqrt{\gamma RT} \tag{1.17}$$

where γ, that is the adiabatic constant of an ideal gas, is equal to 1.4.

The ISA model applied to the real atmospheric conditions, is known as (ISA +/–ΔISA), and may compute the engine/aircraft performance at a particular Flight Level FL (AIRBUS, 2002).

The $(+/-\Delta ISA)$ is a parameter that gives the temperature difference with reference to the MSL, that is the standard temperature deviation (ΔISA), and is measured in ℃.

The temperature is an important factor to provide a safe flight. It has a direct impact on aircraft and aircraft flight operations as it affects the engines, avionics, climbs (when does not climb at predicted rate of climb), True Air Speed (TAS) and icing exposure.

1.3.6.2 IAS and TAS Airspeeds, and Mach number

Since its introduction, computerization has become a dominant tendency in Aerospace due to its contribution to the reliability, the improved performances, and not least to reducing the costs of most aircraft installed avionics systems (i.e. FMSs) (Endsley, 1996). This reliance on computerization emphasizes the need to recognize the critical flight parameters that must be monitored, for example by each crew, in terms of airplane position of important reference points and terrain, by comparing its position with the position of other aircraft along with relevant flight parameters. Besides the crew, the operator of air traffic control systems (ATCs) on the ground, as human decision maker, should be experienced to react to a Situation Awareness (SA) level, and to know what needs should be monitored to reach the fastest response. Therefore, even if there are automated aircraft systems, the ATC systems still need to be well understood and supervised by responsible individuals. In his review of commercial aviation accidents, Ensley showed that 88% of these accidents were caused by problems provoked by SA (Endsley, 1996).

The critical flight parameters include the Pressure Altitude (PA), the Vertical Speed (VS) or RoC (Rate of Climb), the Calibrated Air Speed (CAS), the real speed or Indicated Air Speed (IAS), the Mach number (M), the static pressure (p_S), and the relative atmospheric ratios, which consist of their temperatures ratio (θ):

$$\theta = \frac{T_h}{T_{MSL}} \tag{1.18}$$

The pressure ratio (δ) is:

$$\delta = \frac{p_h}{p_{MSL}} \tag{1.19}$$

The density ratio (σ) is:

$$\sigma = \frac{\rho_h}{\rho_{MSL}} \tag{1.20}$$

as described by Botez in (Botez, 2006). The indices h and MSL represent the given flight altitude and the Mean Sea Level standard atmospheric condition.

The air pressure and temperature data are the:

- Total or Pitot pressure(p_T);
- Total or indicated air temperature (TAT or IAT); and
- The static pressure (p_S).

These data are supplied by redundant input sensors (Botez, 2006; Zimmerman and McIntyre, 1991).

The avionics systems in a commercial aircraft usually monitor navigation and flight conditions information by indicating the altitude h, RoC, IAS, and the M. The electronic engine controls, by using the same redundant input sensors, manage the air/fuel ratio that affects the engine.

Aiming to provide a powerful fail-safe system, in 1991 aircraft design engineers combined the airframe's air data and the electronic engine system into a single integrated system. This system had several advantages, such as improved accuracy of the estimated thrust calculated by the FMS. The information received from the input sensors discussed above is displayed on the board of the aircraft.

The total pressure is the pressure measured by a Pitot sensor mounted on the fuselage. It indicates the sum of the local static pressure (p_S), and the impact pressure caused by the relative motion of the aircraft, called the dynamic pressure (q_c), indicated as:

$$q_c = \frac{1}{2}\rho V^2 \tag{1.21}$$

where V is the aircraft velocity at an altitude h. In our case, V is expressed by the TAS that is the True Air Speed of the airplane.

When an aircraft changes its altitude or its FL, a difference in air pressure occurs. The rate of change in transition from one altitude to another in climb/descent, called the rate of climb/descent, is measured in feet per minute (fpm), and is displayed by an instrument called a Vertical Speed Indicator (VSI) or Vertical Velocity Indicator or Variometer.

The IAS abbreviated *KIAS* (Knots Indicated Airspeed) is the aircraft speed that appears on the Airspeed Indicator (AI). The IAS measurements are not corrected from the instrument errors. This airspeed is determined by subtracting the measured total pressure by the Pitot sensor from the atmospheric static pressure measured at a static port. It can be measured in knots (kn) or in nautical miles per hour (nm or nmi).

The CAS (Calibrated Air Speed) abbreviated $KCAS$ (Knots Calibrated Air Speed), represents the IAS corrected from the instrument, the position of the static port and the installation errors.

The input sensor used for the measurements of the total or indicated air temperature (*TAT* or *IAT*) is essential for the Air Data Computer (*ADC*) as a critical part of the air data airframe systems. The *IAT* is a kinetic temperature influenced by the TAS, so that at a low TAS, the *IAT* is considered to be equal to the local room temperature (Zimmerman and McIntyre, 1991).

By definition, the TAS is the corrected CAS for altitude h and non-standard atmosphere (extreme conditions, i.e. hot/cold, tropical/polar temperature profiles). In other words, the TAS also abbreviated *KTAS* (Knots True Air Speed), represents the airspeed of an aircraft relative to the air mass that is used in flight planning in the absence of wind effects.

Under standard atmospheric conditions, at *MSL* and low airspeeds, for incompressible air, the IAS is approximated to the TAS. For different air densities or temperature conditions, the TAS is computed using the next equation:

$$TAS = \sqrt{\left(\frac{2\gamma}{\gamma-1}\right)\left(\frac{p}{\rho}\right)\left(\left[\left(1+\frac{p_0-p}{p}\right)^{\frac{(\gamma-1)}{\gamma}}-1\right]\right)} \tag{1.22}$$

which depends on the static pressure and dynamic pressures given by the Pitot Tube (Asselin, 1997).

The TAS can be also expressed in terms of the pressure and density ratios, as seen in the following equation:

$$TAS = \sqrt{\left(\frac{2\gamma}{\gamma-1}\right)\left(\frac{p_{MSL}}{\rho_{MSL}}\right)\left(\frac{\delta}{\sigma}\right)\left[\left(1+\frac{q_c}{\delta p_{MSL}}\right)^{\frac{(\gamma-1)}{\gamma}}-1\right]} \tag{1.23}$$

Furthermore, the TAS is the airspeed used in the computation of the aircraft performance in cruise regime. Compressibility errors occur due to changes in atmospheric conditions, so that the TAS must be calculated based on the Mach speed or M; otherwise it will not reflect the aircraft performance. The compressibility factor therefore needs to be incorporated into the expression of the Mach number M (Eurocontrol, 2014). Thus, the TAS at a given altitude h is calculated by equation:

$$TAS_h = Ma_h \tag{1.24}$$

given in (Botez, 2006) and (Asselin, 1997), where a_h is the sound speed corresponding to the TAS_h, and M is the Mach number. The Machmeter is a flight instrument used to indicate the Mach number (M). The measurements are taken via an aircraft's pitot-static system, also considered as the airspeed indicator sensor.

1.3.7 Aero-Propulsive Model Parameters

The Aero-Propulsive Model (APM) was defined in the beginning of this chapter, together with the expectations from the research in this thesis. A short parameters description related to the aircraft geometry and of the forces acting on the airplane is explained in this section. More detailed information regarding these forces and parameters are presented and discussed in Chapter 2, along with the APM modeling methodology.

Aerodynamics and propulsion are two main fields in Aerospace Engineering associated with a new conceptual aircraft design approach. These fields are also part of Aircraft Design discipline, as Corke mentioned in his book (Corke, 2003). The impact of each of these two fields on APM modeling is based on their optimum parameters that control the "size, shape, weight and performance of an aircraft", as stated by Corke ((Corke, 2003), p6).

The wing aspect ratio (AR) is a feature of the main lifting surface used to determine wing's performance of an airplane. The AR is also a basic parameter of airplane wing design expressed as follows:

$$AR = \frac{b^2}{S} \tag{1.25}$$

where b is the wingspan and S is the reference wing area. This characteristic of the wing design indicates how thin and long a wing can be made from tip to tip (NASA, 2015).

The airfoil thickness ratio $\left(\frac{t}{c}\right)$, a geometrical characteristic of the airfoil profile, is defined as the ratio between the wing thickness t and the wing chord c (Cheng and Smith, 1982).

The choice of a low or high wing aspect ratio depends on the flight profile or flight performances for which the aircraft is designed. In other words, an aircraft high AR is

equivalent to an airplane with long and thin wings, expensive from the manufacturing point of view, but that produces more lift. More lift allows for an efficient cruise, offers better stability but less manoeuvrability, and creates much less induced drag, leading to lower fuel consumption. A low AR is more appropriate to a commercial transport airplane because of its structural weight and fuel-carrying capabilities (Blake, 2009). A combat aircraft combines a low AR, with low wing loading to achieve a high degree of manoeuvrability, implying higher fuel consumption and costs. In order to fulfill the customer requirements, a compromise is needed to achieve a safely operating aircraft design.

The leading edge sweep angle (Λ_{LE}) is used to achieve the wing critical M, before the aircraft reaches a_h, with the aim to avoid the occurrence of shock waves. The Λ_{LE}, the AR, the airfoil thickness ratio $\left(\frac{t}{c}\right)$, and the wing weight, will all have an impact on the location of the fuel storage and landing gear retraction in terms of aerodynamical and structural considerations. To achieve an optimum design, trade-offs are required. Most commercial airliners, at transonic M, are designed with sweep angles of approximately 30 degrees (Corke, 2003).

As the principle of flight requires to keep the airplane to a certain height above the ground, some specific forces must sustain it in the air. Four major forces are involved in the airplane flight performances, such as the lift force (L), the weight (W) or the gross weight (GW), the thrust (T), and the drag (D) that is caused by friction with the air mass. In other words, because of these forces, an airplane is moving through the air mass. The engine (propeller or power plant) produces the thrust. In other words, it gives a propulsion force, which opposes to the drag force created by the air resistance. This friction force is influenced by the shape of airfoil, the density ρ of the air mass, and by the TAS of the aircraft.

1.4 The Numerical Database Concept and Research Problem Statement

The concept of an aircraft numerical database will continue to be developed and adapted correspondingly to the research problem of this thesis. The objectives and assumptions of the problem statement are defined at the end of this subsection.
The FMS, an airborne device, is designed to compute the optimal profile based on trajectory optimization function in order to minimize the flight cost, that is given in terms of flight time and/or total fuel burnt. One solution would be to solve the equations of motion. These equations of motion for an aircraft are non-linear. But, the FMS's architecture is not able to solve a set of non-linear equations, due to its complexity, therefore a linearization it is imposed.

Another way to solve this problem would be to build a numerical model, which has to describe the behaviour of an aircraft during a particular flight phase (e.g. climb, cruise). Therefore, this model must be simplified, such that to be able to be performed in the form of a numerical database as shown by Vincent et al. (Vincent et al., 2012), Murrietta (Murrieta Mendoza, 2013), and Ghazi et al. (Ghazi, Botez and Tudor, 2015).

In order to create this numerical database, we need to have access to flight data of the airplane, which later will be used in the model validation process. The database used to build this aero-propulsive model for a commercial aircraft (including business jet) is provided in the form of "text" files (Murrieta Mendoza, 2013). These ". csv" (comma separated values) files are converted into ". mat" format, and adapted at the LARCASE by PhD student Dancila Bogdan, in order to be utilized them by MATLAB environment, highly used in trajectory optimization techniques. Therefore, using this flight data, aero-propulsive models were developed for the climb and cruise regime, in order to create a numerical database for a commercial airplane. In this research thesis, we assumed that all the flight data were accurately recorded.

In Figure 1.4, as a symbolic representation, an aero-propulsive model is compared to a black box, which has numerous inputs and outputs. The selection of the inputs and the outputs depends on the flight conditions or flight regimes (e.g. climb, cruise) given for an aircraft configuration.

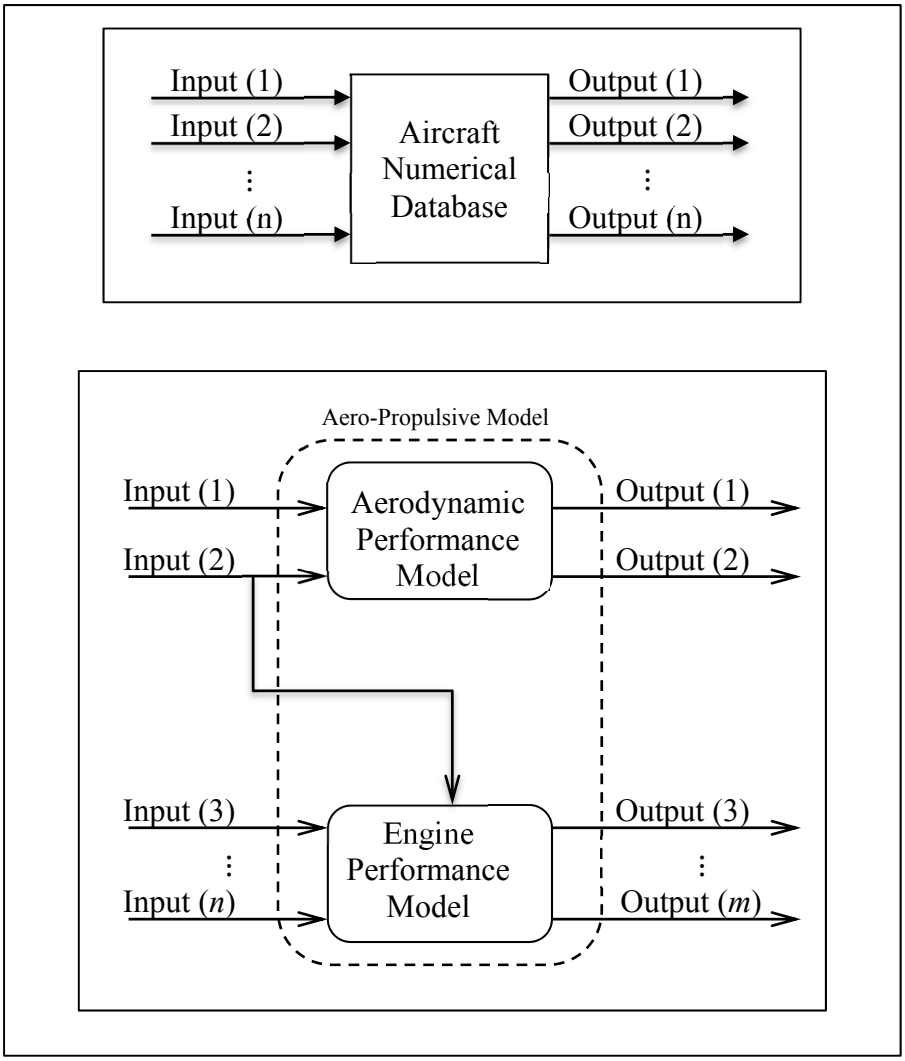

Figure 1.4 Aircraft Numerical Database and
Aero - Propulsive Model (APM) Inputs and Outputs

According to some studies in the flight trajectory optimization problems (Murrieta-Mendoza and Botez, 2014; Patrón et al., 2013), the aircraft's behaviour is affected by the main parameters such as the center of gravity position, the speed, the weight or the gross weight,

the ISA temperature deviation, and the altitude, as multiple inputs, while the outputs are basically the drag and thrust forces.

Therefore, an aero-propulsive model (APM) can be expressed in a mathematical form by the next equation:

$$[D, T, T_{sfc}] = \mathbf{f}(x_{cg}, IAS, GW, \Delta ISA, h) \tag{1.26}$$

where D represents the drag force, T the engine thrust force, T_{sfc} the engine specific fuel consumption coefficient, as unknown parameters regarding propeller data, and x_{cg} is the center of gravity position, IAS is the indicated airspeed, GW is the gross weight, ΔISA is the ISA temperature deviation, h is the geometric altitude, as inputs. The function $\mathbf{f}: \mathbb{R}^5 \rightarrow \mathbb{R}^3$ is the mathematical representation of aircraft performance.

In this thesis, an aero-propulsive model is built for a commercial aircraft, by creating a numerical database in order to improve its performance in both the climb and cruise regimes.

The main objective can be summarized as:

"Identifying an aero-propulsive model of a commercial aircraft from flight data, and building a numerical database to predict the performances in climb and cruise regimes."

To solve this research problem, the following two sub-problems are imposed:

1. "Identifying an aero-propulsive model from flight data in the climb and in the cruise regime" by applying system identification methods; and
2. "Creating a numerical database for a commercial aircraft by employing the identified aero-propulsive model."

Additionally, to simplify the research model the following limitations are assumed:

- Still air environment (wind-free);
- Operational engines; and

- Climb and Cruise at a constant $IAS/Mach$.

The target of this research is to find a methodology to obtain an aero-propulsive function **f** for each flight's regime. This target can be achieved by using system identification methods as presented in the next chapter.

CHAPTER 2

AIRCRAFT IDENTIFICATION AND METHODOLOGY

The main purpose of this thesis is to give the most appropriate solution to research questions that concern a new identification procedure for two mathematical models that best predict a commercial airplane in climb and cruise phases. This new methodology based on the system identification theory, the aero-propulsive model concept and the parameter estimation techniques create the aero-propulsive model (APM) from Aircraft Flight Manual or the Flight Tests data without knowledge of prior propulsion data.

2.1 Aircraft mathematical Climb Model – IAS/MACH constant

Basically, the flight profile for a commercial aircraft consists of take-off, climb, cruise, descent and landing segments. This research thesis, as already mentioned, aims to build an aero-propulsive model only for climb and cruise regimes, which are essential for the vertical trajectory optimization of commercial airplanes (Air Traffic Management applications).

The complexity and the difficulty of this research problem proposed compel us to restrict the studied domain by applying a set of assumptions. These assumptions are fundamental to simplify the approach to the problem, even if it must be solved with lack of data (e.g. no engine data). However, the solution of the problem in question is an approximation of the real system (i.e. the aircraft) under this research. The accuracy level relies on both the assumptions and the proposed methodology. Therefore, for an airplane, the coordinate frame, the assumptions, the acting forces and the other essential parameters in the climbing flight are presented in Figure 2.1 below:

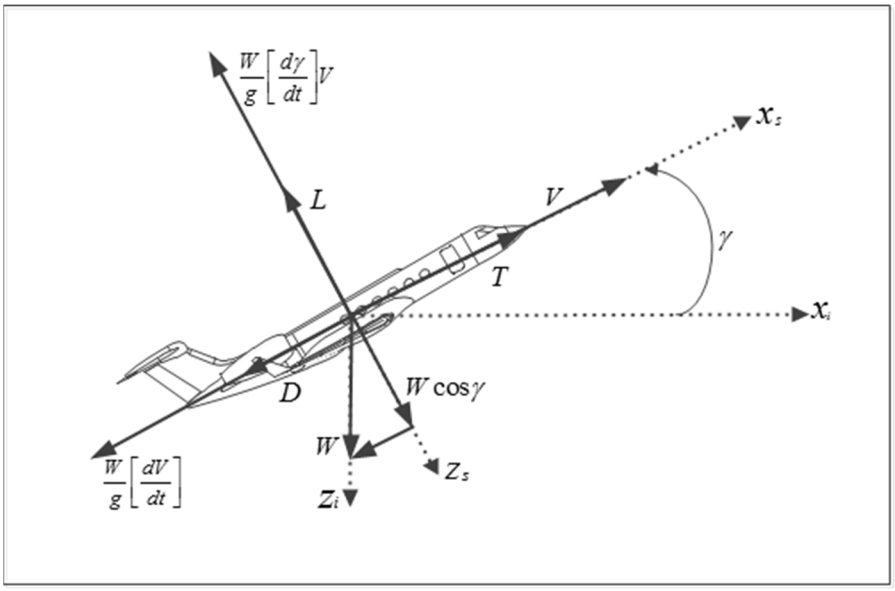

Figure 2.1 The acting forces in the climb flight

The (xz) plane is the vertical plane (plane perpendicular on the surface of the Earth or ground) with the x axis oriented in the direction of motion and the z axis pointing Earthward (Figure 2.1). The (x_i, z_i), and (x_s, z_s) are the inertial and stability axes, T is the propeller thrust force, V is the TAS (aircraft true airspeed or velocity vector), L is the lift force (perpendicular to the velocity vector V), D is the drag force (parallel to the velocity vector V), W is the aircraft weight or gross weight, g is the acceleration due to gravity, α is aircraft angle of attack and γ is the flight path angle. The airplane used in most of the figures is a Gulfstream G500 (Kaboldy, 2013).

To keep an airplane flying in the air, three essential features must be guaranteed: the lift provided by the wings, its system of propulsion and stability. The aircraft is assumed to be a variable-mass rigid body (Hull, 2007). For an airplane motion, the Earth is an approximate inertial reference frame (in order to obtain small errors in the analyses), and for thus the Newton's laws can be applied. Based on the Newton's second law:

$$\frac{W}{g}\mathbf{a} = \sum \boldsymbol{F} \tag{2.1}$$

where **a** is the airplane acceleration relative to the inertial frame (Earth or ground) that is mathematically expressed in the form:

$$\mathbf{a} = \frac{d\mathrm{V}}{dt} \tag{2.2}$$

and $\sum \boldsymbol{F}$ is the net force applied to the airplane.

There are four main forces acting at the center of gravity of an airplane: lift, drag, thrust and weight (using point-mass considerations). In aircraft flight mechanics, the lift and drag forces, as aerodynamic forces, according to several references (Stevens and Lewis, 2003), and (Nelson, 1998), are expressed as:

$$L = q_c S C_L \tag{2.3}$$

and

$$D = q_c S C_D \tag{2.4}$$

where C_L and C_D represent the lift and drag coefficients. The wing lift coefficient C_L is expressed by the well-known formula:

$$C_L = \frac{L}{S q_c} \tag{2.5}$$

The aerodynamic drag coefficient C_D for the entire aircraft is also known as the drag polar, and is expressed as follows:

$$C_D = C_{D0} + \frac{C_L^2}{\pi A R e} \tag{2.6}$$

The dimensionless C_{D0} is the zero-lift drag coefficient or the minimum drag coefficient C_{Dmin}. The second term of the right hand side equation (2.6) is the representation of the induced drag coefficient C_{Di}, in which e is the aerodynamic efficiency or the airplane efficiency factor. This factor is also known as Oswald efficiency coefficient, and is usually less than 1.

During climb, the motion of an airplane along its stability axes is described by the kinetic equations, as shown in Figure 2.1:

$$\frac{W}{g}\left[\frac{d\mathrm{V}}{dt}\right] = T\cos\alpha - D - W\sin\gamma \tag{2.7}$$

$$\frac{W}{g}\left[\frac{d\gamma}{dt}\right]\mathrm{V} = -T\sin\alpha - L + W\cos\gamma \tag{2.8}$$

These two equations describe the complete longitudinal motion of the airplane.

The parameter estimation algorithm must solve the set of equations (2.7) and (2.8). However, because their arrangement is non-linear, the parameter estimation algorithm encounters difficulties. In order to effectively describe a flight phase in the climb or cruise, the system has to be repositioned and adapted correspondingly. An aircraft mathematical model that is less complicated or much simpler must be developed instead of equations' set (2.7) and (2.8). More assumptions must be added; therefore by considering that the angle of attack α is small, thus approximately zero, the following statement can be made:

$$\alpha \approx 0 \Rightarrow \begin{cases} \sin\alpha \approx 0 \\ \cos\alpha \approx 1 \end{cases} \tag{2.9}$$

and therefore α from equation (2.9) is replaced in the equations (2.7) and (2.8). It should be mentioned that the angle of attack α was not shown in Figure 2.1, as it was small.

One of the main aims of this research is that is directed towards climb performances improvement of a commercial aircraft. In the climb regime, the climb performance consists of the rate of climb (RoC), an unknown parameter, which thus should be part of the above motion equations. In the vertical plane, an aircraft in climb is described in scalar form by the next two equations through which the following performance parameters are expressed by equations (2.10) and (2.11):

$$\dot{x} = GS = V\cos\gamma \tag{2.10}$$

where $\dot{x}$ is the ground speed (GS) or the horizontal velocity, V is the local velocity (TAS), and γ is the flight path angle. In equation (2.11) the vertical velocity is represented as:

$$\dot{h} = V\underbrace{\sin\gamma}_{\frac{dh}{H_{dist}}} = \frac{dh}{dt} \tag{2.11}$$

where $\dot{h}$ is also known in the literature under the name of the rate of climb (RoC), and ($\sin\gamma$) represents the climb gradient. By definition, the climb gradient is the ratio between the vertical distance (dh) and horizontal distance (H_{Dist}) traveled by an aircraft (Corke, 2003). The vertical velocity and the climb gradient are illustrated in Figure 2.2, also known as the velocity triangle.

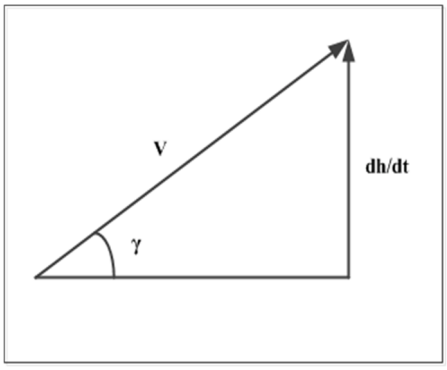

Figure 2.2 Velocity triangle

To solve the first sub-problem of this research we study the climb performance, represented by the rate of climb of the DS (i.e. aircraft). The rate of climb is computed by means of some mathematical calculation steps as follows. In the first step, the assumptions of equation (2.9) are applied to equation (2.7) that becomes:

$$\frac{T-D}{W} = \overbrace{\sin\gamma}^{\frac{\dot{h}}{V}} + \frac{1}{g}\underbrace{\left[\frac{d\mathrm{V}}{dt}\right]}_{\frac{d\mathrm{V}}{dh}\frac{dh}{dt}} \tag{2.12}$$

Thereafter, employing the chain rule:

$$\frac{d\mathrm{V}}{dt} = \frac{d\mathrm{V}}{dh}\frac{dh}{dt} \tag{2.13}$$

and by replacing also the climb gradient ($\sin\gamma$) from equation (2.11) in equation (2.12), we finally obtain an expression of the climb performance. This form of the equation of motion describes the rate of climb $\dot{h}$, as follows:

$$\frac{T-D}{W} = \left(1 + \frac{V}{g}\frac{d\mathrm{V}}{dh}\right)\frac{\dot{h}}{V} \tag{2.14}$$

and in which the term in the brackets:

$$\left(1 + \frac{V}{g}\frac{d\mathrm{V}}{dh}\right) = AF \tag{2.15}$$

is known as the acceleration factor (AF). The AF is a correction taken into consideration when climbing at constant TAS, and it cannot be neglected at high altitudes (Blake, 2009). Therefore, by replacing equation (2.15) in equation (2.14), the rate of climb $\dot{h}$ formula is obtained:

$$\dot{h} = \frac{\left(\frac{T-D}{W}\right)V}{AF} \tag{2.16}$$

This equation (2.16) is very important, because is the expression that reveals the climb performance relative to aero-propulsive forces. As indicated in equation (2.16), for a specific airplane with known rate of climb (as the airplane's climb performance), the difference $(T - D)$ between the two aero-propulsive forces T and D can be calculated. The other way around, by knowing the thrust T and drag D forces, their difference $(T - D)$ can be calculated, and then the climb performance can be estimated as well. Therefore, the aerodynamic forces must be predicted using the estimation techniques as presented below.

2.1.1 Aerodynamics: Lift and Drag Forces Estimation

The lift force, as an aerodynamic parameter, can be described by applying equation (2.9) to the kinetic equation of motion presented in equation (2.8), so that:

$$L = W\cos\gamma - \frac{W}{g}\left[\frac{d\gamma}{dt}\right]\mathrm{V} \xrightarrow{\frac{d\gamma}{dt}\to 0} L = W\cos\gamma \tag{2.17}$$

For a small flight path angle, the acceleration term $\left(\frac{d\gamma}{dt}\right) = \dot{\gamma}$ is neglected for quasi-steady flight. However, the lift force L is also represented as a function of the atmospheric factors as shown in equation (2.3).

Therefore, by replacing equation (2.5) for the quasi-steady assumption into equation (2.17), the lift coefficient can be expressed in the next equation:

$$C_L = \frac{W\cos\gamma}{Sq_c} \tag{2.18}$$

The drag force D cannot be estimated exactly from the set of the equations of motion (2.7) and (2.8) because the thrust force T is also an unknown variable of the parameter estimation

problem. In contrast to the computation of the lift force L, which is using equation (2.8), the drag force D will be estimated from equation (2.4). It is worth noticing that the drag polar equation (2.6) is usually only utilized for airplane wing. However, assuming that the lift and drag forces are predominantly performed by the airplane wing, this equation can be extended to the entire airplane. Also, equation (2.6) is given by Corke (Corke, 2003) as it shows the wing loading effect on climb rate. In the drag polar expression, another unknown parameter to our research problem, which has to be estimated, is the Oswald efficiency factor. The Oswald efficiency factor for an aircraft wing leading edge greater than 30 degrees is given by an empirical formula taken from Raymer (Raymer, 1992) or Brandt (Brandt, 2004).

$$e = 4.61(1 - 0.045AR^{0.68})[\cos(\Lambda_{LE})]^{0.15} - 3.1 \tag{2.19}$$

According to Gudmundsson, the Oswald span efficiency e, as shown by the drag polar formula in equation (2.6), is a vital parameter for the lift-induced drag (drag due to lift) in the airplane identification process (Gudmundsson, 2013). It was named after W. Bailey Oswald, who labelled it the *airplane efficiency factor* in the NACA TR-408 report (1933) (Gudmundsson, 2013). Later, Raymer (Raymer, 1992) and Brandt (Brandt, 2004) recommended equation (2.19) as "e" an empirical estimation formula for swept wings. Snorri G. has used this equation as a statistical expression to estimate the airplane efficiency factor (Gudmundsson, 2013). The empirical methods are used in the preliminary design phase of the aircraft design process. The two parameters, C_{D0} and e, as unknown parameters, in the final evaluation phase of an aircraft‘s design must be optimized to better estimate the airplane’s performances using parameter estimation methods.

The total drag, for subsonic climb, consists of the base drag, characterized by C_{D0}, and the lift-induced drag. By replacing C_D given by equation (2.6) into equation (2.4), the total drag D is obtained:

$$D = q_c S C_{D0} + q_c S \left(\frac{C_L^2}{\pi ARe}\right) \tag{2.20}$$

This term $\left(\frac{1}{\pi ARe}\right)$ describes the induced drag parameter or the drag due to lift factor $\boldsymbol{k}$.

$$\boldsymbol{k} = \frac{1}{\pi ARe} \tag{2.21}$$

where AR is known as the wing aspect ratio and e is the Oswald efficiency factor.

The aero-propulsive model must also be investigated from the aspect of propulsion performances. It should be recalled, that the airplane propulsion data are unavailable.

2.1.2 Propulsion: Engine Thrust and Specific Fuel Consumption Estimation

The second part of an aero-propulsive model involves the engine performance. The thrust force is expressed from the set of equations of motion. The drag force is calculated to obtain an initial value of it. This is also the starting point corresponding for the calculation of this unknown force that is a very important initial value in the parameter estimation algorithm realized.

$$T = \frac{W}{g}\left[\frac{d\mathrm{V}}{dt}\right] + D + W\sin\gamma \tag{2.22}$$

Equation (2.22) is rearranged by applying further the chain rule to the acceleration term $\left[\frac{d\mathrm{V}}{dt}\right]$.

$$\frac{d\mathrm{V}}{dt} = \frac{d\mathrm{V}}{dh}\frac{dh}{dt} \tag{2.23}$$

Then equation (2.23) is replaced into equation (2.22), which becomes:

$$T = D + W\frac{1}{g}\left[\frac{d\mathrm{V}}{dh}\frac{dh}{dt}\right] + W\sin\gamma \tag{2.24}$$

The thrust equation (2.24) can be written also under the following form:

$$T = D + W\underbrace{\left(1 + \frac{V}{g}\left[\frac{dV}{dh}\right]\right)}_{AF}\sin\gamma \tag{2.25}$$

in which we recognize the acceleration factor AF as presented in equation (2.15).
The thrust formula can then be represented in a more compact form by use of equation (2.11) in equation (2.25) that becomes:

$$T = D + W(AF)\frac{\dot{h}}{V} \tag{2.26}$$

Equation (2.26) is further used to obtain the first initialization of the engine thrust force. It should be recalled that we are building this mathematical model with no engine data provided. The thrust force and the thrust specific fuel coefficient are the two engine performance parameters. Both are unknown parameters and dependent functions of the altitude. The true airspeed V as well as the altitude h have an impact on the thrust T as indicated below:

$$T = T(h, V) \tag{2.27}$$

By definition, the thrust specific fuel consumption (SFC or T_{sfc}) represents the effect of the altitude or of the pressure altitude (ft) on engine performance as estimated by:

$$T_{sfc} = \frac{\dot{w}_f}{T} \tag{2.28}$$

where $\dot{w}_f$ represents the weight of fuel consumed in kg or pound mass per hour for a given thrust force T, or the engine fuel flow $(\dot{w}_f)$ in the cruise regime, formulated as:

$$\dot{w}_f = \frac{dFB}{dt} = \frac{\Delta FB}{\Delta t} \tag{2.29}$$

in which FB is the fuel burnt. It should be also noted that the differentials could be approximated as algebraic quantities.

The thrust force depends on the altitude, and therefore, the thrust specific fuel consumption can be expressed as follows:

$$T_{sfc} = T_{sfc}(h) \tag{2.30}$$

The model's parameters that were calculated based on the AFM data or the flight data represent the first estimates of the described physical model. They are the initial values (i.e. initial guesses or initial approximation) used by the parameter estimation algorithm.

2.1.3 Estimation Methods and Algorithms

CMC Electronics Esterline provided the flight data of two commercial aircrafts (Aircraft A and B) for this research thesis. The numerical database of an aircraft in climb has inputs and outputs that may differ for different aircraft. For this reason, the numerical database has been formatted from Table 2.2, according to the general structure presented in Table 2.1.

Table 2.1 Sample data for a commercial aircraft

$GW = 90{,}000\ kg \parallel x_{cg} = 27\% \parallel IAS = 220\ kts \parallel \Delta IAS = 0°$				
Altitude (ft)	*Fuel Burn* (Kg)	*Horizontal Distance* (nmi)		*Fuel Flow* (Kg/h)
0	0	0		–
1,000	15.00	0.73		–
2,000	69.00	1.64		–
3,000	130.0	2.05		1010
⋮	⋮	⋮		⋮
23,000	789.0	25.4		1075
24,000	894.0	25.9		1080
25,000	953.0	26.4		1094

The parameters values presented into Table 2.1 are not the real values of a commercial aircraft, due to confidentiality concerns. However, this representation of the aircraft performance is very similar to those found in any aircraft flight manual (AFM). The methodology developed in this thesis can therefore be extended and applied to any commercial aircraft.

The available numerical database for the Aircrafts A and B can be observed in Table 2.2, which contains all the flight tests (e.g. 2184 flight tests of aircraft A). The number from the example represents the combination of all the flight data inputs for the climb phase that were formatted, when the aircraft flies with the airspeeds IAS, as were presented by Table 2.1.

Table 2.2 Inputs and Outputs Flight data of the Aircrafts A and B in the Climb phase

Flight data of Phase	**Inputs Aircraft**		**Outputs Aircraft**	
	A	**B**	**A**	**B**
Climb	Center of gravity (3) Gross weight (8) IAS (7) ISA deviation (13) Altitude (N/A)	Center of gravity (-) Gross weight (16) IAS (12) ISA deviation (13) Altitude (N/A)	Fuel Burn Horizontal Distance	Fuel Burn Horizontal Distance

In this research, some of the flight tests provided are used to identify the physical model and the others to check or validate the resulting model. Therefore, the flight tests were divided into the following two categories: identification and validation.

The first category was targeted to identify the aero-propulsive model, while the second category was used to validate the estimated model. It should be emphasized that even though one of the aims is to minimize the number of required flight tests, their selection corresponding of each flight category must be carefully done.

2.1.3.1 Model Identification Process

The proposed methodology consists of a climb model identification process, which allows estimating of three parameters (D, T, T_{sfc}) that define the aero-propulsive model.

In order to estimate a combination of the aero-propulsive forces, which best predicts the rate of climb described by equation (2.16) for a specific flight configuration, we selected among optimization available algorithms in the Matlab® Optimization Toolbox™, the Nelder-Mead algorithm. This algorithm known also as the *simplex search* algorithm (or downhill simplex method) is an iterative method. For this reason, it is critical to know how to choose correctly the initial values of these parameters. Therefore, it is essential in order to start this algorithm to find a vector containing initial values for every parameter. The model identification process can be structured in the following steps:

1. Flight parameters estimation,
2. Propulsion initial approximations,
3. The *simplex search* algorithm execution $(C_{D0}, e, T)_{min}$,
4. The thrust specific fuel consumption coefficient estimation.

The identification process begins with the flight parameters estimation, through which the aircraft aerodynamic and propulsion parameters are calculated first, based on the aircraft flight manual's data or the given flight data. In the flight data of an Aircraft A, which were presented in Table 2.1, by the discrete values, the altitude h has been partitioned into N sub-segments at each $\Delta h = 1000$ ft, as illustrated in Figure 2.3.

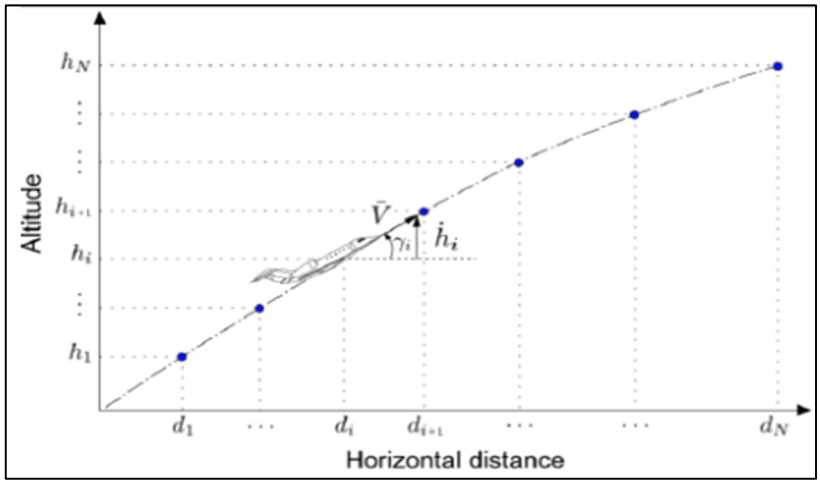

Figure 2.3 The trajectory of an aircraft

with $i \in [\![1, N]\!]$, and where γ_i is the flight path angle, $\bar{V}$ the average true airspeed ($\overline{TAS}$), h_i represent the altitude (ft), H^i_{Dist} the horizontal distance traveled d_i (nmi), and $\dot{h}_i$ is the rate of climb related to a position i.

The estimation algorithm code was created and studied for two cases regarding the speed from the available flight data: in the first case, the speed is given as the Indicated Air Speed (IAS), and in the other case, the speed is given as Mach number (M).
The readings from the speed indicator are measured in knots indicated airspeed (KIAS) or nm/h. However, the true airspeed (TAS) must be used in the algorithms, which is why the correction is needed. The TAS can also be calculated by increasing the IAS with 2% for each 1000ft of altitude. It should be mentioned that all of the measurement units of the variables and parameters used in the estimation algorithm's code are British and American Engineering (AE) units. Also, the mean true airspeed $\overline{TAS}$, measured in knots or nm/h or KTAS, refers to the mean speed used by the estimated algorithm's codes.

The estimation algorithm code starts by computing the aircraft true airspeed V or TAS, and the Mach number from the given indicated airspeed IAS based on the speed conversion function *IAS_to_TAS* for each sub-segment. This function was created at LARCASE by Ghazi Georges PhD student, but was applied in the International System Units (SI).

Therefore, the function was adapted for the British units in order to work within the developed algorithms of this thesis. The conversion function consists of a parameterized lapse rate atmosphere model to compute the pressure and the speed of sound for a given altitude and temperature deviation.

In order to compute the climb performance for one configuration of the aircraft, the estimation procedure first has to calculate the climb gradient (c_{grad}) or $(\sin\gamma)$. The flight path angle γ_i was estimated using Euler method for each sub-segment as shown in Figure 2.3 and in the next equation:

$$\gamma_{\mathrm{i}} = \arctan\left[\frac{\Delta h_i}{\Delta H^i_{Dist}}\right] = \arctan\left[\frac{h_i - h_{i-1}}{d_i - d_{i-1}}\right] \tag{2.31}$$

where Δh_i is the difference between two consecutive altitudes, and ΔH^i_{Dist} is the distance travelled by the aircraft during the i^{th} sub-segment. Thereafter, the time to climb t^i_c between two consecutive altitudes can also be calculated using the Euler method as in the equation below. The Δt^i_c is a function of the mean true airspeed ($\overline{TAS}$), as follows:

$$\begin{aligned} t^i_c &= t^{i-1}_c + \frac{h_i - h_{i-1}}{\overline{TAS} \times \sin\gamma_i}, \\ \Delta t_c &= \frac{\Delta H^i_{Dist}}{\overline{TAS} \times \sin\gamma_i} = \frac{\Delta h}{\overline{TAS} \times \sin\gamma_i} = \frac{\Delta h}{RoC} \end{aligned} \tag{2.32}$$

in which RoC_i is the rate of climb corresponding to the Δt^i_c. The Δt^i_c represents the time to climb for each sub-segment, and is measured in minutes (min).

During a flight, an aircraft is also characterized by its fuel consumption, the last but not the least as importance of its flight performance. The average engine fuel flow $\dot{w}_f$, as shown in equation (2.29) is determined directly from the flight data, along each sub-segment, with respect to its time to climb.

The climb gradient (c_{grad}) expression is thus presented below, as a dimensionless parameter.

$$c_{grad} = \frac{\Delta h_i}{\Delta H^i_{Dist}} = sin(\gamma) = \frac{\dot{h}}{\overline{TAS}} \tag{2.33}$$

Now, all the information required to converge to the rate of climb (RoC), measured in ft/min, is assembled. The RoC is a function of the $\overline{TAS}$ and the c_{grad}, and can be expressed by:

$$RoC_{data} = RoC_{data}(\overline{TAS}, c_{grad}) \tag{2.34}$$

or from Figure 2.3, and also from equation (2.33):

$$\dot{h} = RoC_{data} = \overline{TAS} \times c_{grad} \tag{2.35}$$

This method of computing the rate of climb is based on the aircraft flight manual (AFM) data or the given flight data.

In order to reach the first approximation of rate of climb, the first estimates of the lift, the drag, and the thrust forces have to be firstly calculated.

The dynamic pressure q_c of the compressible free stream air is therefore expressed as a function of the density altitude ρ_h and the true airspeed $\overline{TAS}$, and is expressed as:

$$q_c = q_c(\rho_h, \overline{TAS}) \tag{2.36}$$

The q_c is measured in lbf/ft^2 or slug/(ft s^2) in the American Engineering (AE) unit system. However, the q_c is calculated using equation (1.21). The dynamic pressure is the parameter used in computing the lift force, which is measured in lb$_f$ or slug ft/s^2.

The lift force is function of the given aircraft gross weight (GW), measured in kg, and the fuel burn (FB), measured in kg. It is expressed in the mathematical form:

$$L = L\,(GW, FB) \tag{2.37}$$

and is computed within the estimated algorithm's code, as follows

$$L = W\cos\gamma \xrightarrow{small\,(\gamma)} L = g \times (GW - FB_{data}) \tag{2.38}$$

As described by the above equation (2.5), dimensionless lift coefficient C_L could also be expressed as function of the lift force L, the dynamic pressure q_c and the aircraft wing area S, as follows:

$$C_L = C_L(L, q_c, S) \tag{2.39}$$

Another dimensionless aerodynamic coefficient is C_D. It is function of the C_L at low subsonic speeds (Torenbeek, 1995) and could be also expressed as follows:

$$C_D = C_D\,(C_L) \tag{2.40}$$

The C_{D0} is assumed to be within the range of (0.01, 0.05) (Brandt, 2004). In this study, C_{D0} is treated as representative for the entire aircraft body even if it is only assigned to the wing area. However, the zero-lift drag coefficient C_{D0} is initialized by the nominal value of 0.03, and the empirical Oswald efficiency factor e is calculated based on equation (2.19).

The induced drag parameter $\boldsymbol{k}$ is then calculated using equation (2.21). The drag-due-to lift factor is dimensionless. This parameter is necessary for the drag polar estimation as indicated in equation (2.6). The predicted drag force D, measured in lbf or slug ft/s^2, can now be computed by applying equation (2.20). The estimated thrust is computed with equation (2.26), in which the acceleration factor AF is computed with equation (2.15). The both variations of velocity dV, expressed as ΔTAS, and of the Δh are used in the calculus of the acceleration factor AF, as well as of the thrust force T.

The thrust force T is approximated using equation (2.26) in which the rate of climb (RoC_{data}) is computed by applying equation (2.35). The difference between the thrust and the drag ($T - D$) forces is finally calculated. In order to estimate the rate of climb was applied equation (2.16).

An optimization routine was used to determine the unique local minima (i.e. the initial guesses) of the unknown parameters (C_{D0}, e, T). It is always applied a step ahead of the pre-estimation or the first prediction of the model's parameters $\left(T_{sfc}, (T - D)\right)$.

The optimal rate of climb $\widehat{RoC}$ depends on the following three unknown parameters C_{D0}, e, and T as shown by equation (2.41):

$$\widehat{RoC}(C_{D0}, e, T) = \frac{\left[\frac{T - D(C_{D0}, e)}{GW}\right] V}{AF} \tag{2.41}$$

In other words, the optimal of these parameters is computed using the Least Squares (LS) technique, by minimizing the sum of squared errors. Thus, the model's error function between the rate of climb from the flight data (measured) and the predicted rate of climb is expressed as:

$$f_{err} = \sum_{1}^{N} \left(\underbrace{RoC_{data}}_{measured} - \underbrace{\widehat{RoC}}_{predicted} \right)^2 \tag{2.42}$$

The model error f_{err}, also known as the residuals, was illustrated in the block diagram of Figure 1.3 and expressed in general terms in equation (1.1).

A minimization routine based on the Nelder-Mead (NM) *simplex search* algorithm (Lagarias et al., 1998) was used to adapt the minimum drag coefficient C_{D0}^{min}, the Oswald efficiency factor e_{min}, and the thrust T_{min} in order to minimize the errors f_{err} between the estimated

rate of climb $\widehat{RoC}$ obtained with equation (2.16) and the computed rate of climb RoC_{data} from the AFM data with equation (2.35).

The function *fminsearch* is applied to this optimization routine. This MATLAB function based on the NM method finds the solution to the problem of Least Squares (LS). It is designed to converge to a local minimizer, as the solution of a non-linear system of equations, and it can be applicable nearly from any crude approximations or starting points (Dennis Jr and Schnabel, 1996). The optimal values of the $(C_{D0}, e, T)_{min}$ are helping to minimize the modelling errors. The proposed steps of the optimization routine are described in the flow chart of Figure 2.4.

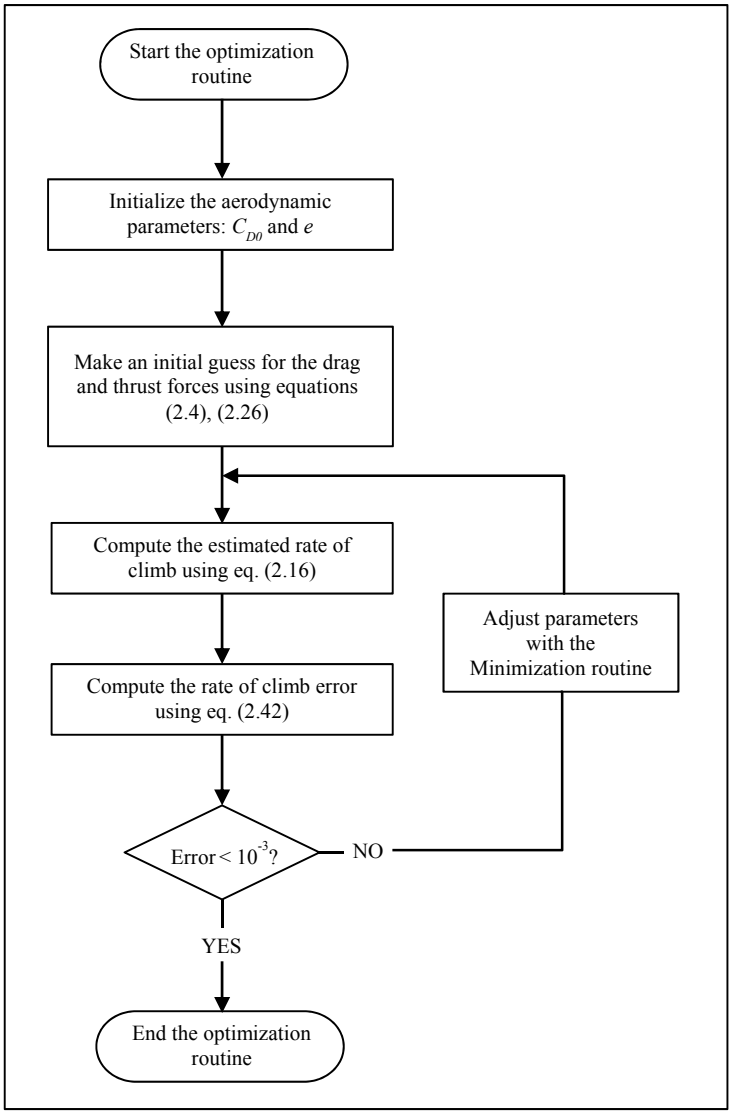

Figure 2.4 The optimization routine

Thereafter, the optimal of the drag force is also computed. The difference between the aero-propulsive forces can now be calculated, in order to determine its optimal value.

The engine specific fuel consumption T_{sfc} is then computed using equations (2.28) and (2.29), such that:

$$T_{sfc} = \left(\frac{dFB}{dt}\right) \times \frac{1}{T} = \frac{\Delta FB}{\Delta t} \times \frac{1}{T} = \frac{1}{T} \times \frac{\Delta FB}{\Delta h} \frac{\Delta h}{\Delta t} = \frac{\Delta FB}{\Delta h} \times \frac{\dot{h}}{T} \tag{2.43}$$

The optimal rate of climb $\dot{h}_{opt}$ is known, by applying the equations (2.35) and (2.32). The optimal specific fuel consumption can be expressed as:

$$T_{sfc}^{opt} = \frac{\Delta FB}{\Delta h} \cdot \frac{\dot{h}_{opt}}{T_{opt}} \tag{2.44}$$

and where ΔFB represents the fuel burnt between two altitudes.

A linear interpolation is performed within the aircraft flight data inputs structure, for the optimal values of the thrust T denoted by T_{opt}, of the difference between the thrust and the drag $(T - D)$, and of the specific fuel consumption SFC. For this reason, a MATLAB function *interpn* is applied. Thereafter, the calculation of the model estimation process is reversed, so that the estimated rate of climb RoC^{estim} is calculated based on equation (2.16) in which the airspeed V is the $\overline{TAS}$ along a sub-segment. The estimated climb gradient c_{grad}^{estim} is then determined by applying equation (2.33), where the rate of climb used is the RoC^{estim}. Next, the estimated horizontal distance traveled H_{Dist}^{estim} at each altitude i is found with equation (2.33):

$$H_{Dist(i)}^{estim} = H_{Dist(i-1)}^{estim} + \frac{\Delta h}{c_{grad}} \tag{2.45}$$

Ultimately, the estimated time to climb Δt_c^{estim} for each sub-segment, an important parameter utilized in executing the Required Time of Arrival (RTA) instructions in the FMS, is computed using following formula:

$$\Delta t_c^{estim} = \frac{\Delta h}{RoC^{estim}} \tag{2.46}$$

In order to reveal the other output parameter of the estimated model, called the estimated fuel burnt FB^{estim}, the estimated fuel consumption rate $\dot{w}_{f\,(i)}^{estim}$ is calculated based on equation

(2.28) for each of the position i. Then, the estimated fuel burnt FB_i^{estim} is computed using equation (2.29), as follows:

$$FB_i^{estim} = FB_{i-1}^{estim} + \dot{w}_{f\,(i)}^{estim} \times \Delta t_c^{estim} \tag{2.47}$$

All the estimation process steps described thus far are summarized in the flow diagram in Figure 2.5.

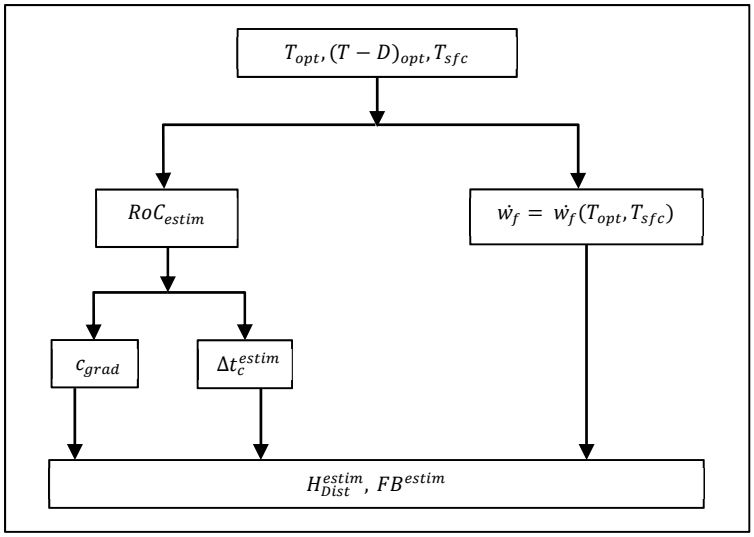

Figure 2.5 Flow chart of the model estimation process

For a given flight test whose inputs include the altitude, the gross weight, the airspeed IAS, and the temperature deviation ΔISA, and its outputs as a set of the thrust values T, the difference between the thrust and drag forces $(T - D)$, and the specific fuel consumption SFC, a look-up table structure equivalent to the black box model is created. The altitude is declared N/A, meaning not applicable for a particular case (Table 2.2). This strategy has been applied for a total of 27 flight tests and is shown in the flowchart of Figure (2.6).

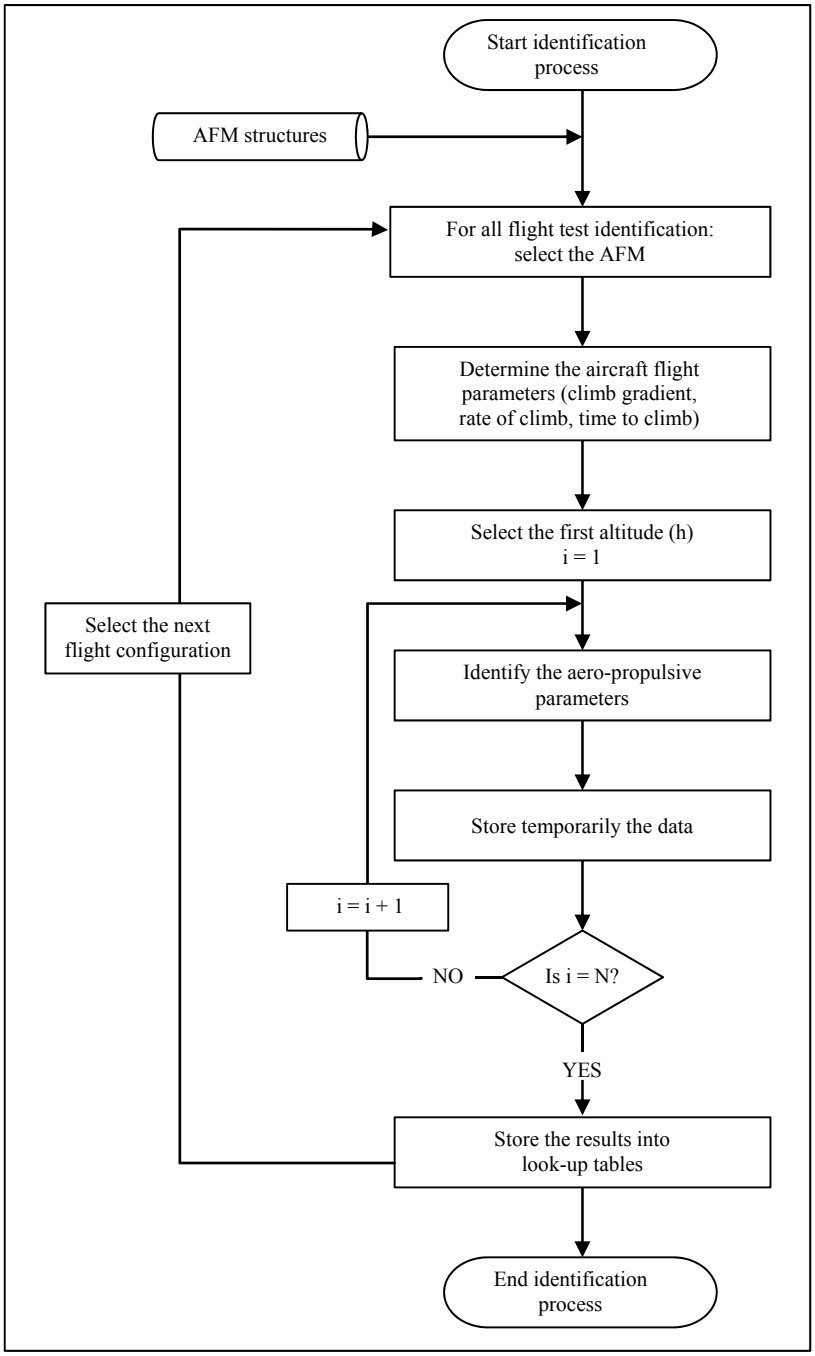

Figure 2.6 Parameter estimation algorithm in the climb regime

The results of the parameter estimation process were stored and formatted into 3D look-up tables (Figure 2.7) or expressed in the mathematical form by the following set of equations:

$$\begin{cases} [T] = f_T(h, GW, IAS, \Delta ISA) \\ [T-D] = f_{T-D}(h, GW, IAS, \Delta ISA) \\ [T_{sfc}] = f_{sfc}(h, GW, IAS, \Delta ISA) \end{cases} \tag{2.48}$$

It must be noted that in order to respect the confidentiality of the subject, the parameter values from Figure. 2.7 are not the real values of the computed aircraft parameters.

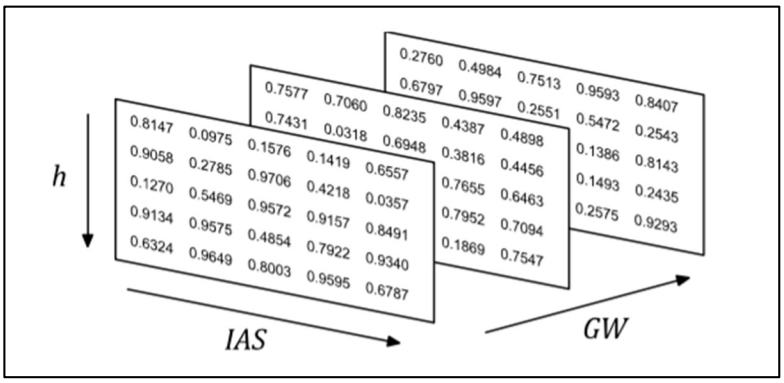

Figure 2.7 3D Look-up tables representation

An estimation technique based on the prediction parameter errors was applied. We noted that the parameters prediction process is critical to achieve good optimization of the unknown parameters. The percentage errors ($\%_{err}$) or the relative errors are calculated for the fuel burnt as follows:

$$\%_{err}^{FB} = \frac{\overbrace{\|FB^{data} - FB^{estim}\|}^{residual}}{\|FB^{data}\|} \times 100 \tag{2.49}$$

and for the horizontal distance traveled:

$$\%_{err}^{H_{dist}} = \frac{\overbrace{\left\|H_{Dist}^{data} - H_{Dist}^{estim}\right\|}^{residual}}{\left\|H_{Dist}^{data}\right\|} \times 100 \tag{2.50}$$

There is no specific criteria to validate or verify an aero-propulsive model, and therefore the proposed flight tests were considered a success if the maximum error between the two models (i.e. the numerical database (AFM) and the developed APM) were found to be within $\pm$ 5% for whole flights. Harada in (HARADA et al., 2013) quantitatively studied the accuracy of an aircraft performance model (i.e. the BADA model) in Air Transportation Systems (ATS).

The aero-propulsive model for the cruise regime is also evaluated in the same viewpoint regarding the model's verification as well the one in the climb regime. An analysis of a commercial aircraft during the cruise phase is described in the following sections, as part of the aero-propulsive model design methodology.

2.2 Aero-Propulsive Cruise Model

The cruise regime is the longest phase in flight for an aircraft. Developing an aero-propulsive model for this flight phase will be useful to the airlines and aircraft manufacturers, especially from a cost perspective. The physics involved during this flight process are described via the aerodynamics and propulsion parameters, and by the specific steps applied to simplify the mathematical model to reduce its modeling errors. These steps as parts of a new approach, together with its input configuration are different than those described for the climb regime.

2.2.1 Aerodynamics and Propulsion Estimation

The cruise regime, a three-degree of freedom dynamic model is characterized by the point variable-mass (i.e. the aircraft), by preserving a steady flight; the forces and vectors are illustrated in Figure 2.8.

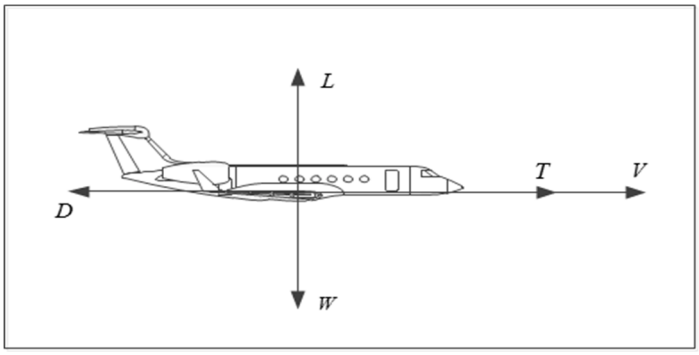

Figure 2.8 The acting forces in the cruise regime

Where V represents the true airspeed (TAS) or Mach number M, L the lift force, D the drag force, W the aircraft weight or gross weight, and T indicates the engine thrust. Considering the flight as symmetric, all the forces act in the plane of the aircraft's symmetry, and the effects of winds are not considered.

Steady flight means that the flight path angle γ is considered as follows:

$$\gamma = 0 \tag{2.51}$$

and velocity V, as the true airspeed (TAS) or the Mach number M remains constant.

Level flight is characterized by constant speed segment, with no external force, but with four acting forces balancing each other, as shown in Figure. 2.8.
The forces equation in the vertical plane consists of the lift force from aircraft's wings that counteract the weight force. The flight path angle assumed in equation (2.51) and applied in equation (2.8) gives the resulting formula:

$$L = W \tag{2.52}$$

This formula is determined also from Figure 2.8.

The engine thrust (T) balances the total drag (D) of the airplane in the horizontal plane, in the following mathematical form, as shown also in Figure 2.8.

$$T = D \tag{2.53}$$

Examining equations (2.52) or (2.53), we can declare that based on the equalities between the acting forces, we cannot build an aero-propulsive model with the strategy applied to the climb regime; a new approach is required, that is described next.

Equation (2.53) replaced in equation (2.28) lead to the following relation between the fuel flow $\dot{w}_f$, the thrust specific fuel consumption coefficient T_{sfc} and the drag force D.

$$\dot{w}_f = T \times T_{sfc} \approx T_{sfc} D \tag{2.54}$$

Equation (2.54) reveals that the fuel flow $\dot{w}_f$ is proportional to the product of the thrust specific fuel consumption coefficient T_{sfc} and the drag force D. Thus, the new approach is based on the analysis of fuel flow $\dot{w}_f$ from equation (2.54). Instead of building a model for each of the parameters, which define the fuel flow $\dot{w}_f$, a parametric model identification of the fuel flow is proposed. This approach involves a minimum of modeling errors. In order to identify this parametric model, the fuel flow $\dot{w}_f$, according to equations (2.27) and (2.30), was analyzed with respect to the altitude h and aircraft speed TAS, assuming constant gross weight (GW) and ISA temperature deviations (ΔISA). We should note that at high subsonic speeds, the effect of compressibility must be considered, and thus, the drag coefficient is also dependent upon the Mach number. The fuel flow varies also with respect to the Mach number M, and is computed by applying equation (1.24).

According to Torenbeek, the variations of center of gravity location x_{cg} have an effect on the drag polar, but these are generally neglected in the preliminary design (Torenbeek, 1995).

Figure. 2.9 presents the variation of the fuel flow from the flight data with respect to the altitude and speed, for a flight configuration that is characterized by a constant gross weight and a temperature deviation.

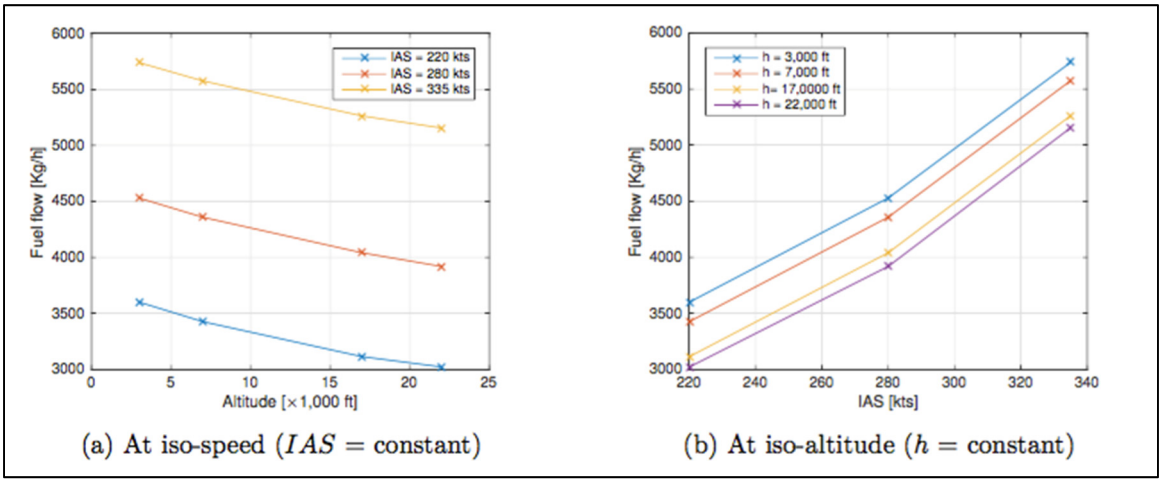

Figure 2.9 Aircraft configurations in cruise flight phase

The following observations can be made from Figure 2.9:

- Fuel flow at constant speed (iso-speed) seems to behave as a quadratic function of the altitude, and
- Fuel flow at constant altitude (iso-altitude) seems to behave as a quadratic function of the speed.

This fuel flow variation, which acts as a quadratic polynomial can be written in the following form:

$$\dot{w}_f(IAS, h, \boldsymbol{\theta}) = \theta_1 + \theta_2 IAS + \theta_3 h + \theta_4 IAS^2 + \theta_5 (IAS)h + \theta_6 h^2 \qquad (2.55)$$

in which the coefficients θ_i, $i = \{1, \ldots, 6\}$ are constant parameters that must be identified to approximate the sampled flight data. It must be noted that in equation (2.55) the coefficients θ_i are computed for a given gross weight and a temperature deviation, as mentioned. To extend the aero-propulsive model of the cruise phase, this methodology should be repeated for other combinations of the gross weight and the temperature deviation. Each of those

combinations is characterized by a set of coefficients. As mentioned, these coefficients must be identified and their values must be then stored in the look-up tables, as the flight data in the AFM. The linear interpolation techniques are then applied to the look-up tables to predict the fuel flow within the aircraft flight envelope.

2.2.2 Parameter Estimation Algorithm

The identification process allows the main parameters associated with the aero-propulsive model in cruise to be approximated. The Least Squares (LS) method is used to identify the coefficients θ_i, $i = \{1,\ldots,6\}$, as the best fuel flow estimates. The method is applied to equation (2.55) for the inputs that are composed of a specific gross weight and the temperature deviation. The procedure is a gradual process, as follows:

1. Compute the information matrix, and then
2. Compute the inverse of the information matrix.

The development of each of the above steps is explained below.

2.2.2.1 Information matrix computation

Taking into account that aircraft performance in cruise is stated in discrete values, the fuel flow is shaped up as a function of altitude h and airspeed IAS, as shown in Figure. 2.10.

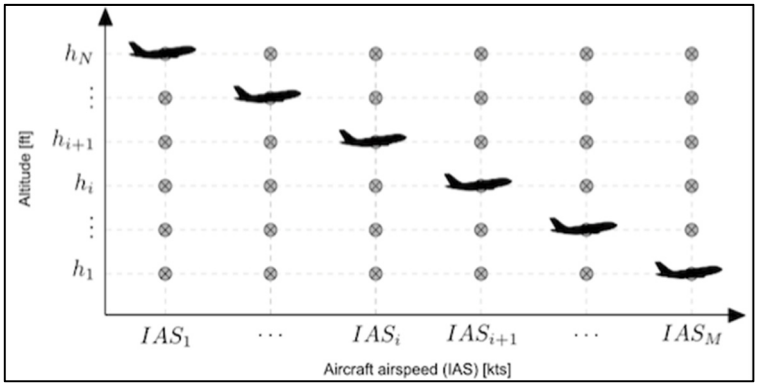

Figure 2.10 Discrete cruise trajectory of an aircraft

Each point of the matrix illustrated in Figure. 2.10 describes a particular flight condition, as a set of altitude/airspeed for a recognized aircraft fuel flow (i.e. the AFM). The grid in Figure 2.10 is not a square grid, as the number of altitudes N may differ from the number of airspeeds (IAS/M).

The algorithm of the identification process begins by computing the information matrix, regarding each flight configuration (i.e. the flight test) as a set of a gross weights (GW) and a temperature deviation (ΔISA). This matrix consists of independent variables matching the structure of the polynomial $\dot{w}_f\ (IAS, h, \boldsymbol{\theta})$, as shown in equation (2.56). For instance, the fuel flow $\dot{w}_f$ is modelled by a bi-quadratic polynomial, as the one presented in equation (2.55). Therefore, by applying it to each grid point, the $N \times M$ matrix will be shaped as follows:

$$\begin{aligned}
\dot{w}_{f_1} &= \theta_1 + \theta_2 IAS_1 + \theta_3 h_1 + \theta_4 (IAS_1)^2 + \theta_5 (IAS_1) h_1 + \theta_6 (h_1)^2 \\
\dot{w}_{f_2} &= \theta_1 + \theta_2 IAS_2 + \theta_3 h_2 + \theta_4 (IAS_2)^2 + \theta_5 (IAS_2) h_2 + \theta_6 (h_2)^2 \\
\vdots \quad &= \qquad\qquad\qquad\qquad \vdots \\
\dot{w}_{f_N} &= \theta_1 + \theta_2 IAS_1 + \theta_3 h_N + \theta_4 (IAS_1)^2 + \theta_5 (IAS_1) h_N + \theta_6 (h_N)^2 \\
\dot{w}_{f_{N+1}} &= \theta_1 + \theta_2 IAS_2 + \theta_3 h_1 + \theta_4 (IAS_2)^2 + \theta_5 (IAS_2) h_1 + \theta_6 (h_1)^2 \\
\vdots \quad &= \qquad\qquad\qquad\qquad \vdots \\
\dot{w}_{f_{N \times M}} &= \theta_1 + \theta_2 IAS_M + \theta_3 h_N + \theta_4 (IAS_M)^2 + \theta_5 (IAS_M) h_N + \theta_6 (h_N)^2
\end{aligned} \tag{2.56}$$

The matrix data $\mathbf{M}_{LS}$ from equation (2.56) can then be presented in the next form:

$$\mathbf{M}_{LS} = \begin{bmatrix}
1 & IAS_1 & h_1 & IAS_1^2 & IAS_1 h_1 & h_1^2 \\
1 & IAS_1 & h_2 & IAS_1^2 & IAS_1 h_2 & h_2^2 \\
\vdots & \vdots & \vdots & \vdots & \vdots & \vdots \\
1 & IAS_1 & h_N & IAS_1^2 & IAS_1 h_N & h_N^2 \\
1 & IAS_2 & h_1 & IAS_2^2 & IAS_2 h_1 & h_1^2 \\
\vdots & \vdots & \vdots & \vdots & \vdots & \vdots \\
1 & IAS_M & h_N & IAS_M^2 & IAS_M h_N & h_N^2
\end{bmatrix} \tag{2.57}$$

where N and M are the number of altitudes and airspeeds, respectively, selected for the model identification process. According to equation (2.57), the computation of the matrix

$\mathbf{M}_{LS}$ is automatically executed by a Matlab code of the parameters estimation algorithm and illustrated in Figure. 2.11. The predicted parameters are stored into a structure containing the independent variables of equation (2.57).

2.2.2.2 The inverse of the information matrix computation

The information matrix shown in equation (2.57) is needed to compute the Moore-Penrose pseudo-inverse matrix, which solves the LS problem, in order to find the estimates of fuel flow parameters. The Moore-Penrose method is working as long as the matrix $\mathbf{M}_{LS}$ is non-singular (Jategaonkar, 2006). In order to build this pseudo-inverse matrix $\mathbf{M}_{\boldsymbol{LS}}^{\dagger}$ that returns the $\mathbf{M}_{LS}$, the proposed cruise model estimation uses the function *pinv* of the Matlab® program. This Matlab function allows to compute, fast and accurate, the Moore-Penrose inverse matrix, as a solution of the Linear Least Squares (LS) problem, as mentioned in equation (1.9).

To extend the model, the complete procedure of the estimation algorithm (i.e. Figure 2.11) was applied to all of the identification flight tests by identifying a polynomial for each set containing a gross weight and a temperature deviation. The coefficients of these polynomials were stored and formatted into 3-D lookup tables. By applying this aero-propulsive model a numerical performance data was created, which is necessary to be used in the trajectory optimization of a commercial airplane in vertical profile. The source information comes from shared reference sources, some of which have the proprietary rights. To protect these sources, this work must be presented only in partial formats.

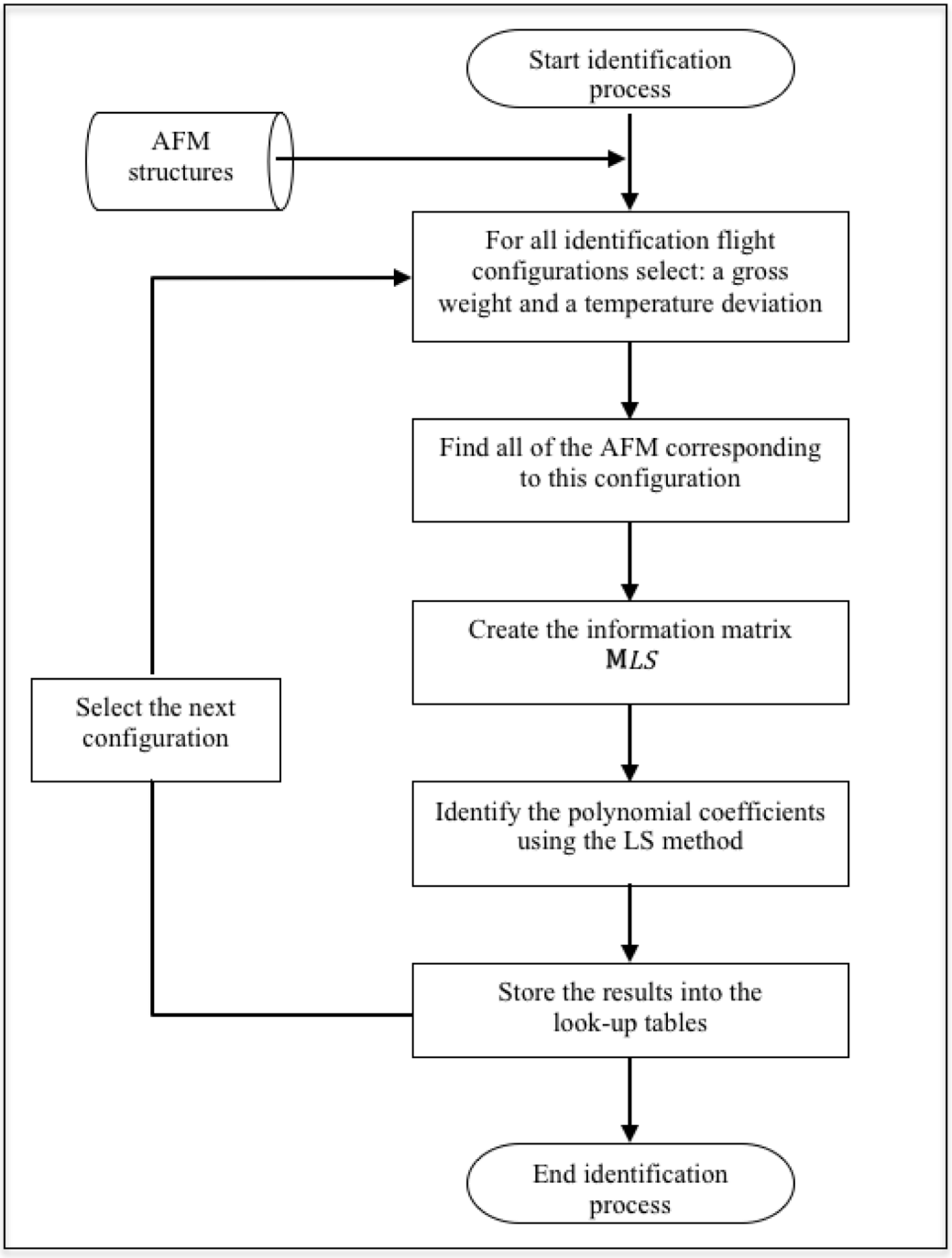

Figure 2.11 Parameter estimation algorithm for the cruise phase

The propulsion model is characterized by its specific fuel consumption, in other words, by the fuel flow rate consumed during the cruise phase.

2.2.3 Cruise performance prediction

The last phase of the cruise process analysis involves the aircraft fuel flow prediction using the created APM for the cruise regime. The available flight data of the Aircrafts A and B are described in Table 2.3. The table contains, for example for the aircraft A, four inputs, among which the Gross Weights GW in number of 29, seven airspeeds IAS (7), ten ISA temperature deviations ΔISA (10), and one output represented by the fuel flow. The proposed methodology was also applied to both aircrafts when flying to the $Mach$ (M) speeds, and is analyzed correspondingly of the IAS speeds' cases.

Table 2.3 Inputs and Outputs Flight data
of the Aircrafts A and B in the Cruise phase

Flight data of Phase	**Inputs Aircraft**		**Output Aircraft**	
	A	**B**	**A**	**B**
Cruise	Gross Weight (29) IAS (7) ISA Deviation (10) Altitude (25)	Gross Weight (26) IAS (11) ISA Deviation (9) Altitude (20)	Fuel flow	Fuel flow

Because the built model parameters are given for discrete values of the gross weight and the temperature deviation, a 2-D linear interpolation was then performed for each of the polynomial coefficients belonging to every identification category, in order to compute their values within aircraft flight envelope.

A polynomial was proposed to model the estimated fuel flow in the cruise regime with respect to the altitude and the airspeed. A new structure consisting of the predicted fuel flow values was created in the form of lookup tables.

A validation of the model identification, for a number of 27 flight profiles or flight tests, was executed for the presented inputs/output in Table 2.3. The fuel flow of the flight data was then interpolated into the reduced structure created during the model identification process

using the Matlab function *interpn*. The interpolated fuel flow values w_f^{interp} were used to compute the percentage error of the validation of model identification using equation (2.58) where the *residual* was represented by the difference between the fuels flow data w_f^{data} and the fuel flow validation of model identification w_f^{valid}.

For the other flight tests, the fuel flow w_f^{valid} values were interpolated inside the AFM structure. The fuel flow percentage error was then computed by applying formula corresponding to validation of the aero-propulsive model in the cruise phase, as follows:

$$\%_{w_f}^{valid} = \frac{\overbrace{\left\| w_{f\ data}^{\ valid} - w_{f\ estim}^{\ valid} \right\|}^{residual}}{\left\| w_{f\ data}^{\ valid} \right\|} \times 100 \tag{2.58}$$

Thus, if the maximum error between the two numerical data is less than 5%, then the flight test is considered successful. The model's accuracy during the cruise phase will be analyzed in Chapter 3.

CHAPTER 3

RESULTS AND DISCUSSIONS

The research findings are presented here, as well as the analyses of the developed aero-propulsive model's reliability and of the effectiveness of the generated numerical data. These analyses are based on the model identification and verification procedures. The methodologies validation proposed in the Chapter 2 consists of comparing the parameters of the AFM (i.e. the numerical flight data provided by CMC Electronics Esterline) with the predicted numerical data using the created aircraft aero-propulsive models.

3.1 Results and Discussions

The validation of models parameters for both climb and cruise regimes are presented in this chapter, along with the results and discussions thereof. The accuracy of the modelled numerical data was verified by comparing its performances. Therefore, a comparison between the provided flight data (or any AFM data) and the predicted parameters, which have been generated using the APM, was performed in climb and cruise for both aircrafts.

The flight tests were assigned to the following two categories: the model identification and the model validation. The first category had the intention to build the aero-propulsive model, while the second category was used to validate the obtained model. As mentioned in the previous chapter, not all flight configurations (tests) were used to identify the model. The core idea was to minimize the number of flight tests. Therefore, to minimize this number, these flight tests were carefully chosen according to the following three assumptions:

1. The center of gravity does not affect the aircraft performance in climb,
2. The variation of the gross weight and of the speed can be expressed by a quadratic function. In consequence, only three gross weights and three speeds were used to identify the climb and the cruise models. The gross weights and the speeds were selected for a minimum value, a middle value and a maximum of the values range.
3. The temperature deviation ΔISA is piecewise linear between $+30°C$ and $-30°C$ of Aircraft A and between $+30°C$ and $-35°C$ of Aircraft B.

There is one exception from the above assumptions, which was applied to Aircraft B related to using the three $Mach$ speeds in cruise regime corresponding other range than the one evaluated for the presented cases.

3.1.1 Validation of the Aero-Propulsive Model in Climb Phase

There are two sets of output parameters for the same input parameters, which were compared to verify the accuracy of the modelled APM during the climb phase. The model identification input/output parameters are described for each of Aircrafts A and B, in Table 2.2 of the Chapter 2.

The model identification of Aircraft A during the climb phase was carried out for 27 flight tests, wherein the inputs ($x_{cg}, GW, ISA/M, \Delta ISA, h$) were based on the above mentioned assumptions, and the outputs were computed in terms of the fuel burnt and the horizontal distance traveled (FB, H_{dist}) from the available flight data or the AFM data. The model identification of Aircraft B contains the inputs ($GW, ISA/M, \Delta ISA, h$). The outputs (FB^{data}, H_{Dist}^{data}) belonging to the flight tests data were sorted from the lookup tables (AFMs). The other set of outputs (FB^{estim}, H_{Dist}^{estim}) contains the estimates of the model parameters (an estimation using flight data). These (inputs/outputs) as predicted parameters' values were tabulated into the lookup tables (i.e. in the model's structure) corresponding to each of the given flight tests. A detailed presentation of the input parameters used by the parameter estimation algorithm is described below in order to present the models' validation results.

The flight envelope of the Aircraft A was used in order to fulfill and complete the APM study in climb, by choosing a number of 2157 flight tests, which represents 99% of the total of 2184. The flight envelope of the Aircraft B was used in order to fulfill and complete the APM study in climb, by choosing a number of 1728 flight tests with IAS speeds and 1296 flight tests with $Mach$ speeds.

A total of 27 flight tests were used to validate the model identification of Aircraft A in the climb phase, from a total number of 2184 flight tests, i.e. only 1% of the total. The other 2157 flight tests were used to validate the identified model in the climb regime. As 2157 is a high number, the validation is performed for the aircraft flight envelope.

The model's efficiency in climb regime is illustrated in Figures 3.1 to 3.6 and in Figures 3.7 to 3.12. These twelve sets of results show several examples of the successful investigations based on three different gross weights (i.e. $GW_1 < GW_2 < GW_3$) and three speeds (i.e. $IAS_1 < IAS_2 < IAS_3;\ M_1 < M_2 < M_3$) of the speed's range of each of both aircrafts under study. Thus, an analysis example is based on a constant speed (IAS/M), one center of gravity position and one ISA temperature deviation ΔISA of the Aircraft A as well as the Aircraft B, while the simulation is performed for the three gross weights of each of the aircrafts. The results shown in these figures were grouped in order to emphasize the accuracy of the aircraft performance under investigation.

Figure 3.1 shows the variation of the horizontal distances that were predicted and their relative errors with respect to the altitude, which were simulated using the lowest IAS. The errors were found to be higher at lower altitudes; the relative error was computed with respect to the total horizontal distance traveled that is dependent on the aircraft GW. In other words, the relative error decreases noticeably when the aircraft is climbing, so the estimated model becomes much more accurate when is applied to a heavier aircraft, for GW_3. The APM data shows a very good approximation with the given flight data because of the fact their errors are generally under 5%; in this case a flight test is considered a success.

Figure 3.2 shows the variation of the estimated fuel burn and its relative error with the altitude. Figure 3.2 also shows that during the aircraft climbing, at the higher gross weights GW_3, the relative errors are higher; i.e. the higher fuel burnt occurs along with the distance traveled, that is evident, too. Consequently, from Figure 3.2, the maximum relative error between the measured fuel burnt and the estimated fuel burn was found to be less than 1%. Therefore, the resulting model that was analyzed for the same gross weights seems to be much more accurate for the estimated fuel burn than the estimated horizontal distance, but overall good approximations were obtained.

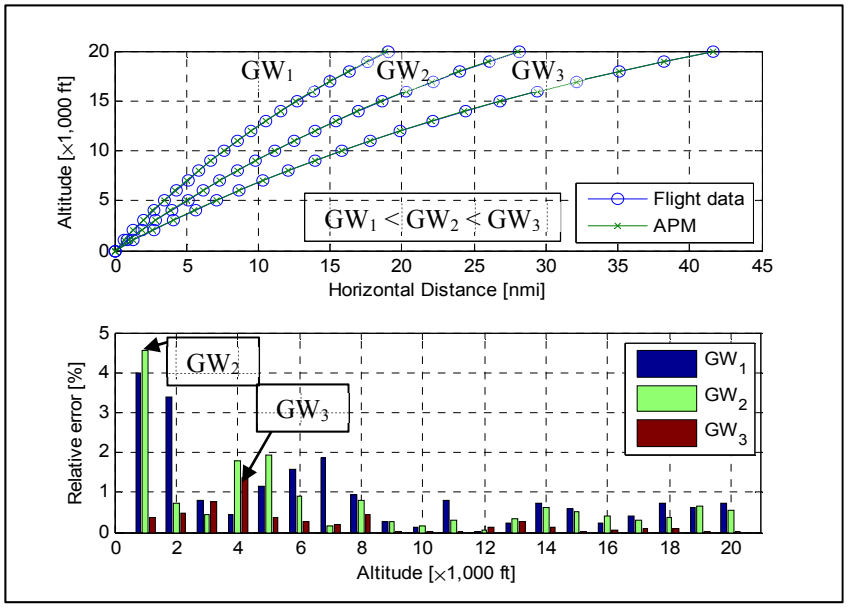

Figure 3.1 Estimated Horizontal Distance of Aircraft A in Climb at the lowest *IAS* and for three *GW*s

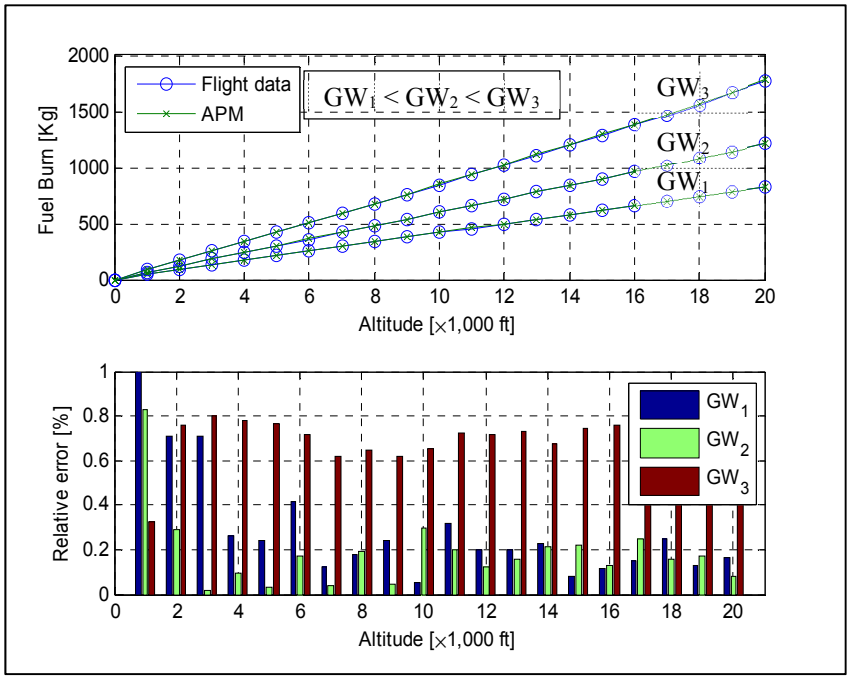

Figure 3.2 Estimated Fuel Burn of Aircraft A in Climb at the lowest *IAS* and for three *GW*s

Figures 3.3 and 3.4 were illustrated in the case of the middle speed IAS of its range. The aircraft performances under these circumstances were also visualized for the estimated horizontal distance and the estimated fuel burn, whose accuracies were quantified by their errors. Those examples based on the developed model have shown that the APM data matched the given flight data (AFM) for all three gross weights taken in consideration. The relative error of the horizontal distance is less than 5%, which means that the trajectory is well approximated by the numerical data derived from the APM.

Figure 3.3 shows also that when the aircraft climbs at its maximum gross weight value GW_3, the relative error is the lowest of them with respect to the altitude reached.

Figure 3.4 shows that the maximum relative error of the fuel burn estimation is less than 1% for all three gross weights tested and a better prediction could be observed to the gross weight GW_1 of the range studied in terms of smallest error.

The performances validation continues with another example of investigation on the Aircraft A in climb that is performed at the highest speed IAS on the gross weights' range, and is illustrated in Figures 3.5 and 3.6. Both figures prove a good prediction between the given flight data and predicted data (i.e. the APM). The results of their relative errors of the estimated horizontal distances and the fuel burn predicted with respect to the altitude have also showed a good estimation of the model proposed, with an accuracy less than 5% for the horizontal distances (Figure 3.5), and less than 1% for the fuel burn (Figure 3.6).

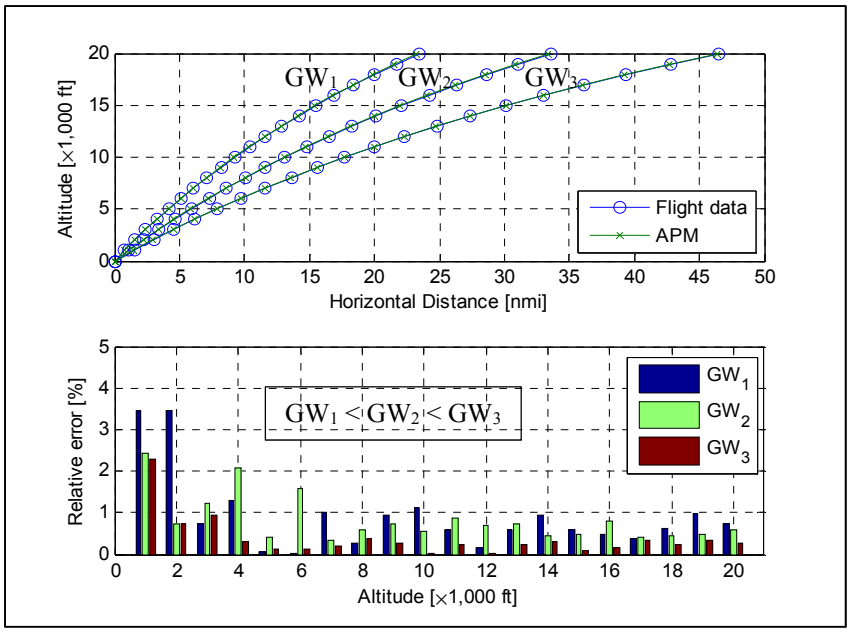

Figure 3.3 Estimated Horizontal Distance of Aircraft A in Climb at a middle *IAS* and for three *GW*s

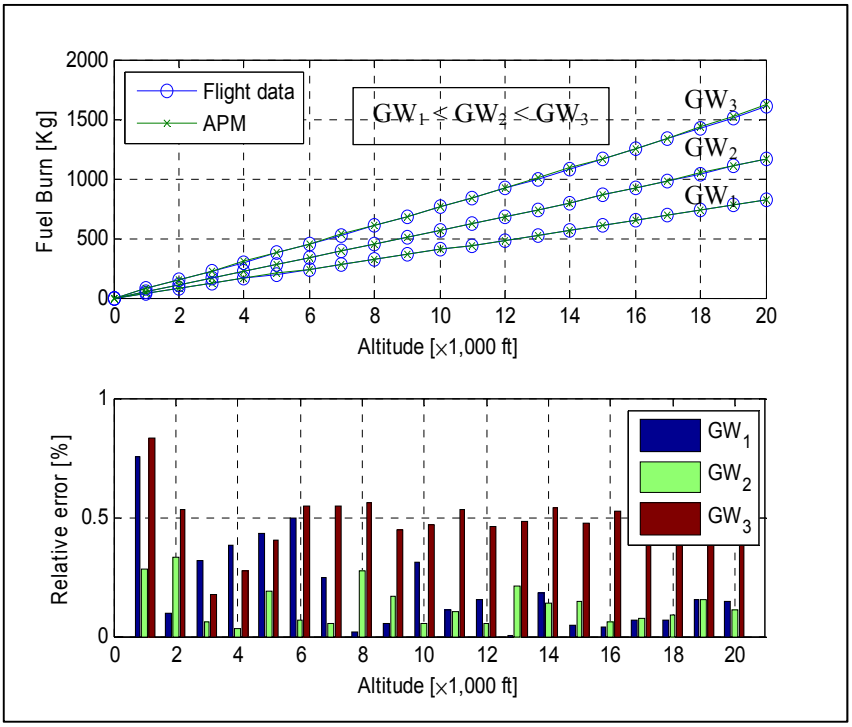

Figure 3.4 Estimated Fuel Burn of Aircraft A in Climb at a middle *IAS* and for three *GW*s

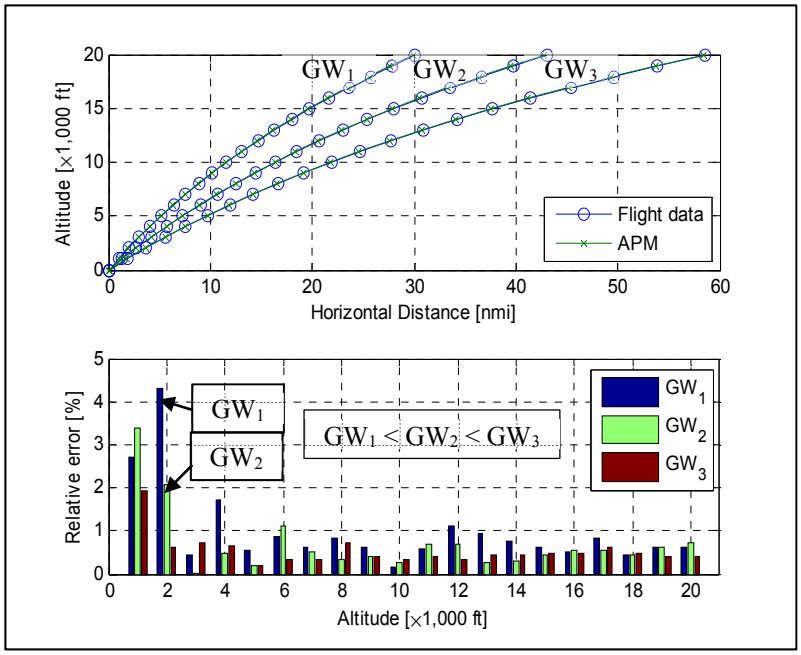

Figure 3.5 Estimated Horizontal Distance of Aircraft A in Climb at the highest IAS and for three GWs

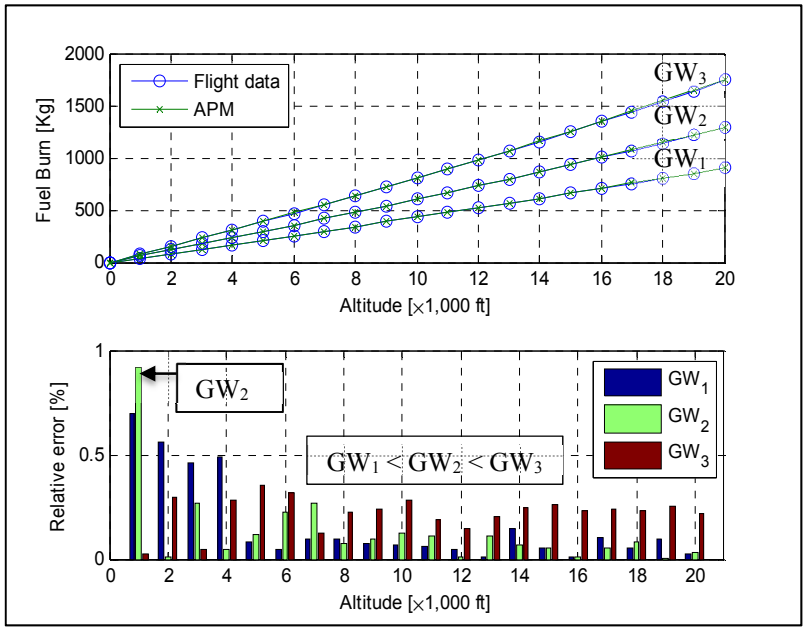

Figure 3.6 Estimated Fuel Burn of Aircraft A in Climb at the highest IAS and for three GWs

A graphical validation of the identified model for the Aircraft B in climb regime is further illustrated in the same way as for the Aircraft A. The following Figures 3.7 to 3.12 illustrate the accuracy of its APM. Other several examples of three simulation's cases were performed on its aircraft' gross weights (i.e. the minimum, the middle and the maximum of value) for each of the three IAS speeds.

A flight configuration which has to validate the APM data against the flight data (AFM) of the Aircraft B contains as the previous ones: the airspeed IAS (i.e. taking the minimum medium and eventually maximum speed), the ISA temperature deviations ΔISA, the altitudes and is analyzed for the three gross weights as mentioned. The following six figures demonstrate how well the estimated model is fitting the flight data for the Aircraft B.

Figure 3.7 illustrates that the horizontal distance' predictions with respect to the altitudes are matching very well the given experimental data. They are tested for three of the gross weights and at the speed that corresponds to the lowest value of the flight speed in climb. The relative error of the horizontal distance is higher at lower altitudes because is computed with respect to the total distance traveled. Generally, these relative errors are less than 2%, meaning the horizontal trajectory is well approximated by the derived numerical data of the Aircraft B. The highest error is 5% for the gross weight GW_1 and occurs at 2000ft.

Figure 3.8 shows that the maximum prediction errors between the estimated fuel burn and the fuel burnt belonging of the flight data are less than 1%. Therefore, we could declare that the numerical data obtained from this APM demonstrate a good fit with the experimental data for this research.

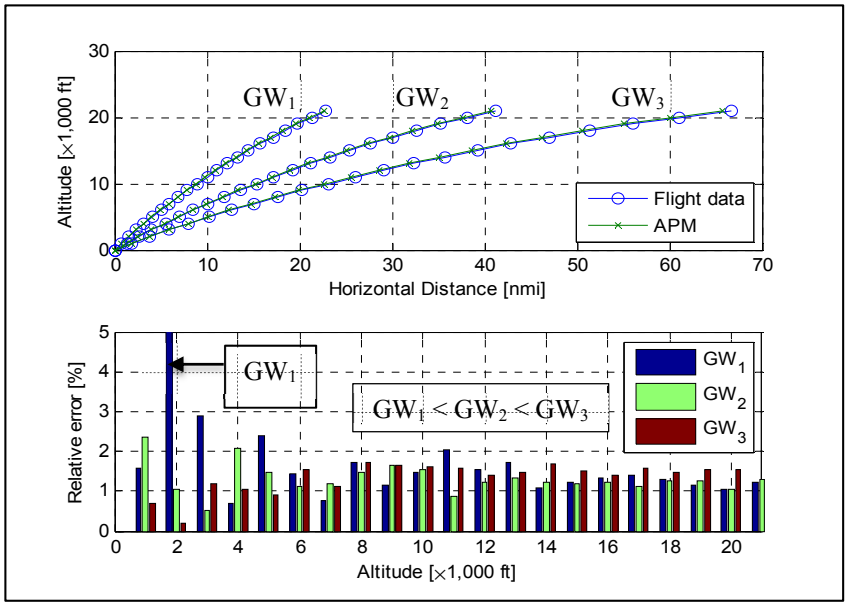

Figure 3.7 Estimated Horizontal Distance of Aircraft B in Climb at the lowest IAS and for three GWs

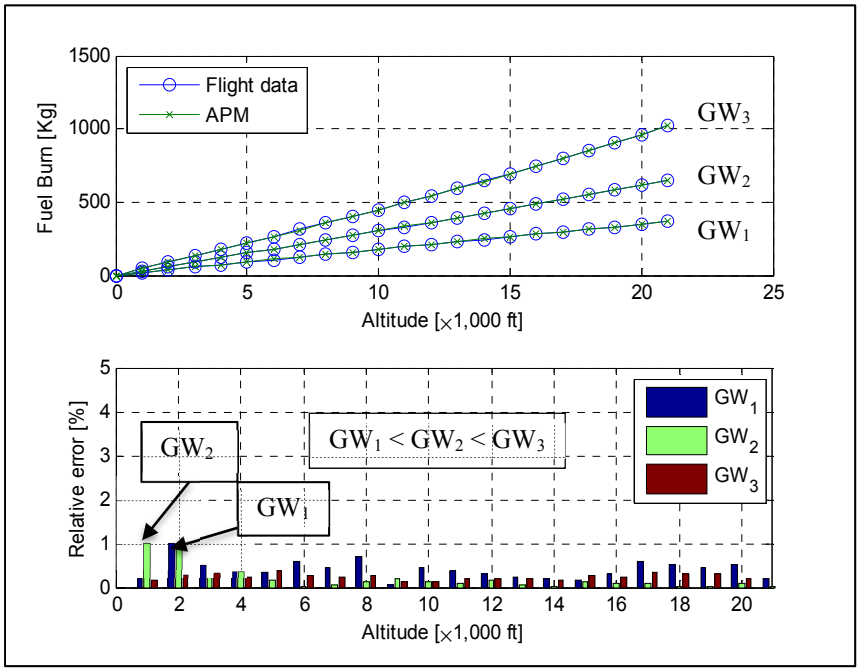

Figure 3.8 Estimated Fuel Burn of Aircraft B in Climb at the lowest IAS and for three GWs

The validation analysis continues with the case when the speed (IAS) is chosen at its middle value from the flight envelope. This case is described into Figure 3.9 where a validation of the horizontal distances estimated against the one from the flight data was performed. Indeed, as shown in Figure 3.9, there is a very good match between the predicted and the experimental data for the horizontal distance traveled with the altitude.

For the simulation case at middle speed value, the horizontal distance was well estimated. The relative errors of the horizontal distance are less than 3%, and are almost all under 2% for the altitudes higher than 5000ft. Therefore, even if the aircraft travels more in terms of its horizontal distance, the predicted model, for this case, does not change too much in accuracy.

Figure 3.10 describes the results obtained in terms of aircraft fuel burn estimation that was tested for a middle speed (IAS) of the range. The estimated data for the three gross weights investigated demonstrate also that a good fit of the given flight data, with errors of less than 1% is obtained. For the flight configuration chosen and illustrated in Figure 3.10, when the gross weight is at the middle GW_2 of their range, it can be noted that their errors are decreasing with increasing in the altitude. And so, the model is more predictable than for the lowest GW_1, for example.

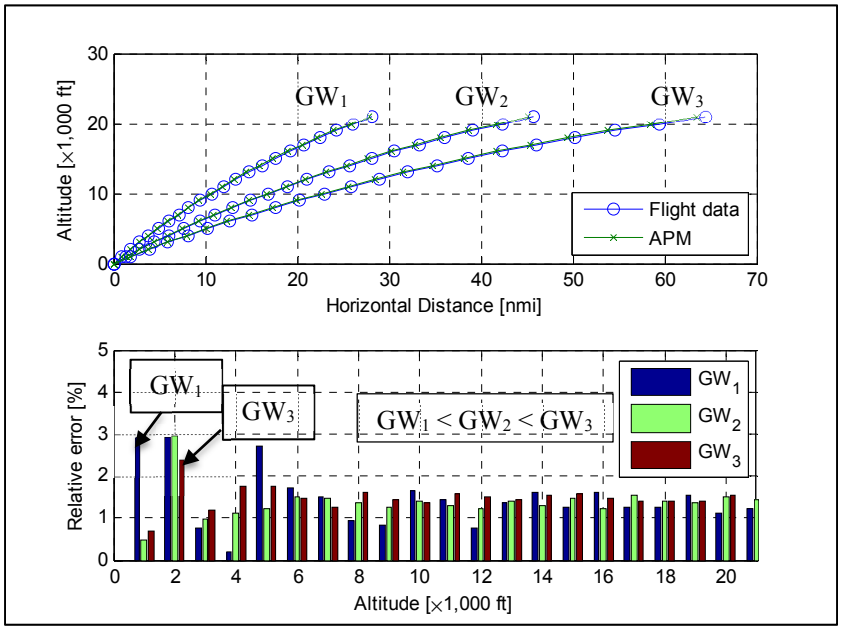

Figure 3.9 Estimated Horizontal Distance of Aircraft B in Climb at a middle IAS and for three GWs

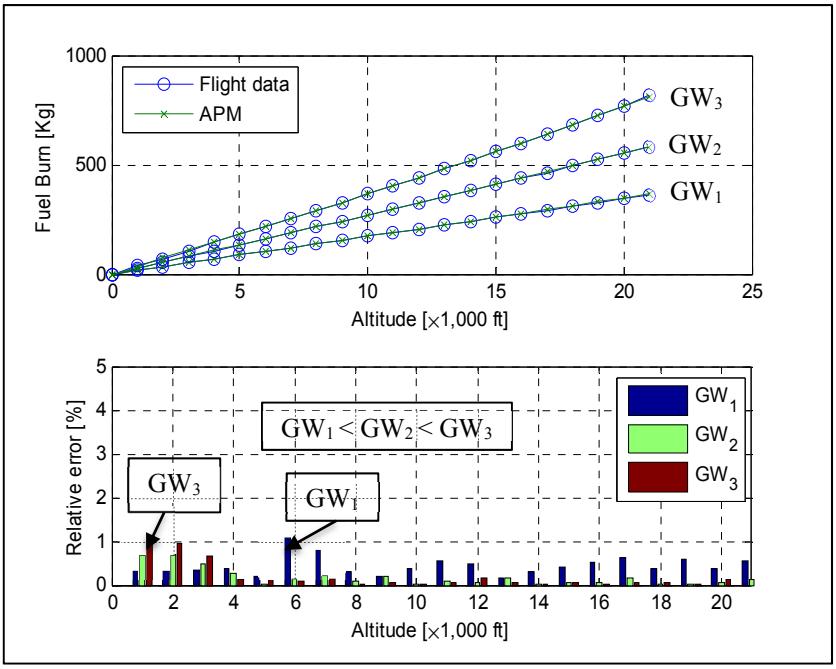

Figure 3.10 Estimated Fuel Burn of Aircraft B in Climb at a middle IAS and for three GWs

The results in the climb regime of the proposed methodology for the Aircraft B are shown next in two validation examples of the horizontal distance and of the fuel burnt when the aircraft flies at maximum IAS, and for three aircraft' gross weights. These results are illustrated in Figures 3.11 and 3.12 and demonstrate that the proposed methodology gives a good fit between the horizontal distances of the available flight data and the predicted horizontal distances traveled, as well as for the fuel burnt estimation. The relative error is less than 5% for the horizontal distance (Figure 3.11), and the relative errors remain almost under 2% along the investigation for the fuel burnt (Figure 3.12).

The fuel burnt prediction when the aircraft flies with their middle and maximum gross weights is better with increasing in altitude. That means that once the aircraft begins to reach higher altitudes (e.g. above 5000ft), the proposed model is much more efficient, especially for the highest gross weight of its range (where the relative errors are the lowest).

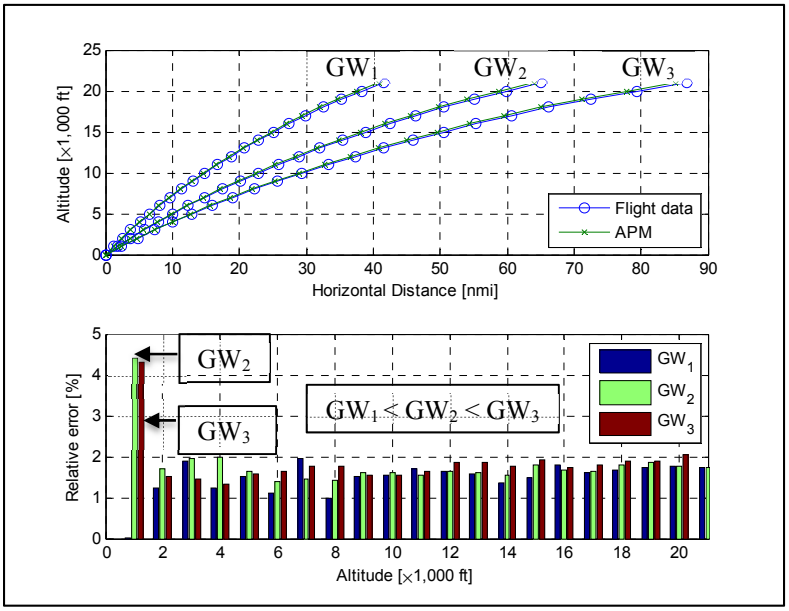

Figure 3.11 Estimated Horizontal Distance of Aircraft B in Climb at the highest IAS and for three GWs

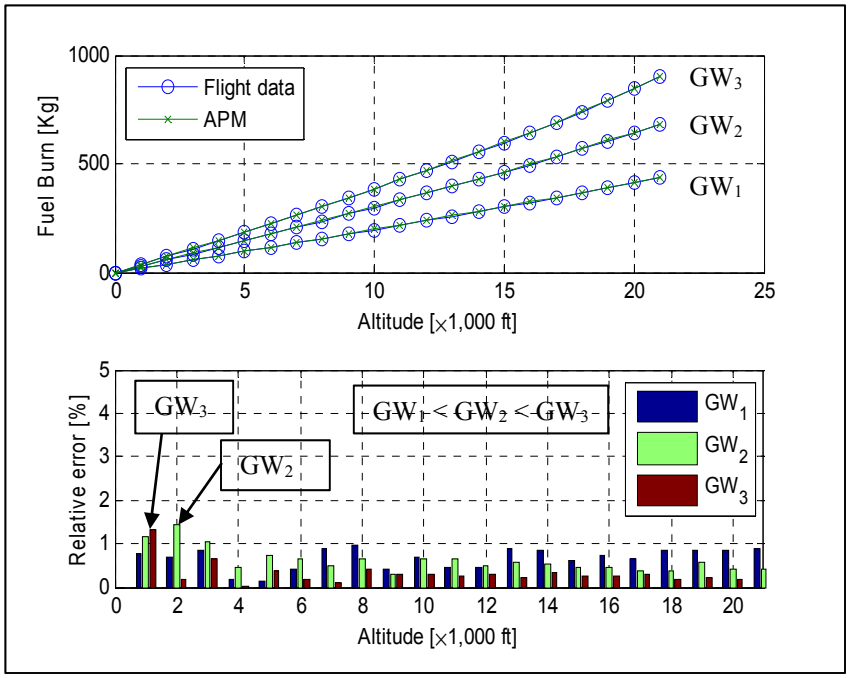

Figure 3.12 Estimated Fuel Burn of Aircraft B in Climb
at the highest IAS and for three GWs

The obtained model is then verified for both aircrafts in the cruise regime and is illustrated through other several examples when the gross weight of the airplane is kept constant (at the minimum, the middle and the maximum values) for each of the three speeds (IAS and $Mach$) analyzed.

3.1.2 Validation of the Aero-Propulsive Model in Cruise Phase

To illustrate how each of the flight tests were validated in cruise for Aircraft A, more examples were performed that are illustrated in Figures 3.13 to 3.15 at three IAS ($IAS_1 < IAS_2 < IAS_3$) and in Figures 3.16 to 3.18 at three Mach speeds ($M_1 < M_2 < M_3$). The simulations were executed for the gross weight at the minimum, then middle and the maximum value.

The results were analyzed each time for three IAS speeds, also of the minimum, medium and maximum of their range. The same graphical validation was performed for three $Mach$

speeds, respectively. When the maximum error between the experimental numerical data and the predicted numerical data was less than 5%, then the flight test was considered to be goal reached. Figure 3.13 shows that the relative errors of the estimated fuel flow of the Aircraft A for all the examples performed at the three IAS speeds are smaller than 2%. Figure 3.13 also demonstrates that the best prediction is for the case of minimum IAS (IAS_1) and the minimum GW (GW_1).

Figure 3.14 shows that for the middle GW value chosen, the estimated fuel flow has relative errors smaller than 1.5% for all speeds.

Figure 3.15 describes the case of the Aircraft A that flies with its maximum GW and for the smallest IAS. For this configuration, and over 8000ft, there are no flight data for this region of airplane flight envelope. The relative errors are smaller than 1.5%.

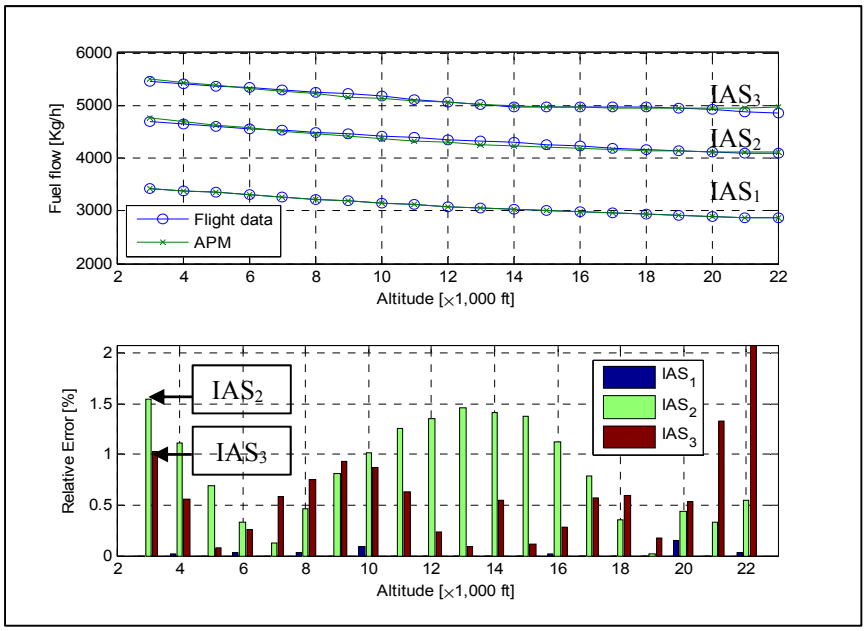

Figure 3.13 Estimated Fuel Flow of Aircraft A in Cruise
at minimum GW and for three IASs

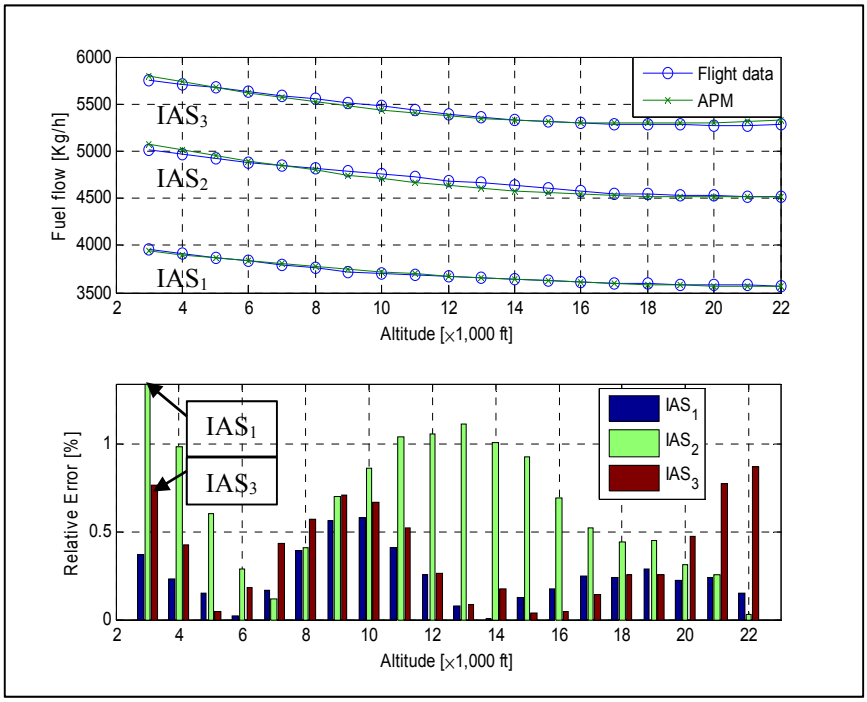

Figure 3.14 Estimated Fuel Flow of Aircraft A in Cruise at a middle GW and for three IASs

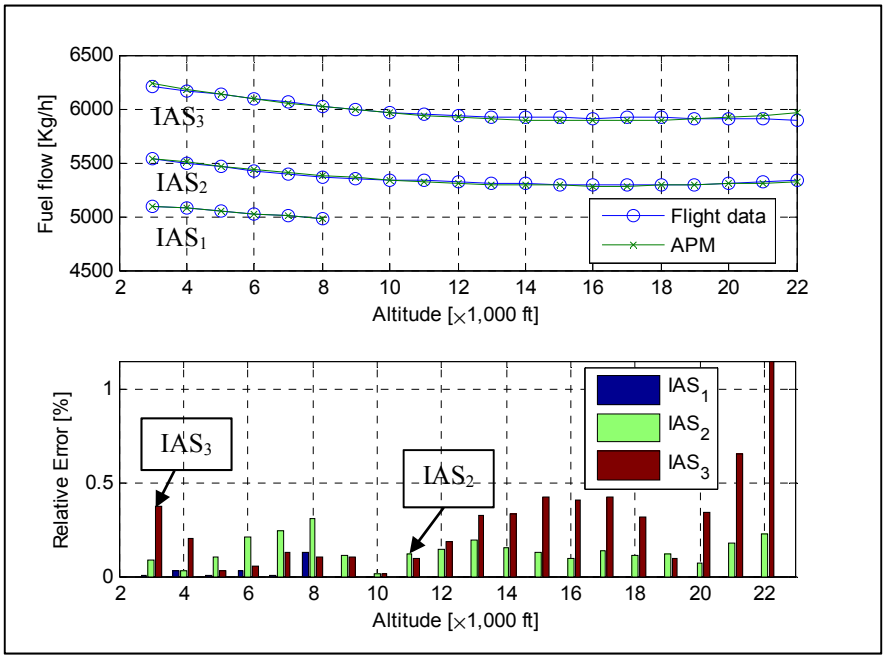

Figure 3.15 Estimated Fuel Flow of Aircraft A in Cruise at maximum GW and for three IASs

The estimated fuel flow model of the Aircraft A is further validated for three $Mach$ speeds, and to the minimum, medium and maximum values of gross weights. The results are illustrated in Figures 3.16 to 3.18. These figures show good approximation of the fuel flow between the flight data and the APM data, with the relative errors under 2%. For altitudes lower than 13,000ft, demonstrates that the flight test data are zeros, which means that the aircraft cannot fly at $Mach$ speeds under these circumstances. The developed APM in cruise is not a physical model as mentioned in Chapter 2, and there is no information about engine(s) for none of the aircrafts studied; therefore the speed curves are just fitting curves, reason for which they have the shapes shown in Figures 3.17 and 3.18.

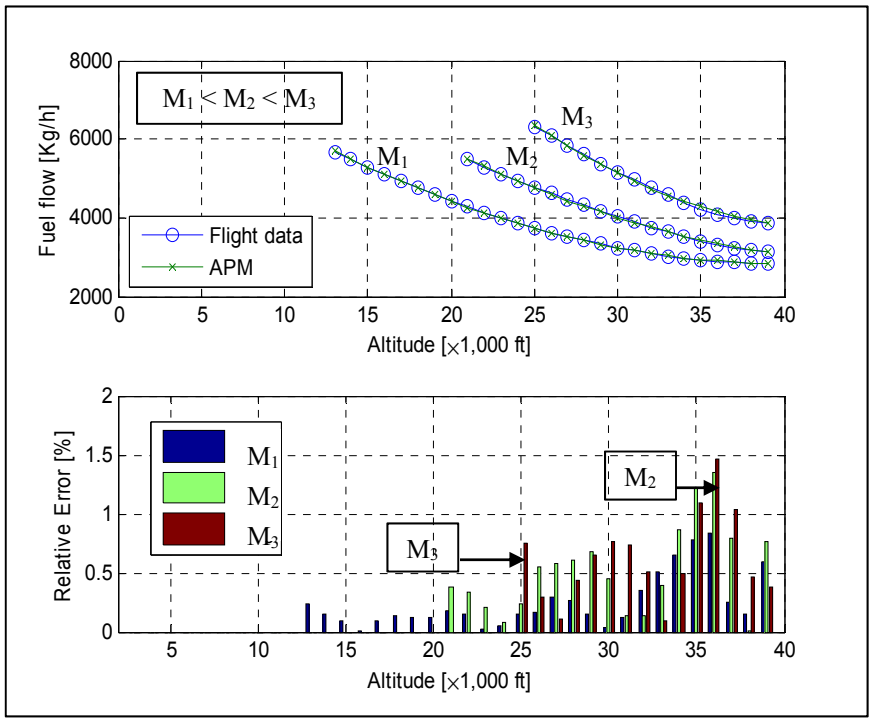

Figure 3.16 Estimated Fuel Flow of Aircraft A in Cruise
at minimum GW and for three $Mach$ speeds

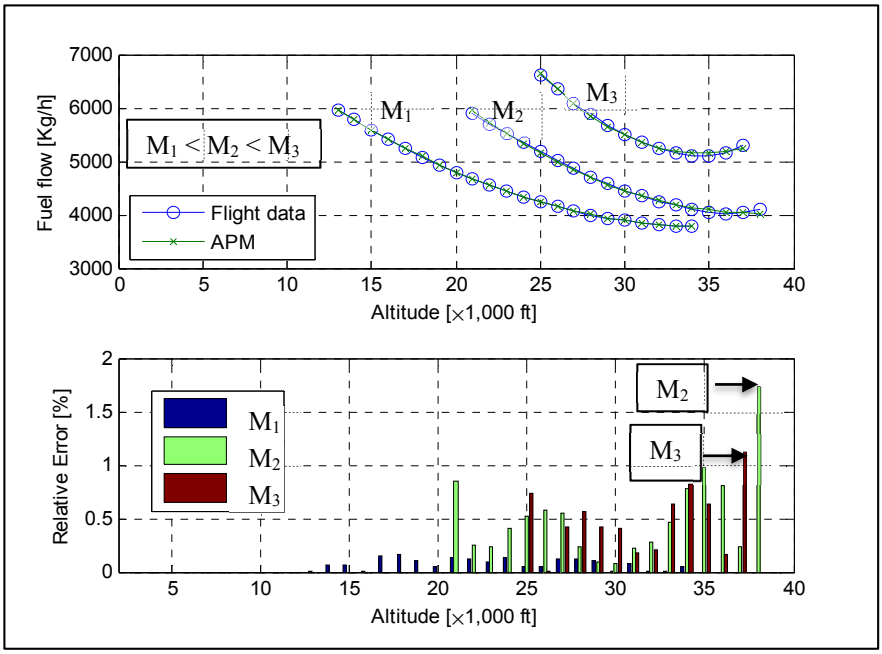

Figure 3.17 Estimation Fuel Flow of Aircraft A in Cruise at middle GW and for three $Mach$ speeds

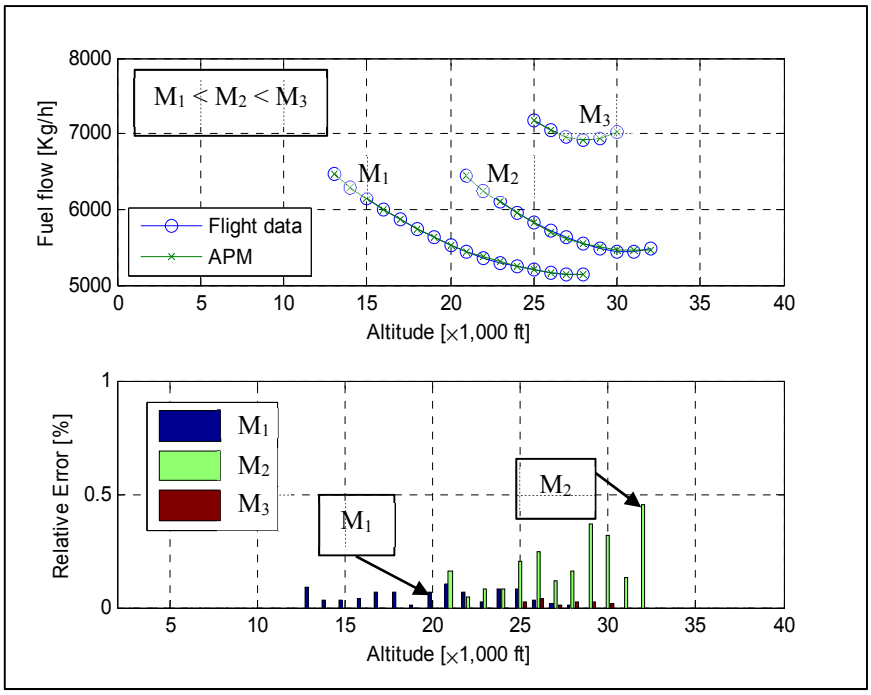

Figure 3.18 Estimation Fuel Flow of Aircraft A in Cruise at maximum GW and for three $Mach$ speeds

The validation of the created APM in cruise is sustained by several examples illustrated in Figures 3.19 to 3.21 for three IAS speeds, and in Figures 3.22 to 3.24 for three $Mach$ speeds; each set of cases was analyzed for three gross weights (minimum, middle and maximum). The first example of the first case analyzes the estimated fuel flow in cruise regime at its minimum gross weight.

Figure 3.19 illustrates that for each of three IAS speeds, a good fit between the flight data and the APM data was obtained. The fuel flow relative errors are less than 0.5% when the aircraft flies at the minimum IAS and the middle IAS, while when these errors are less than 3% at the maximum IAS. The verification of the model continues with the example of the fuel flow prediction at middle gross weight, which is illustrated in Figure 3.20, and where the relative errors are smaller than 2.5%, and so demonstrating a good prediction, too. Another analysis in terms of gross weights at its maximum limit is represented in Figure 3.21. The fuel flow given by flight test data is better approximated by the proposed methodology in this case, when the aircraft performance in cruise has been predicted with errors that are lower of 2%.

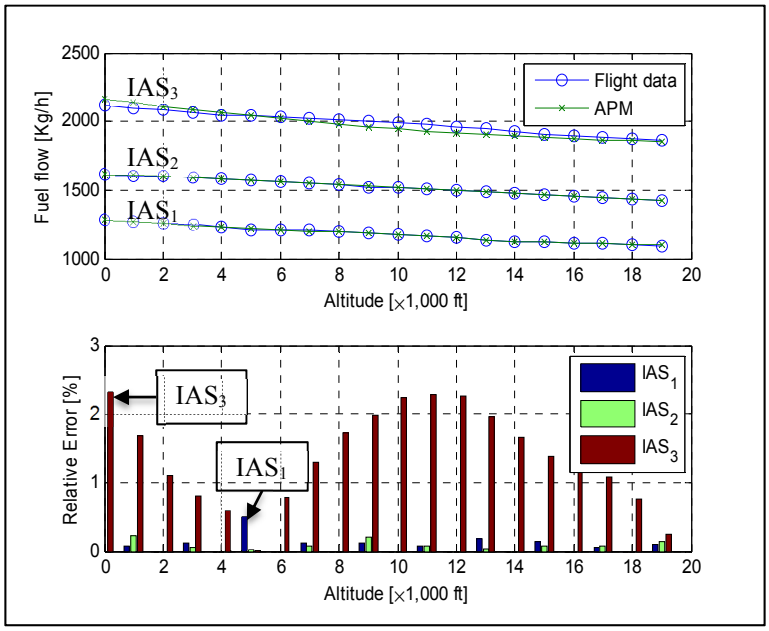

Figure 3.19 Estimated Fuel Flow of Aircraft B in Cruise at minimum GW and for three IASs

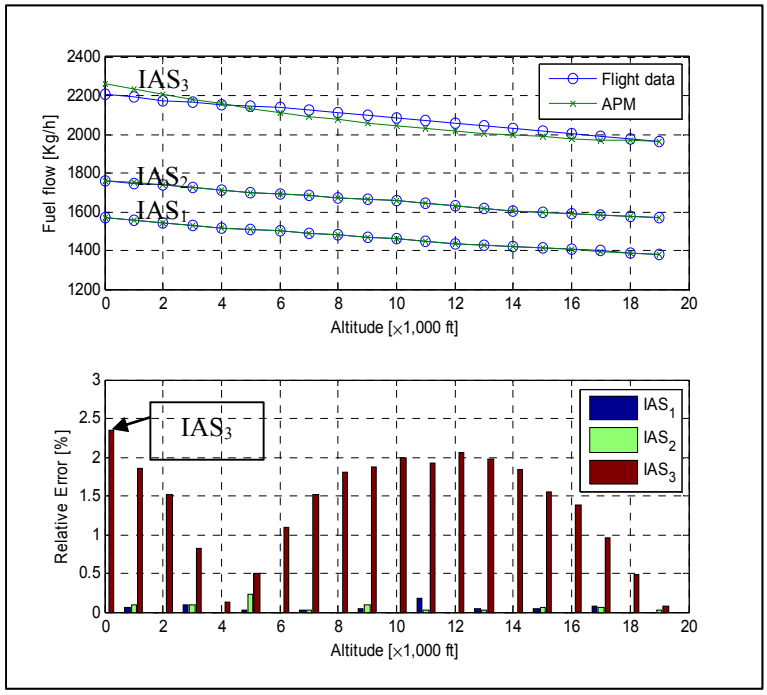

Figure 3.20 Estimated Fuel Flow of Aircraft B in Cruise at middle GW and for three IASs

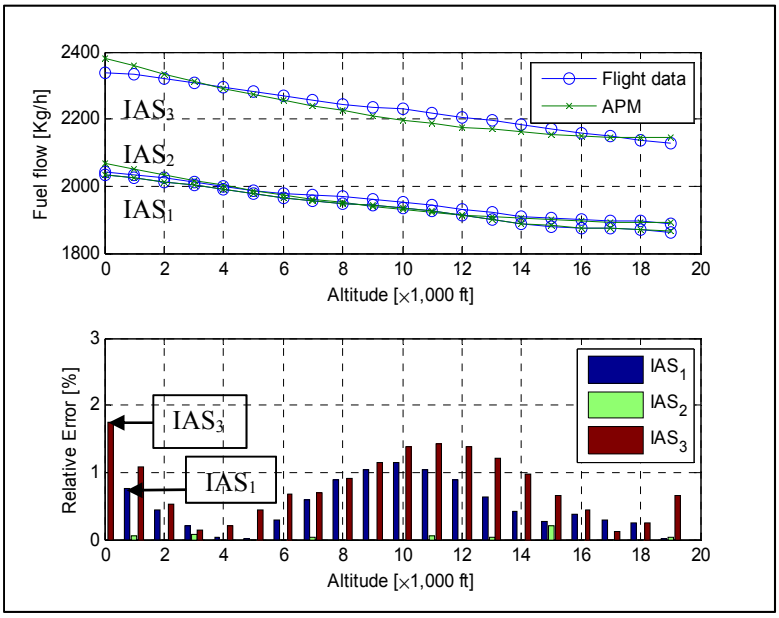

Figure 3.21 Estimated Fuel Flow of Aircraft B in Cruise at maximum GW and for three IASs

The second case analyzes the estimated fuel flow of the Aircraft B in cruise regime for an evaluation at three specific $Mach$ speeds. The prediction of fuel flow is verified at minimum gross weight and is pictured in Figure 3.22, followed by the example when the predicted fuel flow is evaluated at middle gross weight and illustrated in Figure 3.23, and finally this estimation is validated at maximum gross weight and is shown in Figure 3.24. The relative errors are less than 1% for all three examples, which means that the model gives a good prediction to the available flight data. Also, these figures demonstrate that the aircraft cannot fly at the maximum $Mach$ speed M_3 for any of the gross weights at altitudes lower than 14,000ft.

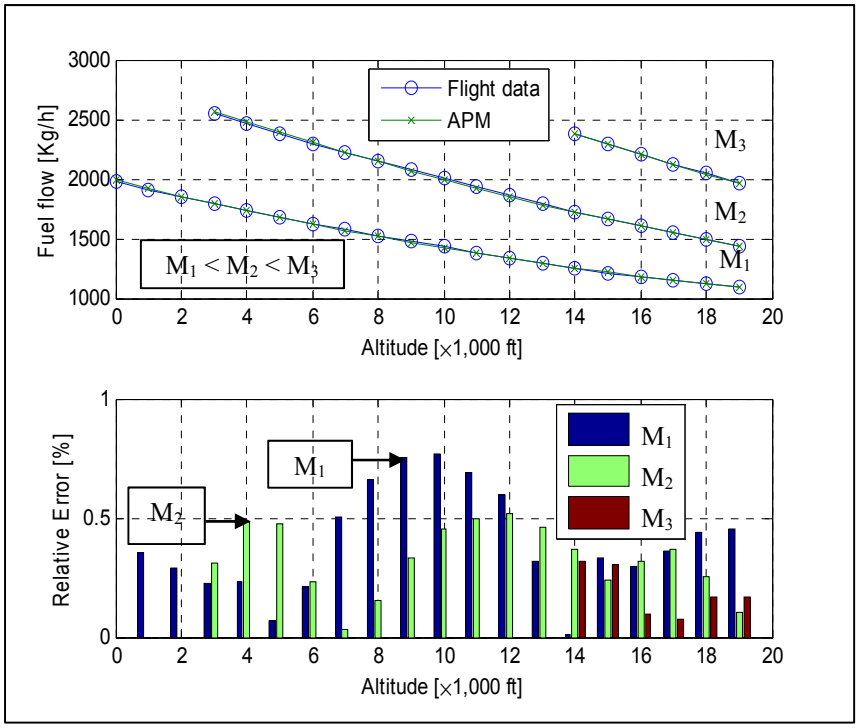

Figure 3.22 Estimated Fuel Flow of Aircraft B in Cruise at minimum GW and for three $Mach$ speeds

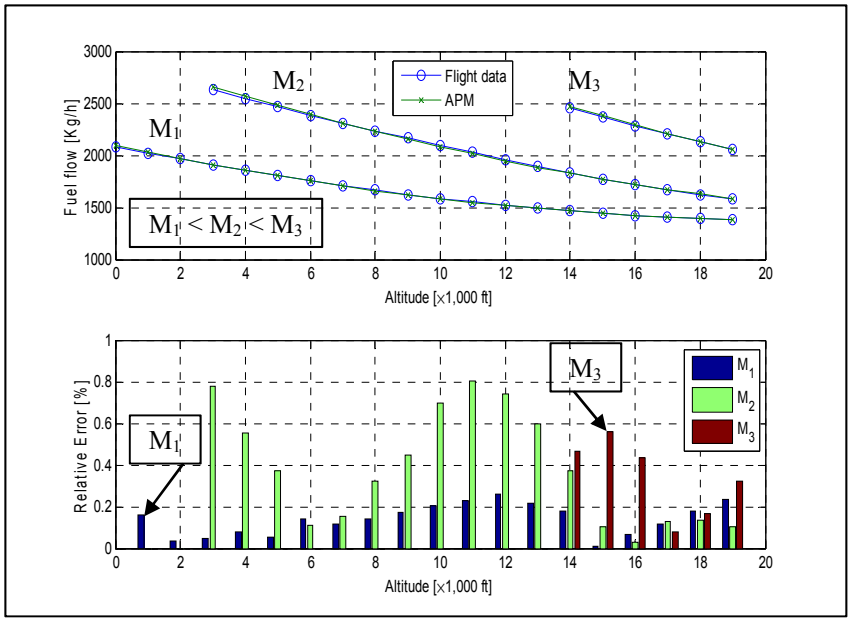

Figure 3.23 Estimated Fuel Flow of Aircraft B in Cruise at middle GW and for three $Mach$ speeds

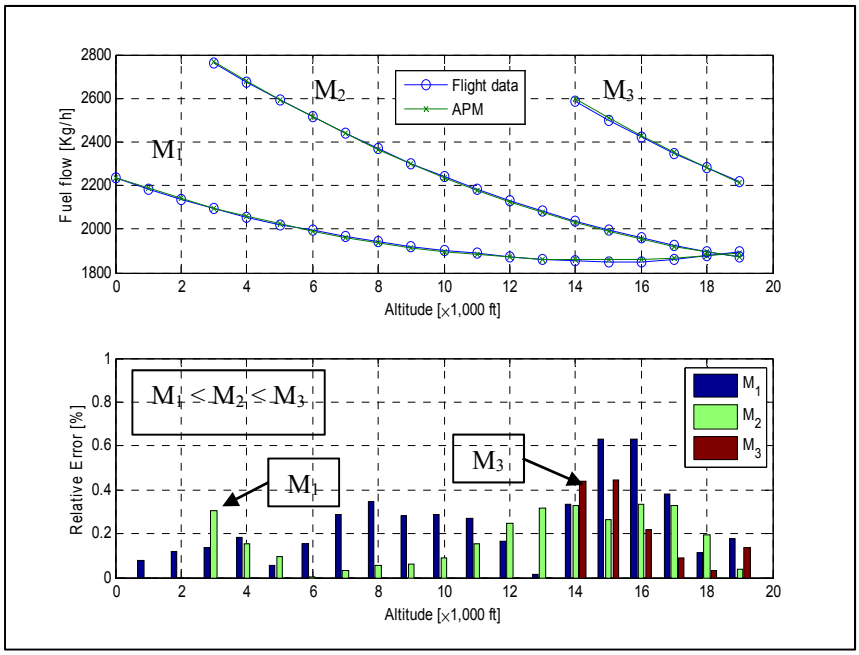

Figure 3.24 Estimated Fuel Flow of Aircraft B in Cruise at maximum GW and for three $Mach$ speeds

A similar analysis to the examples illustrated in Figures 3.1 to 3.6 was extended for a total of 2184/2107-flight tests of Aircraft A, in the climb regime. The success ratio and the number of flight tests performed for both identification and validation models in the climb regime for Aircraft A are presented in Table 3.1. Both the identification and the validation of the resulting model were executed for the $IAS/Mach$ speeds (e.g. Table 2.2). The model identification in the climb procedure shown in Table 3.1 gives an excellent prediction of 100% of the performances, for H_{Dist} and FB, for the IAS speeds. A number of 27 flight tests were also performed for the $Mach$ speed in the model identification process and gave a success of 93% for both climb performances. For the rest of the flight tests (i.e. 2080 flight tests) that were used for the validation model process a success ratio of 86% for H_{Dist} and of 74% for FB were obtained.

Table 3.1 Success ratios and number of flight tests
in the Climb regime for Aircraft A

Flight Test Category	**Number of flight tests**		**% of total flight tests**	**Climb Performances Aircraft A**	**Success ratio (%)**	
	IAS	**Mach**			**IAS**	**Mach**
Identification	27	27	1.24	Horizontal Distance (H_{Dist}) / Fuel Burn (FB)	100 / 100	92.86 / 92.86
Validation	2157	2080	98.76	Horizontal Distance (H_{Dist}) / Fuel Burn (FB)	99.62 / 99.86	85.83 / 74.07

The verifications for the Aircraft B in the climb regime in terms of relative errors, as analyzed in Figures 3.7 to 3.12 were repeated for a total number of 1755 flight tests for the IAS. These flight tests were divided, so that most of them were performed for the model validation. Both identification and validation processes were performed for the IAS and $Mach$ speeds and their success ratios are summarized in Table 3.2. It should be noted that for the identification model process, for 1.24% of the total flight tests used, a success rate of

100% was reached for IAS speeds, while a success rate of 96% was reached for $Mach$ speeds; 1.56% or 27 flight tests of the total flight tests was used, for both $IAS/Mach$ speeds. The rest (98.44% of the total flight tests or 1728/1296 flight tests) of flight tests were used for the validation of the predicted model, and the results were not as good as those success ratios of the model identification because the experimental data contained plenty of zeros meaning that the airplane could not fly in those zones. This has a negatively influence on the horizontal distance results performance. In Table 3.2 a success rate of 78% was obtained for the horizontal distance and around 93% was obtained for the fuel burnt when the flight tests were performed at the IAS speeds. For the case when the airplane flies with the $Mach$ speed, a total number of 1323 flight tests were used from which 27 flight tests took place for model identification, and 1296 flight tests (i.e. 98 % of the total flight tests) took place for the model validation. The success ratios of each of the flight test categories were obtained with a success of 96% for model identification and of 55%, and 59% respectively for model validation.

Table 3.2 Success ratios and number of flight tests
in the Climb regime for Aircraft B

Flight Test Category	**Number of flight tests**		**% of total flight tests**	**Climb Performances Aircraft B**	**Success ratio (%)**	
	IAS	**Mach**			**IAS**	**Mach**
Identification	27	27	1.56	$\frac{\text{Horizontal Distance } (H_{Dist})}{\text{Fuel Burn } (FB)}$	$\frac{100}{100}$	$\frac{95.83}{96.30}$
Validation	1728	1296	98.44	$\frac{\text{Horizontal Distance } (H_{Dist})}{\text{Fuel Burn } (FB)}$	$\frac{77.94}{92.55}$	$\frac{55.43}{58.79}$

Overall, these percentages are reasonable for both aircrafts under investigation. These positive results indicate that manufacturers could eliminate approximately 99% of flight tests in the climb regime, by making substantial financial savings, as seen on the 2nd row of Table 3.1 and of Table 3.2, for the two aircrafts of commercial class. The model designed for this

flight phase has created the numerical data with an acceptable degree of accuracy, to the extent that it can now be adapted for its application to other commercial aircraft.

The simulation for the Aircraft A model' identification in the cruise regime was executed for a number of 675 flight tests. The success ratio for the aero-propulsive model in the cruise phase indicates that the designed model could bring significant economies to the aircraft manufacturers close to 99% of flight tests costs, as presented by the 2nd row of Table 3.3.

Table 3.3 Success ratios and number of flight tests
in Cruise regime of Aircraft A

Flight Test Category	**Number of flight tests**		**% of total flight tests**	**Cruise Performances Aircraft A**	**Success ratio (%)**	
	IAS	**Mach**			**IAS**	**Mach**
Identification	675	675	1.33	Fuel flow (w_f)	100	96.30
Validation	50,750	79,750	98.67	Fuel flow (w_f)	96.61	94.93

The required performance for the Aircraft A is described in Table 3.3, and shows a very good conformity between the fuel flow flight data and the predicted fuel flow (w_f). The estimated fuel flow was achieved, for the model identification and validation with respect to flight tests data with 100% and 96.61% accuracy for the IAS speeds, and with 96% and 95% accuracy for the identification and validation processes due to investigations at $Mach$ speeds. Additionally, the model in cruise has been applied to the Aircraft B and the results are presented in Table 3.4, these results have also a good accuracy.

Table 3.4 Success ratios and number of flight tests
in Cruise regime of Aircraft B

Flight Test Category	Number of flight tests		% of total flight tests	Cruise Performances Aircraft B	Success ratio (%)	
	IAS	Mach			IAS	Mach
Identification	540	540	1.05	Fuel flow (w_f)	100	92.59
Validation	51,480	46,800	98.95	Fuel flow (w_f)	100	86.75

These positive results indicate the fact that this aero-propulsive model inserted into a FMS application could reduce almost 99% of the required number of flight tests needed to achieve accurate numerical data, during the cruise phase, thereby realizing significant savings, and therefore advantageous for commercial aircraft designers.

CONCLUSION AND RECOMMENDATIONS

Aerospace industries are still seeking to improve the solutions that have already been implemented in the commercial aviation sector to reduce the industry's environmental impact. Advances in the design and technology of aircraft and engine models have improved the efficiency of Air Traffic Control (ATC) decisions, while remaining within airworthiness rules. The efficiency of those decisions is also dependent upon by the Air Traffic Management Systems (ATMs) and Flight Management systems (FMSs), whose reference source is a performance database accessed by both the aircraft manufacturers and by their collaborators or subcontractors. Usually, the aircraft manufacturer provides to his collaborators, in addition to aircraft flight manual, the software and/or the performance database, as tools with which the aircraft was designed and built. However, there are some obstacles that limit direct collaboration with the aircraft manufacturer; one such obstacle is that the performance database represents its Intellectual Property (IP). Another difficulty, in terms of the direct use of this product is linked to the limited capacity of the FMSs applications for processing information. It is known in the literature that an FMS application uses a set of look-up tables that contains an experimental database of a particular airplane. This database is playing an essential role in trajectory' optimization algorithms. But, solving the flight's trajectory problems allows better prediction of an aircraft's flight plan in terms of safety, efficiency and environmental consequences. The performances of systems applications (i.e. ATMs and FMSs) are influenced by the accuracy of the created mathematical models for their operational needs. There are few aircraft performance models for ATM-FMS applications, and even fewer, that refer to an aero-propulsive model built for climb flight, by using the inverse engineering problem.

In fact, there are no aero-propulsive models created, without access to engine(s) data, for commercial airplanes in the climb and cruise flight, and by their use, to solve flight trajectory optimization problems. This research aims to fill up this gap of the domain. The research problem concerns the generation of numerical databases, for a commercial airliner, that relies on the aero-propulsive models, which describe the airplane in the climb and cruise phases.

An aircraft is a complex dynamic system based on others systems. The performance of each system must be described through a mathematical model. Therefore, the traditional approach widely used in the aerospace industry was to apply the system identification theory, with the goal to find a crude approximation of each of studied systems performances. To solve this research problem, a new methodology to build an aero-propulsive model in accordance to each of two flight regimes (climb and cruise) has been done.

Description of thesis chapters

This research thesis was structured in three major chapters covering the background topic, a complete methodology, the results that have shown the degree of success of the argued methodology and recommendations needed for further work. An overview of each of these chapters is presented as follows.

Chapter 1 has began with an introduction in which this research topic was explored in a global context regarding fuel reduction with implications in the control and management of the emissions, and the motivation besides the contribution of this research in solving this problem. The research problem has dealt serious and important environmental issues, since the distance traveled as well as the fuel consumption have been seen as potential time and money savings that could have positive implications for our ecosystem. The originality of the research is also supported by the fact that the models investigated and the numerical databases produced, to predict the optimal flight planning, were both accurately realized with the least possible flight data access and for a minimal number of flight tests; a unique and valuable addition is thus brought to the investigations improvement in the aerospace area. The chapter ends by presenting the research problem, which has been directed to two main objectives (i.e. identifying an APM and generating a numerical database derived from the identified APM), which have to answer this research question (i.e. identifying an APM of a commercial aircraft from available flight test data, that generates a numerical database which contains the estimated performances in climb and cruise regimes).
By definition, an aero-propulsive model (APM) was represented by an aerodynamic performance model and an engine performance model, with multiple inputs and outputs.

The methodology developed in the Chapter 2 responds to both research questions by (a) the design of two mathematical models for climb and cruise regimes, utilizing the numerical databases of two commercial aircrafts, provided by our research partner, and (b) the conception of the numerical databases derived from the resulting models.

To answer to the first research question, this methodology recommends the application of system identification theory to a dynamic system (i.e. the aircraft) within specific assumptions for climb and cruise regimes. These models were subjected to common assumptions, for each flight test, such as wind-free, operational engine(s), and the constant Indicated Air Speeds and Mach speeds.

For an aircraft flight in the vertical plane, the assumptions are:

1. An aircraft is considered as a rigid body in an inertial reference frame;
2. A set of equations, which describes the aircraft longitudinal motion, is also subject to aerodynamic forces (i.e., the drag and lift), propulsive forces (i.e., the thrust) and gravitational forces (i.e., the weight); thus a physical model is expressed by its flight dynamics equations (e.g., in the climb regime). The physical model was modified to best present the aircraft motion corresponding to the climb phase.

More exactly, the specific identification methods were applied to the linear (i.e. used for the cruise regime) and non-linear models (i.e. used for the climb regime), which are mathematically represented by several functions that describe the relationships between the aircraft's parameters under investigation. These mathematical functions of the airplane's behavior in the climb and cruise regimes were based on the inputs and outputs measurements of a “black box” model (i.e. the given numerical database or the AFM structures). The inputs of the given flight data (e.g. the measured parameters by the onboard aircraft instruments) consist of the parameters describing the behaviour of the aircraft in the climb such as the gross weights, the center of gravity positions (only in the climb phase), the speeds (i.e. IAS and $Mach$), the ISA temperature deviation and the altitudes, while the outputs of the given flight data correspond to the horizontal distance traveled and the fuel burned as the climb performances and to the fuel flow as the cruise performance. The inputs and outputs may differ for another aircraft, but their structure should remain similar to that found in any

aircraft flight manual (AFM). However, this methodology can be no doubt applied for the design of other aircraft performance models.

This proposed aero-propulsive model relies on two estimation algorithms, corresponding to each flight regime studied, climb and cruise. According to the identification system principle, each estimation algorithm received the residuals (i.e. the model error), and produced an update on the parameters defining the mathematical model. The aim of each of these estimation algorithms was to find that set of parameters for which the difference between the outputs observed and predicted output was minimal. The prediction error (PE) method and the least square (LS) method were the two methods used in this study for the aircraft' parameter estimation algorithms.

The model identification procedure in the climb regime was performed in two steps. The first step has consisted in the computation of the rate of climb based on the available flight data or the AFM data. In the second step of the model identification few crude approximations of the parameters of the physical model have been chosen, and all the other necessary computations to it were emphasized through a parameter estimation algorithm. In the climb estimation algorithm, the prediction error (PE) method was applied, in order to estimate the output parameters of a non-linear function that minimize the sum of squared errors (i.e. the residuals) between the measured (i.e. the measured aircraft parameters) output and the predicted (i.e. the identified model parameters) output. The climb performance estimates were then optimized to find their local minima as unique solutions. An optimization routine based on the *simplex search* algorithm (Nelder-Mead method) was chosen to adjust a set of three variables (C_{Dmin}, e, T) in order to minimize the sum of squared modeling errors. The climb estimation' error was expressed by the difference between the estimated rate of climb and the rate of climb computed. However, the mathematical model is automatically fed with these optimized parameters.

The specific fuel consumption was then computed, based on the optimal values of the engine thrust and rate of climb, and the available fuel burnt for each of the altitude climb sub-segments.

The obtained equation of the rate of climb $\dot{h}$ is essential for a specific flight condition, because it involves the aero-propulsive forces performance. The difference between the two aero-propulsive forces (i.e. the thrust T and the drag D forces) could then be calculated, in order to obtain the first estimate of the rate of climb. On the other hand, if each of these forces T and D is known, then the climb performance could be estimated.

For each flight test corresponding to the model identification procedure, the thrust force T, the specific fuel consumption T_{sfc} and the difference $(T - D)$ between the thrust and the drag forces were tabulated and formatted into different 4-D (i.e. the altitude, the speed, the gross weight, the temperature deviation) look-up tables (used by the FMS applications).

The methodology used for climb ends with the aircraft trajectory prediction using the aero-propulsive model (APM). The horizontal distance traveled and the fuel burn are the two needed parameters used to predict the aircraft trajectory and its performance for each specific flight configuration. Thereafter, the horizontal distance traveled and the fuel burn were determined using an "Euler integration technique".

For the cruise model, a new approach was proposed for the case, when the aircraft' behaviour cannot be represented by a physical model. A parameterization of the fuel flow to identify its model has been used instead of finding approximate representations for each of its parameters (i.e. the thrust specific fuel consumption coefficient and the drag force) that are defining it. An engine fuel flow analysis with respect to the altitude and the speed revealed that the fuel flow behaves as a bi-quadratic function. These coefficients were identified to best approximate a flight test data.

In the cruise estimation algorithm, the Least Squares (LS) method was also used to compute the residuals between the measured and the estimated parameters.

The estimated parameters of the identified model for the climb or cruise were then tabulated into look-up tables in order to allow an interpolation within each flight envelope of each of the aircrafts. A 4-D linear interpolation was performed into the look-up tables for each of these parameters in order to extend the aircraft flight trajectory within its flight envelope.

The flight tests corresponding to one investigated flight phase (climb or cruise) were divided such that some of tests were used in the model identification process, and the most of them were assigned to the model validation process.

Chapter 3 describes the research findings and assesses the reliability of the aero-propulsive models in climb and cruise regimes for two aircrafts of the commercial class. The results and the discussions were based on the validation of the proposed methodologies needed to develop the aero-propulsive models in the climb and cruise regimes, and show how well these models have approximated the available flight data. The model validation consisted on the analogy between the real flight data acquired and provided by our research partner, and the predicted numerical data based on our suggested methodology. Predicted performances of the aero-propulsive models were verified using different flight tests for the validation process than the ones used in the identification process. Therefore, a very small percentage (%) of the total flight tests number was attributed to the identification model compared to the validation model, in order to minimize the number of the flight tests, and thus their costs. The number of flight tests used in the identification process was chosen as around 1% of their total number of flight tests in the climb regime for Aircraft A, while the rest of these flight tests of 99% of their total were used for validation purposes.

Savings of almost 99% in flight tests, for Aircraft A, sustain the effectiveness of the model identification with 100% accuracy in climb phase, for the total distance traveled and fuel burn, at constant IAS. The validation of the climb model has 99.62% for the total distance traveled and 99.86% success ratio for the fuel burnt when the aircraft flies at constant IAS.

For the simulation performed at a $Mach$ speed constant, a good accuracy was obtained for the model identification (i.e. 93%) for both climb performances analysed. While, 86% success ratio for the horizontal distance traveled and 74% success ratio for the fuel burnt were obtained for the validation of the identified model; the reason is that the supplied flight data contain flight regions to which the aircraft is not intended to fly.

The methodology was also verified for the Aircraft B in the climb regime; an accuracy of 100% was obtained for both performances (H_{Dist}, FB) of the model identification case where 1.56% of the total flight tests were performed at IAS speeds.

For the validation, when 98.44% of the total of the flight tests were used, accuracy of 78% was obtained for the horizontal distance, and 93% for the fuel burnt. A success ratio of 96% was achieved for both climb performances (H_{Dist}, FB) at $Mach$ speeds in the model identification process, while for the validation of the identified model, only 55% for the horizontal distance traveled and 59% for the fuel burnt consumption were obtained.

In cruise regime for the Aircraft A were obtained the following accuracies for the model identification process performed with only 1.33% of the total of the flight tests: 100% fuel flow at constant IAS and 96.30% at constant $Mach$ speeds. While, for the model validation process, the simulation results have shown also a good cruise performance (i.e. the fuel burnt) accuracy, which is of 96.61% at constant IAS, and of 94.93% at constant $Mach$.

The model's methodology in cruise was also verified for an Aircraft B and again a good accuracy of 100% was found at IAS speeds for both identification and validation processes, and 92.59% and 86.75% were obtained as success ratios in model identification, respectively in the model validation at $Mach$ speeds.

The cruise regime was considered to be the most efficient, economically speaking, thus these results have emphasized that this aero-propulsive model that was tested for two commercial aircrafts A and B, it can be seen as a valid and reliable economic alternative solution for any FMS providers. As already mentioned, the literature did not impose a special criterion regarding the accuracy degree of a numerical database generated using this type of model. However, in this research thesis, we considered that the model was reliably predicted within a maximum errors range of 5%. Additionally, its effectiveness is sustained by the fact that the numerical databases derived from these models can be used in the trajectory optimization of FMS applications. Consequently, this aero-propulsive model applied as the simulation (Matlab script) tool in ATM-FMS applications will improve the global efficiency of commercial aircraft.

Therefore, the designed methodology responds very well to the addressed research questions by creating these models in the climb and cruise phases, whose numerical databases derived have experimentally have shown an excellent accuracy of 100% for both aircrafts A and B studied at the IAS speeds.

Recommendations

The flight trajectory prediction could further be improved, and thus an optimal and safer flight trajectory could be obtained by adding the wind effect and the weather data as a complement to this aero-propulsive model in the climb and cruise regimes.

The methodologies suggested in this research thesis can be applied for the development of other numerical databases that correspond to the descent, acceleration and deceleration phases; the wind, thus the weather effects could also be taken in consideration.
The numerical databases generated from these aero-propulsive models might be further used in the flight trajectory optimization of any commercial airplane. All of them are intended for the full characterization of a commercial aircraft flight (of all the flight regimes).

An analysis between the aero-propulsive model and the BADA model can be also considered part of a future research. The results and recommendations of this study are addressed to the aeronautical research community, consisted of students and researchers, as well as of aeronautical engineers.

LIST OF BIBLIOGRAPHIC REFERENCES

AIRBUS. 2002. *Getting to Grips with Aircraft Performance*. Coll. « Flight Operations Support & Line Assistance », November 26, 12 p. < http://www.skybrary.aero/bookshelf/books/2263.pdf >.

Airbus. 2014. « Global Market Forecast (2014–2033) ». < https://www.airbusgroup.com/.../Airbus_Global_Market_Forecast_2014-2033_Presentation_by_John_Leahy.pdf >. Consulté le September 26, 2015.

Airbus. 2015. « Winglets Airbus, a leading aircraft manufacturer ». < http://www.airbus.com >. Consulté le September 29, 2015.

Asselin, Mario. 1997. *An introduction to aircraft performance*. Coll. « AIAA Education Series: An Introduction to Aircraft Performance ». AIAA, 339 p.

ATAG. 2014. *Aviation benefits beyond borders*. 72 p. < http://www.aviationbenefits.org >.

Baklacioglu, T, and M Cavcar. 2014. « Aero-propulsive modelling for climb and descent trajectory prediction of transport aircraft using genetic algorithms ». *AERONAUTICAL JOURNAL,* vol. 118, n° 1199, p. 65-79.

Blake, Walt. 2009. *Jet Transport Performance Methods*. Coll. « Boeing Commercial Airplanes, Boeing Document D6-1420 », 21-6 p.

Bosch, Paul P.J. van den, and Alexander C. van der Klauw. 1994. *Modeling, identification and simulation of dynamical systems*. CRC Press, 208 p.

Botez, Ruxandra (Ed). 2006. *GPA-745: Introduction à l'avionique: notes de cours*. GPA-745. Bachelor and Master's engineering programs. Montreal: École de technologie supérieure, multiple pagination 394 p.

Brandt, Steven A. 2004. *Introduction to aeronautics: a design perspective*. Aiaa.

Budd, Lucy, and Andrew R Goetz. 2014. *The Geographies of Air Transport*. Ashgate Publishing, Ltd.

Camilleri, William, Kenneth Chircop, David Zammit-Mangion, Roberto Sabatini and Vishal Sethi. 2012. « Design and validation of a detailed aircraft performance model for trajectory optimization ». In *AIAA Modeling and Simulation Technologies Conference, Minneapolis, Minnesota, August*. p. 13-16.

Cavcar, Mustafa. 2000. « The International Standard Atmosphere (ISA) ». Vol. 26470, p. 7. < http://fisicaatmo.at.fcen.uba.ar/practicas/ISAweb.pdf >. Consulté le November 11, 2015.

Cheng, HK, and FT Smith. 1982. « The influence of airfoil thickness and Reynolds number on separation ». *Zeitschrift für angewandte Mathematik und Physik ZAMP,* vol. 33, nº 2, p. 151-180.

Collinson, RPG. 2011. « Autopilots and flight management systems ». In *Introduction to Avionics Systems*. p. 415-458. Springer.

Corke, Thomas C. 2003. *Design of aircraft*. Prentice Hall: Pearson College Division, 391 p.

Creedon, JF. 1983. « Flight management systems ». *AIAA-83-2235*, p. 516-528.

Daamen, Winnie, Christine Buisson and Serge P Hoogendoorn. 2014. *Traffic Simulation and Data: Validation Methods and Applications*. CRC Press.

Dancila, Bogdan Dumitru. 2011. « Altitude optimization algorithm for cruise, constant speed and level flight segments ». École de technologie supérieure.

Dennis Jr, John E, and Robert B Schnabel. 1996. *Numerical methods for unconstrained optimization and nonlinear equations*, 16. Siam, (xv + 375) p.

DTTL. 2014. « Current Market Outlook (2014–2033) ». < http://www.boeing.com/assets/pdf/commercial/cmo/pdf/Boeing_Current_Market_Outlook_2014.pdf >. Consulté le September 28, 2015.

Endsley, Mica R. 1996. « Automation and situation awareness ». *Automation and human performance: Theory and applications*, p. 163-181.

Eurocontrol. 2014. « True Airspeed ». In *Theory of Flight | Enhancing Safety*. < http://www.skybrary.aero/index.php/True_Airspeed >. Consulté le December 1, 2015.

FAA. 2015. *Aviation Emissions, Impacts & Mitigation: A Primer*. Report. 38 p. < http://www.faa.gov/regulations_policies/policy_guidance/envir_policy/media/Primer_Jan2015.pdf >.

Flathers III, George W, DJ Allerton and Graham T Spence. 2010. « FMS automation issues for future ATM integration ». In *27th International Congress of the Aeronautical Sciences, Nice, France*. p. 10.

Fleming, Gregg G, Andrew Malwitz, Brian Kim and Lourdes Maurice. 2006. « Using FAA's SAGE Model to Conduct Global Inventories and to Assess Route-specific Variability

in Aviation Fuel Burn, Emissions, and Costs ». In *25th International Congress of the Aeronautical Sciences*.

Gabor, Oliviu Sugar, Andreea Koreanschi and Ruxandra Mihaela Botez. 2012. « Low-speed aerodynamic characteristics improvement of ATR 42 airfoil using a morphing wing approach ». In *IECON 2012-38th Annual Conference on IEEE Industrial Electronics Society*. p. 5451-5456. IEEE.

Gabor, Oliviu Sugar, Andreea Koreanschi and Ruxandra Mihaela Botez. 2013. *Optimization of an Unmanned Aerial System'wing using a flexible skin morphing wing*. SAE Technical Paper.

Gabor, Oliviu Şugar, Antoine Simon, Andreea Koreanschi and Ruxandra Botez. 2014. « Numerical Optimization of the S4 Éhecatl UAS Airfoil using a Morphing Wing Approach ». In *32ndAIAA Applied Aerodynamics Conference*. (Atlanta, GA).

Ghazi, GEORGES. 2014. « Développement d'une plateforme de simulation et d'un pilote automatique-application aux Cessna Citation X et Hawker 800XP ». Master's thesis, University of Quebec-École Polytechnique de Montréal, 2014. DOI: 10.13140/2.1. 1236.7369.

Ghazi, Georges, Ruxandra Mihaela Botez and Magdalena Tudor. 2015. « Performance Database Creation for Cessna Citation X Aircraft in Climb Regime using an Aero-Propulsive Model developed from Flight Tests ». In *AHS Sustainability 2015 Conference*. (Montreal, Quebec, September 22-24), p. 11.

Ghazi, Georges, Ruxandra M. Botez, J. Casas and M. Tudor. 2016. *Climb, cruise and descent trajectory prediction of a transport aircraft using an aero-propulsive model*. École de Technologie Supérieure - LARCASE, 35 p.

Gong, Chester, and William N Chan. 2002. « Using flight manual data to derive aero-propulsive models for predicting aircraft trajectories ». In *Proc. of AIAA's Aircraft Technology, Integration, and Operations (ATIO) Forum, Los Angeles, CA*.

Gudmundsson, Snorri. 2013. *General aviation aircraft design: applied methods and procedures*. Butterworth-Heinemann, 1007 p.

Hamel, Peter G, and Ravindra V Jategaonkar. 1996. « Evolution of flight vehicle system identification ». *Journal of Aircraft,* vol. 33, nº 1, p. 9-28.

HARADA, Akinori, Yuto MIYAMOTO, Yoshikazu MIYAZAWA and Kozo FUNABIKI. 2013. « Accuracy evaluation of an aircraft performance model with airliner flight data ». *TRANSACTIONS OF THE JAPAN SOCIETY FOR AERONAUTICAL AND SPACE SCIENCES, AEROSPACE TECHNOLOGY JAPAN,* vol. 11, nº 0, p. 79-85.

Hull, David G. 2007. *Fundamentals of airplane flight mechanics*, 2007. Springer, 310 p.

IATA. 2013. *Responsibly Addressing Climate Change*. 3 p. < http://www.iata.org/whatwedo/environment/Documents/ policy-climate-change.pdf >.

IATA. 2014. *Report on Alternative Fuels*. 68 p. < http://www.iata.org/publications/Documents/2014-report-alternative-fuels.pdf >.

ICAO. 2010. *Chapter 2 AIRCRAFT TECHNOLOGY IMPROVEMENTS*. Coll. « ICAO Environmental Report 2010 », 94 p. < http://www.icao.int/environmental-protection/Documents/EnvironmentReport-2010/ICAO_EnvReport10-Ch2_en.pdf. >.

Igor, Alonso-Portillo, and Ella M. Atkins. 2001. *Adaptive Trajectory Planning for Flight Management Systems*. AAAI Technical Report SS-01-06, 9 p.

Jategaonkar, Ravindra V. 2006. *Flight Vehicle System Identification A Time Domain Approach*. Coll. « Progress in Astronautics and Aeronautics », volume 216. 534 p.

Jensen, L, R John Hansman, JC Venuti and T Reynolds. 2014. « Commercial Airline Altitude Optimization Strategies for Reduced Cruise Fuel Consumption ». In *14th AIAA Aviation Technology, Integration, and Operations Conference, ed: American Institute of Aeronautics and Astronautics, Atlanta, GA, USA*.

Jensen, Luke, RJ Hansman, Joseph C Venuti and Tom Reynolds. 2013. « Commercial Airline Speed Optimization Strategies for Reduced Cruise Fuel Consumption ». In *2013 Aviation Technology, Integration, and Operations Conference*. p. 1-13.

Junyi, Peng, and Jia Rongzhen. 1997. « Research on flight management system for real-time simulation ». *Journal of System Simulation,* vol. 9, nº 3, p. 88-99.

Kaboldy. 2013. « Gulfstream G500 (Own work) ». < https://commons.wikimedia.org/wiki/File:Gulfstream_G500.svg >.

Lagarias, Jeffrey C, James A Reeds, Margaret H Wright and Paul E Wright. 1998. « Convergence properties of the Nelder--Mead simplex method in low dimensions ». *SIAM Journal on optimization,* vol. 9, nº 1, p. 112-147.

Liden, Sam. 1995. « The evolution of flight management systems ». In *Digital Avionics Systems Conference, 1994. 13th DASC., AIAA/IEEE*. p. 157-169. IEEE.

Ljung, Lennart. 2010. « Perspectives on system identification ». *Annual Reviews in Control,* vol. 34, nº 1, p. 1-12.

Maris, John, and Maxence Vandevivere. 2014. *MGA-856: Ingénierie et principes des essais en vol: notes du cours* MGA-856. Programme de Maîtrise en génie: Concentration en génie aérospatiale. École de Technologie Supérieure, pagination multiple 71 p.

MathWorks. 2013. *MATLAB* (Version R2013). < http://www.mathworks.com/products/matlab/ >.

Murrieta Mendoza, Alejandro. 2013. « Vertical and lateral flight optimization algorithm and missed approach cost calculation ». École de technologie supérieure.

Murrieta-Mendoza, Alejandro, and Ruxandra Botez. 2014. « Method to Calculate Aircraft VNAV Trajectory cost Using a Performance Database ». In *ASME 2014 International Mechanical Engineering Congress and Exposition*. p. V001T01A053-V001T01A053. American Society of Mechanical Engineers.

Murrieta-Mendoza, Alejandro, Simon Demange, François George and Ruxandra Botez. 2015. « Performance DataBase creation using a level D simulator for Cessna Citation X aircraft in cruise regime ». In *IASTED Modeling, Identification and Control Conference, Innsbruck, Austria*.

NASA. 2015. « Wing Geometry Definitions ». < http://www.grc.nasa.gov >. Consulté le December 02, 2015.

Nelson, Robert C. 1998. *Flight stability and automatic control*, 2. WCB/McGraw Hill.

Okamoto, Nicole DeJong, Jinny Rhee and Nikos J Mourtos. 2005. « Educating students to understand the impact of engineering solutions in a global/societal context ». In *8th UICEE Annual Conference on Engineering Education*.

Patrón, RS Félix, Aniss Kessaci, Ruxandra Mihaela Botez and Dominique Labour. 2013. « Flight trajectories optimization under the influence of winds using genetic algorithms ». In *AIAA Guidance, Navigation, and Control Conference*. p. 19-22.

Peeters, PM, J Middel and A Hoolhorts. 2005. « Fuel efficiency of commercial aircraft: an overview of historical and future trends, 2005 ». *National Aerospace Laboratory NLR: Amsterdam*.

Raol, Jitendra R, Gopalrathnam Girija and Jatinder Singh. 2004. *Modelling and parameter estimation of dynamic systems*, 65. Iet.

Raymer, Daniel P. 1992. *Aircraft Design: A Conceptual Approach . Washington DC: American Institute of Aeronautics and Astronautics*. Inc.

Ross, MacAusland. 2014. « The Moore-Penrose Inverse and Least Squares ». < buzzard.ups.edu/ courses/2014spring/420projects/math420-UPS-spring-2014-macausland-pseudo-inverse.pdf >. Consulté le January 27, 2016.

Shin, Ho-Hyun, Sang-Hyun Lee, Youdan Kim, Eung-Tae Kim and Ki-Jung Sung. 2011. « Design of a flight envelope protection system using a dynamic trim algorithm ». *International Journal of Aeronautical and Space Sciences,* vol. 12, nº 3, p. 241-251.

Sibin, Zhu, Li Guixian and Han Junwei. 2010. « Research and modelling on performance database of flight management system ». In *2nd International Asia Conference on Informatics in Control, Automation and Robotics* (Wuhan, 6-7 March 2010). Vol. 1, p. 295-298. IEEE.

Sibin, Zhu, Guixian Li and Junwei Han. 2012. « An Improved PSO Algorithm with Object-Oriented Performance Database for Flight Trajectory Optimization ». *Journal of Computers,* vol. 7, nº 7, p. 1555-1563.

Stevens, Brian L, and Frank L Lewis. 2003. *Aircraft control and simulation*. John Wiley & Sons.

Suchkov, Alexander, S Swierstra and A Nuic. 2003. « Aircraft performance modeling for air traffic management applications ». In *5th USA/Europe Air Traffic Management Research and Development Seminar*. p. 23-27.

Talay, Theodore A. 1975. *Introduction to the Aerodynamics of Flight*, 367. Scientific and Technical Information Office, National Aeronautics and Space Administration, 6-9 p.

Theunissen, Erik, RM Rademaker and AA Lambregts. 2011. « Navigation system autonomy and integration in NextGen: Challenges and solutions ». In *Digital Avionics Systems Conference (DASC), 2011 IEEE/AIAA 30th*. p. 6C5-1-6C5-12. IEEE.

Tomita, Yutaka, Ad AH Damen and PAUL MJ Van Den Hof. 1992. « Equation error versus output error methods ». *Ergonomics,* vol. 35, nº 5-6, p. 551-564.

Torenbeek, Egbert. 1995. *Optimum cruise performance of subsonic transport aircraft*. Delft University of Technology, 69 p. < http://www.tudelft.nl >.

US, Air Force. 1993. *Cruise performance theory*. DTIC Document, 69 p.

Vallone, Michael. 2010. « Parameter Estimation of Fundamental Technical Aircraft Information Applied to Aircraft Performance ». Master of Science DigitalCommons, Faculty of California Polytechnic State University, San Luis Obispo, 174 p. < http://digitalcommons.calpoly.edu/theses/382 >. Consulté le October 22, 2015.

Vallone, Mike, and Robert A McDonald. 2010. « Parameter Estimation of Fundamental Technical Aircraft Information Applied to Aircraft Performance ».

Vincent, Jean Baptiste, Ruxandra Mihaela Botez, Dumitru Popescu and Georges Ghazi. 2012. « New methodology for a business aircraft model Hawker 800 XP stability analysis using Presagis FLsim ». In *AIAA Modeling and Simulation Technologies Conference. AIAA*.

Walter, Randy (Ed). 2001. *Flight Management Systems*. CRC Press, 264-288 p.

Wang, Jiang-yun, and Xiao-yang Yang. 2008. « Modeling and Simulation of the Civil Flight Management System [J] ». *Flight Dynamics,* vol. 43(2), p. 81-84.

Zadeh, L. A. 1962. « From Circuit Theory to System Theory ». *Proceedings of the IRE,* vol. 50, p. 856-865.

Zimmerman, Ward H, and Melville DW McIntyre. 1991. *Integrated aircraft air data system*. US 07/339,675: Boeing Company, 19 p.
< http://www.google.ca/patents/US5001638 >.